Technische Universität München
TUM School of Medicine and Health

Immunometabolism and viral pathogenesis in hepatitis B virus infection

Till Bunse

Vollständiger Abdruck der von der TUM School of Medicine and Health der Technischen Universität München zur Erlangung eines

Doctor of Philosophy (Ph.D.)

genehmigten Dissertation.

Vorsitz: Priv.-Doz. Dr. Maike Buchner

Betreuerin: Prof. Dr. Ulrike Protzer

Prüfende der Dissertation:

1. Prof. Dr. Peter Murray
2. Prof. Dr. Stefanie Eyerich

Die Dissertation wurde am 31.03.2024 bei der TUM School of Medicine and Health der Technischen Universität München eingereicht und durch die TUM School of Medicine and Health am 01.06.2024 angenommen.

Abstract

Chronic infection with the hepatitis B virus (HBV) poses a global challenge to society and affects millions of people worldwide. Despite new treatment options, a functional cure remains often unachieved due to the complex interplay between viral persistence and an inadequate host immune response. This work addresses the relationship between immune metabolism and HBV pathogenesis and aims to generate new insights into viral persistence and immune evasion mechanisms. In vitro cell culture models and in vivo studies in preclinical mouse models were used to investigate the effects of amino acid metabolism on HBV-specific immune responses and identify potential targets for therapy.

First, the influence of amino acid deficiency on the functionality of HBV-specific cytotoxic T cells was investigated, focusing on arginine metabolism. Using an HBV-specific cytotoxicity assay, the central role of this amino acid in modulating the effector functions of T cells was investigated. Broad RNA sequencing and metabolomic analyses of HBV-infected cells were performed to identify potential targets for therapeutic intervention. In particular, transporters responsible for the homeostasis of energy supply were identified as potential targets for intervention. Subsequently, the course of HBV infection was investigated in GCN2 knockout mice. GNC2 is a central factor in the recognition of amino acid deficiency. The aim was to elucidate the influence of the GCN2 signaling pathway on the course of HBV infection. A different course of infection in the mouse model implies the involvement of the GCN2 signaling pathway in the persistence of HBV.

The last section of the thesis investigated the combination of different approaches for the therapy of chronic hepatitis B. The efficacy of a therapeutic vaccine was investigated in a mouse model of chronic hepatitis B in combination with suppression of viral proteins and immune checkpoints. In AAV-HBV infected mice, siRNA was first used to suppress the expression of viral proteins and then additionally the expression of the T cell inhibitory immune checkpoint PD-L1. A therapeutic vaccine was then administered and the course of the infection was monitored in the serum of the mice. The combined application of the two siRNAs and the therapeutic vaccine enhanced the antiviral effect. Due to the increased effectiveness, significantly more people could benefit from therapy who would not

normally be eligible for therapy because therapeutic vaccination fails at high virus titers.

In summary, this work investigated new targets for immunotherapies in chronic HBV infections. The immunologic and metabolic analyses of this work provide a basis for new immunometabolic therapies for chronic HBV infection.

Zusammenfassung

Die chronische Infektion mit dem Hepatitis-B-Virus (HBV) stellt eine globale Herausforderung für die Gesellschaft da und betrifft weltweit Millionen Menschen. Trotz neuer Behandlungsmöglichkeiten ist eine funktionelle Heilung aufgrund des komplexen Zusammenspiels zwischen viraler Persistenz und einer unzureichenden Immunantwort des Wirts schwer zu erreichen. Diese Arbeit befasst sich mit der Beziehung zwischen Immunstoffwechsel und der HBV-Pathogenese und hat zum Ziel, neue Erkenntnisse über die Mechanismen der viralen Persistenz und der Immunevasion zu generieren.

In *in vitro* Zellkultur-Modellen und *in vivo* Studien an präklinischen Mausmodellen wurden die Auswirkungen des Aminosäurestoffwechsels auf HBV-spezifische Immunreaktionen untersucht und potenzielle Ansatzpunkte für eine Therapie identifiziert.

Zuerst wurde der Einfluss von Aminosäuremangel auf die Funktionalität HBV-spezifischer zytotoxischer T-Zellen untersucht, mit Schwerpunkt auf dem Argininstoffwechsel. Unter Verwendung eines HBV-spezifischen Zytotoxizitäts-Assays wurde die zentrale Rolle dieser Aminosäure bei der Modulation der Effektor-Funktionen von T-Zellen untersucht. Breite RNA-Sequenzierungen und Metabolom-Analysen von HBV infizierten Zellen wurden durchgeführt um mögliche Ansatzpunkte einer therapeutischen Intervention zu identifizieren. Hier zeigten sich besonders Transporter, zuständig für die Homöostase der Energieversorgung, als potentielle Ziele einer Intervention.

Anschließend wurde der Verlauf einer HBV-Infektion an GCN2-Knockout-Mäusen untersucht. GNC2 ist ein zentraler Faktor in der Erkennung eines Aminosäuremangels. Das hatte zum Ziel, den Einfluss des GCN2-Signalwegs, am Verlauf einer HBV-Infektion aufzuklären. Ein unterschiedlicher Infektionsverlauf im Mausmodell impliziert die Beteiligung des GCN2 Signalweges an der Persistenz von HBV.

Der letzte Abschnitt der Arbeit untersuchte die Kombination verschiedener Ansätze zur Therapie einer chronischen Hepatitis B. Die Effektivität einer therapeutischen Vakzine wurde in einem Mausmodell für chronische Hepatitis B in Kombination mit der Suppression von viralen und Immun-Checkpoints untersucht. In AAV-HBV infizierten Mäusen wurde mittels siRNA zuerst die Expression von viralen Proteinen supprimiert und anschließend zusätzlich die

Expression des T Zell inhibierenden Immun-Checkpoints PD-L1. Anschließend wurde eine therapeutische Vakzine verabreicht und der Verlauf der Infektion im Serum der Mäuse verfolgt. Die kombinierte Applikation der beiden siRNA und der therapeutischen Impfung erzielte eine Verstärkung des antiviralen Effekts. Durch die gesteigerte Effektivität könnten deutlich mehr Menschen von einer Therapie profitieren, die normalerweise nicht für eine Therapie in Frage kommen würden, weil bei hohen Virus-Titern die therapeutische Impfung versagt.

Zusammenfassend untersuchte diese Arbeit neue Ansatzpunkte für Immuntherapien bei chronischen HBV-Infektionen. Die immunologischen und metabolischen Analysen dieser Arbeit bieten eine Grundlage für neue immunometabolische Therapien bei chronischer HBV-Infektion.

Abbreviations

AAV	adeno-associated virus
ALT	Alanine aminotransferase
AST	Aspartate aminotransferase
ATF4	Activating Transcription Factor 4
cccDNA	covalently closed circular DNA
CHB	chronic hepatitis B
DAMPs	Damage-associated molecular pattern molecules
DNA	deoxyribonucleic acid
eIF2α	eukaryotic translation initiation factor 2 subunit 1
h	hours
HAMPs	Homeostasis-altering molecular processes
HBc	hepatitis B virus core protein
HBeAg	hepatitis B e antigen
HBsAg	hepatitis B surface antigen
HBV	hepatitis B virus
HCC	hepatocellular carcinoma
HCV	hepatitis C virus
HDV	hepatitis D virus
HIF1α	hypoxia-inducible factor 1α
HIV	human immunodeficiency virus
HSPGs	heparan sulfate proteoglycans
i.v.	intravenously
IDO	indoleamine-2,3-dioxygenase
IFN	interferon
iNOS	inducible nitric oxide synthase
MFI	mean fluorescence intensity
mg	milligram
MOI	multiplicity of infection
mTOR	mechanistic target of rapamycin

NF-κB	nuclear factor-κB
NK	natural killer cell
NTCP	sodium taurocholate co-transporting polypeptide
PAMPs	Pathogen-associated molecular patterns
PBMC	peripheral blood mononuclear cells
PegIFNα	pegylated interferon-α
pgRNA	pregenomic RNA
PKM2	Pyruvate kinase isoenzyme M2
qPCR	quantitative PCR
rcDNA	relaxed circular DNA
RNA	ribonucleic acid
RNAi	RNA interference
Rpm	rounds per minute
RT	room temperature
sec	seconds
siHBV	siRNA targeting HBV
siPD-L1	siRNA targeting PD-L1
siRNA	short interfering RNA
TCA	Tricarboxylic acid
TCR	T-cell receptor
TLR	Toll-like receptor
Treg	regulatory T cell
wt	wildtype

1. Introduction

1.1. Hepatitis B virus (HBV)

With approximately 290 million chronically infected individuals and over 800,000 deaths annually, according to estimations by the WHO, the hepatitis B virus (HBV) is one of the leading causes of infectious disease-related mortality (WHO 2021). While the general trend shows a decline in the death toll of infectious diseases, the numbers for viral hepatitis are on the rise. HBV not only causes acute infections but has found its niche as a persistent virus that heavily relies on vertical transmission. Besides causing acute hepatitis in adults, HBV infection in children manifests with very few symptoms during the early phase; most infected individuals don´t know that they are chronic HBV carriers. In 2019, only 30.4 million people living with hepatitis B knew their status, and merely 6.6 million received treatment (WHO 2021).

1.1.1. Classification

As a part of the Hepadnaviridae family, HBV is a partially double-stranded, enveloped DNA virus with a strong tropism for hepatocytes (Schaefer 2007). Transmission is possible between humans and other hominids, such as chimpanzees or macaques. Closely related, several HBV-like viruses have been identified to infect a wide range of hosts, e.g. woodchuck hepatitis virus or duck hepatitis B virus (Hu 2016). Nine different genotypes have been described, A to I. Worldwide, genotype C is the most frequent genotype, mainly found in Eastern and Southeastern Asia, Australasia, and Oceania (Velkov, Ott et al. 2018).

1.1.2. Viral life cycle

Virus replication exclusively takes place in hepatocytes and eventually leads to the non-cytolytic egress of infectious virions (Fig. 1). The attachment to heparan sulfate proteoglycans (HSPGs) and subsequent binding to sodium taurocholate cotransporting polypeptide (NTCP) initiate viral entry. Subsequent virus internalization is clathrin-mediated, and the virion is transported to the nucleus, where the nucleocapsid uncoating happens (Chakraborty, Ko et al. 2020). Next, the relaxed circular DNA (rcDNA) is imported into the nucleus and repaired by the host´s DNA repair enzymes to establish the persistent form of the HBV genome, the covalently closed circular DNA (cccDNA) (Gao and Hu 2007).

Inside the nucleus, cccDNA will stay as an episomal structure and serve as a template for all viral transcripts. In a total of four open reading frames, seven proteins are encoded in the HBV DNA: the HBV surface antigen (HBsAg), which consists of three proteins of different length, large (L), middle (M), and small (S), HBV core protein (HBc) the subunit of the nucleocapsid, HBV e antigen (HBeAg) which is a proteolytically processed version of HBc with an additional N-Terminal peptide, a viral polymerase (Pol) that harbors a reverse transcriptase activity, and the HBV x protein (HBx) (Miller, Kaneko et al. 1989, Seeger and Mason 2015). Newly synthesized RNA can now, depending on the length, be used for the production of viral proteins or, in the case of the longest transcript, the pre-genomic and pre-core mRNA, it will get encapsidated NS reverse transcribed into rcDNA. Those nucleocapsids are now transported back to the nucleus for nuclear re-import to replenish the cccDNA pool or will be enveloped in multivesicular bodies and consecutively released from the cell together with subviral particles (SVPs), which mainly consists of HBsAg (Wei and Ploss 2021).

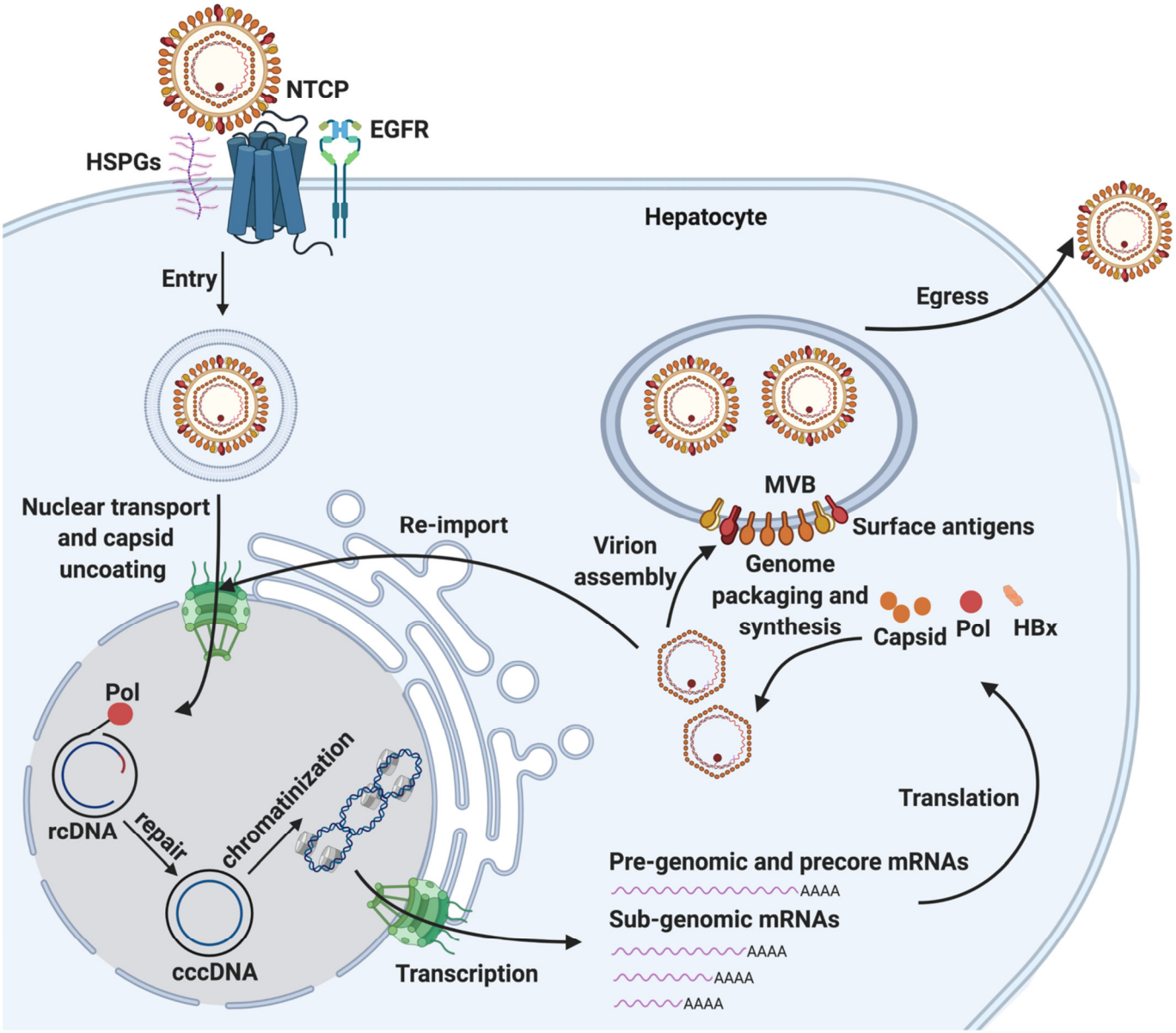

Figure 1 HBV life cycle HBV virions attach via unspecific binding to heparin sulfate proteoglycans (HSPGs) and EGFR on hepatocytes. HBV preS1 binds specifically to the sodium taurocholate co-transporting polypeptide (NTCP). Following endocytosis, nuclear transport, and capsid uncoating take place. Inside the nucleus, relaxed circular DNA (rcDNA) is repaired to form covalently closed circular DNA (cccDNA). After chromatinization, cccDNA serves as a template for pre-genomic and pre-core mRNAs and other sub-genomic mRNAs that encode for the different viral proteins. The binding of HBV polymerase to pre-genomic mRNA initiates nucleocapsid production and triggers the encapsidation and synthesis of rcDNA. Those nucleocapsids are either re-imported into the nucleus to maintain the cccDNA pool or can be enveloped in the multivesicular body (MVB) to form the mature virion. (Wei and Ploss 2021)

1.1.3. Diagnosis, Prophylaxis, and Therapy

Screening of HBV infection is performed by measuring HBsAg, HBcAg, and possibly HBV DNA from the serum. Usually, the presence of HBsAg indicates viral persistence or integration of virus DNA into hepatocytes. HBcAg indicates an immunological encounter with the virus. Screening should be performed on

people showing signs of hepatitis, with immunosuppression, and on people with underlying diseases that could worsen the outcome of a hepatitis B (Cornberg, Protzer et al. 2011). Furthermore, people with an increased risk of being infected should be tested, such as patients from a high prevalence area, sex workers, intravenous drug users or medical employees.

Prophylaxis, especially recommended for the subset of people mentioned beforehand, is carried out by prophylactic vaccination, using HBsAg, or the administration of Hepatitis B-specific immunoglobulins. For active immunization, it is recommended to maintain a neutralizing antibody titer to HBsAg (Anti-HBs) above 100 IU/mL (Cornberg, Protzer et al. 2011) to be protected from a potential infection.

Once an infection with HBV is confirmed (HBsAg positive and/or HBV DNA positive), further diagnostic should be performed to assess the extent of liver disease, which usually includes enzymes released upon liver damage, alanine aminotransferase (ALT), aspartate aminotransferase (AST), haemostasia parameters and albumin to assess the livers synthesis capacity. Additionally, co-infections with the hepatitis C virus (HCV), hepatitis D virus (HCV), and human immunodeficiency virus (HIV) should be excluded.

The course of infection is highly dependent on the age at which the person becomes infected: 90% of neonates and infants will become chronic HBV carriers, whereas only 5% of adults are unable to clear the initial infection (McMahon 2009). Symptoms of acute infection can range from mild symptoms or even absence of any to fulminant hepatitis with consequential liver failure. Viral persistence for more than three months is considered chronic hepatitis B (CHB). It can lead in 8-20% of patients to progressive liver disease and cirrhosis after five years, which is the leading cause of hepatocellular carcinoma (HCC) (Indolfi, Easterbrook et al. 2019). According to the European Association for the study of the Liver (EASL), chronic HBV infection can be divided into five phases, reflecting the dynamic interplay between the virus and the host´s immune response (European Association for the Study of the Liver. Electronic address 2017). Conventionally, levels of HBV markers determine these phases, i.e. HBsAg, HBeAg/antibodies to HBeAg (anti-HBe), and HBV DNA, together with signs of liver disease, e.g. ALT elevations or fibrosis European Association for the Study

of the Liver. Electronic address (2017). Although those phases are not necessarily sequential, an assessment can help with therapy decisions.

Phase 1: Previously termed as “immune tolerant,” now described as HBeAg-positive chronic HBV infection. The patients are HBeAg positive, have high levels of HBV DNA, and ALT is in the normal range, below the upper limit of normal, approximately 40 IU/L. Histologically characterized by the absence of necroinflammation or fibrosis, this phase is usually found early in infection and reflects an insufficient immune response against the virus; therefore, the rate of spontaneous HBeAg seroconversion is very low (Kennedy, Sandalova et al. 2012).

Phase 2: HBeAg-positive chronic hepatitis B, analogous to phase 1, is defined by HBeAg in the serum, high levels of HBV DNA, and elevated levels of ALT. Moderate to severe necroinflammation can be found in the liver, accompanied by progression of fibrosis. Due to the immunologically active nature of this phase, the outcome is variable: most patients will eventually clear HBeAg and achieve HBV DNA suppression, while progression into HBeAg-negative CHB can occur.

Phase 3: Previously “inactive carrier,” HBeAg-negative chronic HBV infection. These Patients present with anti-HBe, undetectable or low levels of HBV DNA, and normal ALT levels. Absence or low levels of necroinflammation and fibrosis can be found in the liver. In this phase, patients usually have a low risk of cirrhosis or HCC, but progression to CHB can occur.

Phase 4: HBeAg-negative chronic hepatitis B describes patients with undetectable levels of HBeAg in the presence of anti-HBe, moderate to high levels of HBV DNA, and fluctuating levels of ALT. In the liver, fibrosis and necroinflammation can be found. HBV variants with mutated core or pre-core regions can be found in most patients, leading to an impaired or abolished HBeAg expression.

Phase 5: The HBsAg-negative phase presents with an absence of HBsAg and antibodies to HBcAg (anti-HBc) in the serum; anti-HBs might be detected or absent, and ALT is within the normal range. HBV DNA in the serum is usually undetectable, whereas cccDNA in the liver is frequently detected. Thus, HBV reactivation during immunosuppression may occur in these patients. If the HBsAg

loss occurred prior to the development of cirrhosis, the risk of developing a progressive liver disease is minimal. If, on the other hand, cirrhosis is developed before HBsAg loss, those patients are still at risk for HCC and should be monitored accordingly.

Therapy for the infection with HBV differs between the acute and chronic settings. The main goal during acute infection is to lower the risk of liver failure, improve quality of life, and reduce the risk of chronicity. Due to the high rate of seroconversion in adults, the majority of patients do not need specific treatment. However, signs of acute liver failure, such as prolonged and severe jaundice or coagulopathy, should be treated with highly potent nucleos(t)ide analogues (NA) (Terrault, Lok et al. 2018).

Management of CHB aims at long-term suppression of HBV DNA levels and, consecutively, disease progression. Furthermore, treatment of extrahepatic manifestations, HBV reactivation, and prevention of mother-to-child transmission should be considered when evaluating antiviral therapy. In general, every patient might be eligible for therapy. However, due to side effects, chances of therapy success, and the risk of resistance development, the decision for therapy should follow the algorithm shown in Fig.2, according to the current German guidelines for the management of HBV infection. Therapy options typically involve either NA or pegylated interferonα (Peg-IFNα)(Lok, McMahon et al. 2016, Terrault, Lok et al. 2018).

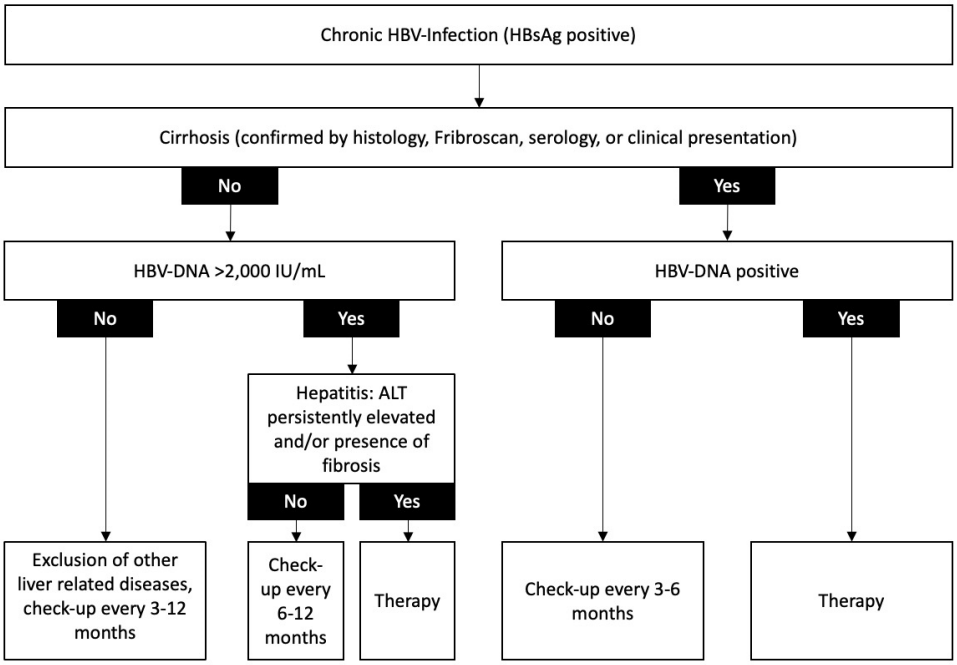

Figure 2 Decision tree for starting therapy in HBV carrier. Adapted from (Cornberg, Protzer et al. 2011)

The target of NAs is the reverse transcriptase domain of HBV polymerase. Incorporated into the enzyme, they will prevent the production of infectious particles, lower HBV DNA levels in the blood, prevent HBV reactivation, and prevent HBV transmission. Further divided into those with a low barrier to resistance, i.e. lamivudine, adefovir dipivoxil, and telbivudine, and those with a high barrier to resistance, i.e. entecavir, tenofovir disproxil fumarate, and tenofovir alafenamide (European Association for the Study of the Liver. Electronic address 2017). Albeit the production of infectious particles is discontinued, already infected hepatocytes will proceed to produce viral proteins. Persistent antigenemia, especially with pre-existing liver cirrhosis, leaves the patient at risk for the development of HCC (Lin and Kao 2023).

As an immune modulator, Peg-IFNα acts by stimulating the patient's immune system to clear the virus. The virus-infected hepatocyte may either be targeted directly by cytotoxic cells, clearing the virus through the killing of the host cell, or in a non-cytolytic way, e.g. IFN mediated pathways (Lucifora, Xia et al. 2014). Although Peg-IFNα treatment leads to a higher eradication rate of HBV compared to NA, due to their unfavorable safety profile and the variability of response, a lot of patients are not eligible for this kind of treatment.

1.1.4. Novel therapeutic approaches

HBsAg loss and absence of HBV DNA in the serum is termed a functional cure. Nevertheless, even after becoming undetectable for the virus in the serum, cccDNA is almost always still detectable in liver biopsies (Gan, Gao et al. 2023). Although integrated HBV DNA can only produce viral proteins and no infectious particles, cccDNA, on the other hand, is able to persist in hepatocytes, and their presence bears the risk of virus reactivation. Despite the good safety profile of the NA, they usually come with the drawback of a lifelong treatment duration. Thus, approaches for therapy in the future are supposed to solve those shortcomings. Drugs that are currently in clinical and pre-clinical evaluation can be divided according to their mechanism of action. Direct-acting antivirals are drugs that directly interfere with the virus by inhibiting parts of its lifecycle, e.g. virus entry inhibitors (Urban, Bartenschlager et al. 2014), capsid assembly inhibitors (Yuen, Gane et al. 2019), or target the cccDNA and their transcripts, e.g. using CRISPR/Cas9 (Kennedy, Kornepati and Cullen 2015), siRNA targeting all HBV transcripts (Michler, Kosinska et al. 2020). Another mechanism of action is the stimulation of the host´s immune system, e.g. Toll-like receptor (TLR) agonists (Zhang, Chai et al. 2019), checkpoint inhibitors (Gane 2017, Bunse, Kosinska et al. 2022), or therapeutic vaccination (Backes, Jager et al.).

1.1.5. Model systems to study HBV

The quality of data generated in pre-clinical studies of HBV infections is highly dependent on the model. It is necessary that the model resembles the real-life situation as closely as possible. The discovery of NTCP as one of the main functional receptors facilitating virus entry (Yan, Peng et al. 2014), allowed for the generation of cell lines supporting the entire life cycle of HBV (Ko, Chakraborty et al. 2018). Nevertheless, *in vivo* models are still scarce. Rodents, commonly used for *in-vivo* studies, are not susceptible to HBV infection, even when transgenic for human NTCP (Li, Wang et al. 2020). As woodchuck hepatitis virus and duck hepatitis B virus are closely related to HBV (Tennant and Gerin 2001, Yao, Chen et al. 2016), woodchucks and Peking ducks have been used as surrogate models. Unfortunately, disease pathogenesis and progression differ from the human counterpart, and therefore, a transfer of insights is not always possible (Mason 2015).

The first mice transgenic for HBV harbored a 1.3 overlength copy of the HBV genome which led to a high-level viral gene expression, preferentially in the liver and kidneys (Guidotti, Matzke et al. 1995). Since then, this model has helped to understand the major characteristics of HBV infection, but it has some shortcomings: the investigation of viral entry and its spread cannot be studied. Due to the integration of the viral genome, viral clearance is also not achievable. Furthermore, a lack of cccDNA restricts the applicability of this model to the natural course of infection.

Vector-based delivery of HBV genomes into mouse livers is a more convenient way of mimicking infection and inducing HBV replication. One of the earliest techniques was the hydrodynamic injection of HBV plasmids. Here, plasmids encoding the viral genome are injected intravenously (i.v.) in a high volume. High pressure caused by the rapid injection leads to the formation of defects in the hepatocyte membrane and facilitates the plasmid´s uptake. This will cause a transient replication and mimic an acute infection, but no cccDNA establishment will take place (Huang, Gäbel et al. 2012). A more recent advance was the construction of minicircles, a circular DNA mainly encoding for the gene of interest with only small fragments necessary for assembly. When injected, a cccDNA-dependent transcription can be established (Protzer 2017), but injection-derived liver damage still limits the applicability of this model (Yan, Zeng et al. 2017). As an alternative to the pressure-dependent uptake of the genomes, viral vectors can be used to promote a more targeted transduction. Adenoviral or adeno-associated viral (AAV) vectors can be used to induce, depending on the dose used, an acute or chronic infection. Although nuclear re-import is most likely not supported, “cccDNA-like” structures are established due to recombination of the AAV genome (Ko, Su et al. 2021), which is also reflected by stable antigenemia in the serum (Dion, Bourgine et al. 2013). Unlike other mouse models, with AAV-mediated HBV transduction of wild-type (wt) mice, there is no need for immunosuppression, allowing for the study of new therapeutic approaches and investigating viral clearance.

1.2. Immunometabolism

The term metabolism refers to the ongoing process of all cells converting nutrients into the building blocks necessary for cell survival while simultaneously

generating the energy needed to sustain the cell´s activities. Those metabolic pathways are highly influenced by intrinsic and extrinsic signals. Immunometabolism describes the specific metabolic prerequisites that are linked to immunological responses. Effector function often relies on the cell´s relocation to the site of the response. This relocation might come with differences in oxygen levels, availability of amino acids, glucose, and many more factors influencing the metabolic capacity (Braun 2021). Despite the high diversity of immunological outputs, growth and survival play a key role in all cells, and although the energy and precursor molecules needed are usually the same, different cells depend more on specific pathways than others. This is possible because of a complex interplay between all those pathways, and its knowledge is necessary to understand how nutrient deprivation can impact certain cell types.

1.2.1. Glycolysis

Glucose metabolism was one of the first big pathways shown to be important for T cells and activated macrophages (Alonso and Nungester 1956, Newsholme, Curi et al. 1986). When inhibited, using 2-deoxyglucose, a decreased activation of macrophages and inflammation was observed (Michl, Ohlbaum and Silverstein 1976, Hamilton, Vairo and Lingelbach 1986). Although not being very effective in generating ATP, only two molecules of ATP per molecule of glucose, its rapid induction of involved enzymes and synthesis of intermediates, which are important for other major pathways, make it a crucial element of immune cell metabolism. Furthermore, the reduction of NAD to NADH, which is an important cofactor for numerous enzymes, enables rapid biosynthesis and growth.

Once activated via lipopolysaccharides (LPS), enhanced glycolysis occurs in almost all effector T cells, most notably in T helper 17 cells (Shi, Wang et al. 2011), Th1 and Th2 cells (Michalek, Gerriets et al. 2011), and CD8+ T cells (Gubser, Bantug et al. 2013). Moreover, B cells (Doughty, Bleiman et al. 2006), natural killer (NK) cells (Donnelly, Loftus et al. 2014), macrophages, and DCs (Rodríguez-Prados, Través et al. 2010) increase glycolysis upon activation, which enables the production of cytokines, phagocytosis, and antigen presentation (Everts, Amiel et al. 2014). This increase in glycolysis can be induced via the activation of hypoxia-inducible factor 1α (HIF1α), known to induce several enzymes involved in glycolysis (Tannahill, Curtis et al. 2013), or via

inhibition of kinases, e.g. TANK-binding kinase 1 or NF-κB kinase and hexokinase 2, independent of HIF1α (Huynh, DuPage et al. 2015). Pyruvate kinase isoenzyme M2 (PKM2), is a key enzyme responsible for the diversion of glycolytic intermediates as it generates pyruvate and ATP from phosphoenolpyruvate. PKM2 is induced by LPS (Palsson-McDermott, Curtis et al. 2015) and is able to translocate to the nucleus, where it promotes the expression of HIF1α-regulated genes (Luo, Hu et al. 2011), including pro-inflammatory factors such as IL-1β. Inhibition of PKM2 can change macrophages from an M1 phenotype, which is pro-inflammatory, into a more M2-like phenotype, therefore being a more pro-reparatory (Palsson-McDermott, Curtis et al. 2015). A similar effect can be observed when glycolysis is inhibited in Th17 cells, the pro-inflammatory phenotype shifts into a regulatory T cell (Treg) cell phenotype (Shi, Wang et al. 2011). Although Treg cells can utilize glycolysis, together with HIF1α, glycolysis is associated with an inflammatory phenotype. This link is further emphasized by the fact that the glycolytic enzyme glyceraldehyde 3-phosphate dehydrogenase (GAPDH) binds to mRNA encoding for interferon-γ (IFNγ) in TH1 cells, and therefore inhibiting translation (Mukhopadhyay, Jia et al. 2009, Chang, Curtis et al. 2013). Upon glycolysis, the mRNA is released, and IFNγ is produced, a crucial step for Th1 cells as IFNγ is one of the main effector cytokines.

1.2.2. Tricarboxylic acid (TCA) cycle

Despite the fact that most effector T cells tend to shift toward glycolysis, the tricarboxylic (TCA) cycle is possible in most T cell subsets (Michalek, Gerriets et al. 2011). The concept for the different roles of the TCA can be observed when looking at M1 and M2 macrophages. M2 macrophages utilize the whole range of the TCA cycle, and the production of intermediates is tightly linked to oxidative phosphorylation, which is especially important for the production of the mannose receptor (Jha, Huang et al. 2015). M1 macrophages, on the other hand, only use the TCA cycle up to a certain point. In their case, the TCA cycle helps to accumulate citrate and succinate (Tannahill, Curtis et al. 2013, Jha, Huang et al. 2015). Citrate will be exported from the mitochondria and used to produce fatty acids, which are highly required for membrane biogenesis. A similar effect is observable in activated DCs to support membrane production needed for antigen

presentation (Everts, Amiel et al. 2014). Furthermore, citrate is utilized in the generation of nitric oxide and prostaglandins (Infantino, Convertini et al. 2011), two important molecules for macrophage function. Accumulating succinate can inhibit prolyl hydroxylase, which in turn stabilizes HIF1α and the production of IL-1β (Tannahill, Curtis et al. 2013). Since this pathway is functional under normoxia, HIF1α activation is not limited to hypoxia but can play a role under aerobic conditions as well.

1.2.3. Pentose phosphate pathway

The pentose phosphate pathway is required for two important functions, the production of nucleotides for cell proliferation and to recycle NADP+ to generate NADPH. As a reducing agent, NADPH is used to generate reactive oxygen species (ROS) during the respiratory burst and, on the other hand, the generation of glutathione and other antioxidants. Both are necessary for macrophages and neutrophils during infection. NADPH is also used for lipid synthesis, and DCs rely on it to regenerate the endoplasmatic reticulum during cytokine secretion (Everts, Amiel et al. 2014). Upon LPS stimulation, the pentose phosphate pathway is highly upregulated in macrophages. Interestingly, the enzyme that limits the substrates for the pathway, the carbohydrate kinase-like protein, is also highly upregulated in M2 macrophages (Haschemi, Kosma et al. 2012). If the enzyme is suppressed, the macrophage will become M1-like, emphasizing the importance of the pathway for the inflammatory phenotype (Tannahill, Curtis et al. 2013).

1.2.4. Fatty acid oxidation

Adaptive and innate immune responses can be orchestrated by fatty acid oxidation. In contrast to inflammatory and rapidly proliferating immune cells, which highly depend on aerobic glycolysis, non-inflammatory cells, such as M2 macrophages or Treg cells, exhibit high levels of fatty acid oxidation. An accumulation and/or the failure to properly incorporate fatty acid into this pathway, for example, happening in macrophages involved in the generation of atherosclerotic lesions, leading to the development of foam cells (Carpenter, van der Veen et al. 1995, Shoelson, Lee and Goldfine 2006), can modulate inflammatory responses. It was shown that accumulated unsaturated fatty acids in foam cells can increase the production of IL-1α and consequentially increase inflammation (Freigang, Ampenberger et al. 2013). Overexpression of

transporters for long-chain fatty acids into mitochondria, thereby increasing fatty acid oxidation, can alleviate the inflammation (Malandrino, Fucho et al. 2015).

A similar effect can be observed in the regulation of T cell responses: not only is fatty acid oxidation increased in Treg cells compared to effector T cells, such as Th1, TH2, and Th17 cells, but it also inhibits the polarization of T cells into the latter (Michalek, Gerriets et al. 2011). This is consistent with a downregulation in effector T cells during activation, as well as in their gene expression patterns for fatty acid oxidation (Gerriets, Kishton et al. 2015). Interestingly, ligation of inhibitory receptors such as programmed death 1 (PD-1) receptors on T cells can reconstitute fatty acid oxidation and, therefore, promote tolerance (Patsoukis, Bardhan et al. 2015). Another example is the generation and maintenance of memory T cells, which only proliferate very slowly and require fatty acid oxidation for cell survival (van der Windt, Everts et al. 2012). Even much so, that complete *de novo* synthesis of fatty acids and subsequent oxidation in a cell-intrinsic cycle was observed (O'Sullivan, van der Windt et al. 2014).

1.2.5. Fatty acid synthesis

As aforementioned, fatty acid synthesis is required for inflammatory immune responses, especially for cells in need of rapid biosynthesis. Upon Toll-like receptor (TLR) stimulation, fatty acid synthesis is upregulated in DCs; this is required for efficient activation of CD8+ T cells (Everts, Amiel et al. 2014). In turn, the deletion of the rate-limiting enzyme in fatty acid synthesis resulted in diminished efficacy and numbers of CD8+T cells upon antigen stimulation (Lee, Walsh et al. 2014). Sphingolipids, a sphingoid backbone N-acetylated with different fatty acids, are highly involved in the modulation of immune responses. They have been shown to be an important part of cell signaling, regulating cell growth and survival, immune cell trafficking, and the emergence of cancer (Hannun and Obeid 2008, Spiegel and Milstien 2011).

1.2.6. Amino acid metabolism

The availability and metabolism of amino acids can have a big impact on immune responses. As a central coordinator of metabolic demand and immunity, the mechanistic target of rapamycin complex 1 (mTORC1) can sense amino acid and growth factors, promote mRNA translation, and influence lipid synthesis for cell growth. Furthermore, it is involved in signaling involved in T cell and monocyte

differentiation (Weichhart, Hengstschläger and Linke 2015, Van de Velde, Subramanian et al. 2017).

Noticeably, sensing amino acid starvation is dependent on multiple factors, resulting in the suppression of global protein synthesis. Upon starvation, an accumulation of uncharged tRNAs is sensed by the General Control Non-derepressible-2 (GCN2), a serine/threonine kinase, which in turn will be auto-phosphorylated and furthermore phosphorylate the eukaryotic translation initiation factor 2 subunit 1 (eIF2α) (Dong, Qiu et al. 2000). This leads not only to reduced global protein synthesis but also to the induction of proteins further regulating amino acid homeostasis. Activating Transcription Factor 4 (ATF4) is one of the proteins induced and initiates the expression of genes for amino acid synthesis, amino acid transporters, and amino acid metabolism (Harding, Zhang et al. 2003, Kilberg, Shan and Su 2009). Additionally, REDD1 and Sestrin2, proteins involved in inhibiting amino acid utilization (Budanov and Karin 2008, Dennis, McGhee et al. 2013), are induced and both are then inhibiting mTORC1-mediated protein expression (Xu, Dai et al. 2020).

Amino acid abundance can influence immune response in a multitude of ways, but the influences of arginine, glutamine, and tryptophan are some of the most prominent and well-studied. Arginine plays an important role in the innate and adaptive immune response. In macrophages, arginine is required for the synthesis of nitric oxide and the arginase pathway (Rath, Müller et al. 2014). Inflammatory M1 macrophages convert arginine via citrulline into nitric oxide, mediated by the inducible nitric oxide synthase (iNOS) (MacMicking, Xie and Nathan 1997). iNOS-deficient mice show an alleviated phenotype for LPS-induced septic shock, concurring the involvement in an inflammatory immune response (MacMicking, Nathan et al. 1995). Contrary to that, if arginine is metabolized through the arginase pathway, a more tolerant phenotype is observable. Not only do macrophages develop into a phenotype associated with wound healing, but they will also limit effector T cell immune responses (Pesce, Ramalingam et al. 2009). However, a direct interaction between arginine and T cell receptor expression together with T cell proliferation has also been observed (Rodriguez, Zea et al. 2002, Rodriguez, Quiceno and Ochoa 2007). Furthermore,

in vitro depletion of arginine can lead to abrogated mTORC1 activity in T cells (Cobbold, Adams et al. 2009).

Mechanistically distinct immunosuppression can be specifically found in glutamine-deprived environments. In vitro experiments showed that IL-1 production of LPS-stimulated macrophages relies on the presence of glutamine (Wallace and Keast 1992). Not only can macrophages use glutamine to generate nitric oxide through the arginine synthesis (Murphy and Newsholme 1998), but it can also be fed into the TCA cycle, where substrates for the hexosamine pathway are produced, promoting an M2 phenotype upon IL-4 stimulation. Interestingly, glutamine is not required for an LPS-induced M1 polarization (Jha, Huang et al. 2015). Furthermore, the adaptive immune response also depends on glutamine. Upon activation, glutamine usage increases and is required for antigen receptor stimulation (Crawford and Cohen 1985, Carr, Kelman et al. 2010). Although glutamine metabolism seems to be essential for the generation and function of Th1 and Th17 cells, the generation of Tregs is not altered when the respective uptake transporter is knocked out (Nakaya, Xiao et al. 2014). Analogous to the in vitro depletion of arginine, glutamine deprivation has a comparable effect on the mTORC1 activity (Nakaya, Xiao et al. 2014).

Lastly, tryptophan has been identified to be involved in numerous immunoregulatory events. As an essential amino acid, cells depend on external supplementation and deprivation is an antimicrobial defense mechanism (Pfefferkorn 1984, Schroten, Spors et al. 2001). Tryptophan catabolism is mainly regulated by the key enzyme indoleamine-2,3-dioxygenase (IDO), induced by LPS exposure or as a response to IFNγ (Yoshida and Hayaishi 1978). In T cells, tryptophan is required for proliferation and activation, both diminished when IDO was overexpressed in antigen-presenting cells, depleting tryptophan (Munn, Shafizadeh et al. 1999, Lee, Park et al. 2002). The overexpression of IDO to inhibit T cell responses is exploited by some cancer types (Uyttenhove, Pilotte et al. 2003, Okamoto, Nikaido et al. 2005) and might play a role in other disease pathogenesis as well.

1.3. Aim of the study

Treatment of CHB continues to be challenging due to viral persistence mediated by cccDNA. Immunotherapies are an elegant way of inducing the host's immune response to fully eradicate the virus. This thesis aims to understand the prerequisites, mechanisms, and effects of potential immunomodulatory therapies against HBV.

The first part of this thesis investigated the effects of arginine depletion and nutrient restriction in *in vitro* models for HBV infection. RNA sequencing, in combination with unbiased metabolomics analysis of HBV-infected cells, was performed to understand cellular changes that occur during viral infection. Furthermore, cytotoxicity assays were performed to understand the functional implications of those changes.

The second part of this work focused on *in vivo* models for HBV infection. GCN2 knockout mice were used to elucidate the influence of the GCN2 signaling pathway on HBV infection. Lastly, combinatory approaches to treating chronic hepatitis B were investigated. Treatments to optimize the microenvironment of the liver for optimal efficacy of a therapeutic vaccination were tested in AAV-HBV-infected mice.

2. Results

By the Thesis aims, this first part investigated the effects of amino acid deprivation on in vitro models for the study of HBV. In particular, the functionality of T cells directed against HBV-infected cells was investigated.

2.1. Immunometabolism in vitro

In many instances of T cell activation, amino acid-dependent immunosuppression was observed and determined as a significant factor for efficient effector function (Brunner, Vulliard et al. 2020). Of particular interest for the HBV setting is Arginine. It has been described that patients suffering from CHB exhibit lower serum arginine levels when compared to healthy controls (Pallett, Gill et al. 2015). Thus, nutrient restriction, including deprivation of arginine, was investigated in *in vitro* models for novel therapy approaches against CHB.

2.1.1. Cytotoxic T cells depend on Arginine.

A T-cell cytotoxicity assay was established to investigate the effects of amino acid deprivation on cytotoxic T cells. Hepatoma cells with a stable expression of HBV proteins (HepG2.2.15) or the parental cell line as control cells (HepG2) were seeded into a 96-well plate. These cells were kept in standard or specific amino acid-deprived cell culture media for 72h. Then, T cells expressing HBV-specific TCRs, i.e. specific for core (6K) and specific for S (4G) (Wisskirchen, Kah et al. 2019), or a non-specific TCR (Mock), were added to the culture. Upon addition of the T cells, cell viability was measured in real-time using an impedance-based measurement on the bottom of the well (Fig 3 A-C). After 72h, the supernatant was collected, and IFNγ concentration was measured by ELISA (Fig. 3 D-F).

As expected, no cytotoxic effect was observed on Hepatoma cells cultured with non-specific TCR-transduced T cells (Fig. 3A). Furthermore, no T cell killing was observed in cultures using the control hepatoma cells (grey lines). In cultures containing HBV-expressing hepatoma cells and HBV-specific T cells, a cytotoxic effect was measurable, starting 2-4h after adding the T cells. T cells transduced with the 4G receptor (Fig. 3B) showed a faster killing of the target cells compared with the 6K receptor (Fig.3C). Interestingly, in cultures deprived of a single amino

acid (blue line: arginine-deprived, yellow line: lysine-deprived) a delayed cytotoxicity was observed compared to cultures with standard media (black line). Furthermore, when the medium was deprived of both amino acids (green line), target cells were again more susceptible to T cell killing, and the effect was similar to that of normal cell culture media. IFNγ concentration in the supernatant correlated with the observed cytotoxic effect. Only supernatants from matching combinations of HBV-producing target cells and HBV-specific T cells contained high amounts of IFNγ when cultured in standard media. Supernatants deprived from arginine, lysine, or both contained reduced amounts of IFNγ.

In summary, this data shows that in this in vitro model, the presence of arginine and lysine in the cell culture medium is indispensable for efficient T cell cytotoxicity and IFNγ release.

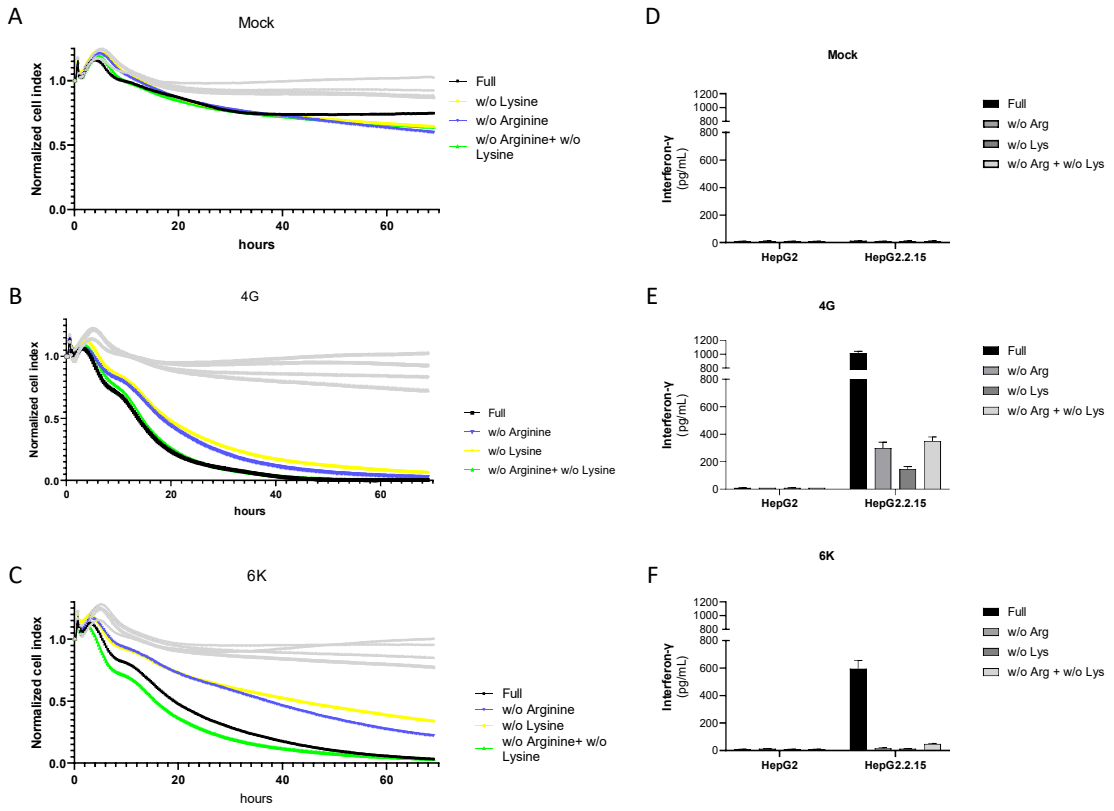

Figure 3 Cytotoxicity in the Presence and Absence of Arginine. T cells were retrovirally transduced with either HBV-specific TCRs (4G+6K) or an unrelated TCR (Mock) and incubated with cells transgenic for HBV. For cultivation, either a completely supplemented medium (Full), arginine deprived (w/o Arginine), lysine deprived (w/o Lysine), or arginine and lysine deprived (w/o Arginine+ w/o Lysine) was used. (A-C) Cell viability was measured in real time using an impedance base method to detect cell detachment. (D-F) Interferon was measured from the supernatant using ELISA. Data is represented as mean ± SD and 8 independent biological replicates per group are shown.

2.1.2. Arginine threshold for efficient activation

To further investigate arginine dependency for T cell activation, T cells transduced with HBV-specific TCRs, 4G and 6K, a non-specific TCR, and peripheral blood mononuclear cells (PBMC) were stimulated using paramagnetic polymer particles (Dynabeads). The cells were stimulated via CD3/CD28 in media containing various amounts of arginine, ranging from 287 µM to 0.29 µM, and completely arginine deprived. After 72 h, IFNγ and TNF concentration in the supernatant was measured by ELISA (Fig 4.), and T cells were analyzed using flow cytometry (Fig.5).

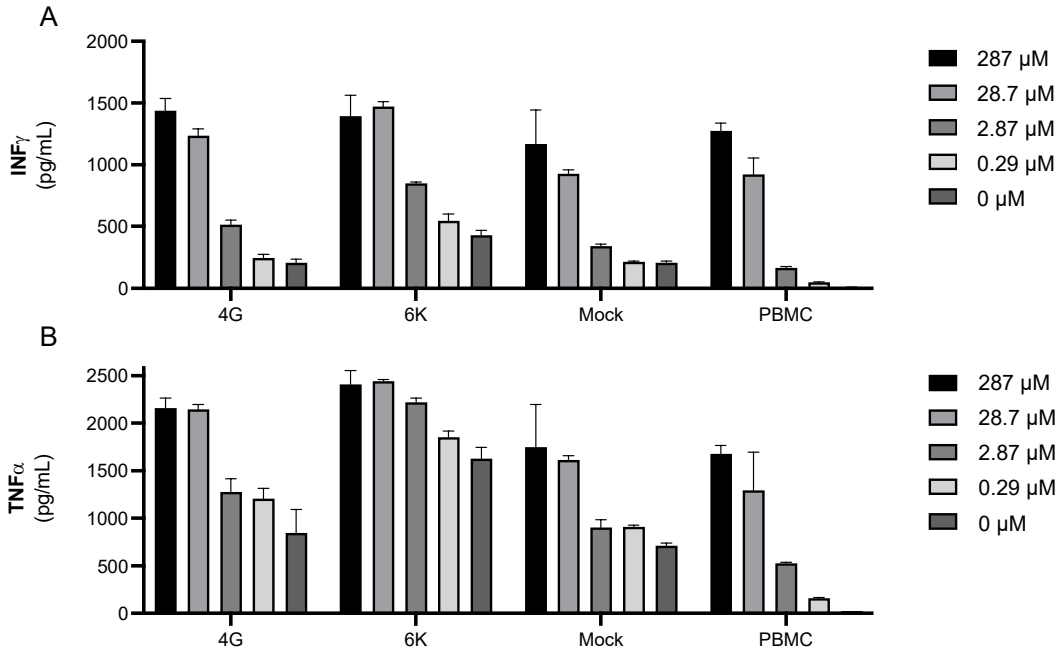

Figure 4 Cytokine Expression in the Presence and Absence of Arginine. T cells were isolated and retrovirally transduced with HBV-specific TCRs (4G+6K) or an unrelated TCR (Mock). Together with T cells directly isolated from peripheral mononuclear blood cells (PBMC), the cells activated using αCD3/αCD28-beads in the presence of different concentrations of Arginine. After three days, INF and TNF were measured by ELISA from the supernatant. Data is represented as mean ± SD and 6 independent biological replicates per group are shown.

T cells stimulated in normal or near-normal amounts of arginine, i.e. 287 to 28.7 µM, showed a high production of IFNγ and TNF (Fig 4 A-B). While TNF production was only reduced when cultured in lower amounts of arginine, it remained at a high level, whereas IFNγ production was almost undetectable. This effect was especially apparent on PBMC and less pronounced in cells that were TCR transduced. A possible confounder responsible for that effect could be the pre-stimulation that is necessary for TCR transduction.

In accordance with the cytokine expression, cell proliferation was similarly tied to the presence of arginine. T cells were stained using cell trace violet to assess the proliferation capacity. Additionally, surface staining for CD4, CD8, and PD1 was performed, and the cells were then analyzed using flow cytometry. For T cells retrovirally transduced with a TCR, at least 28.7 µM arginine was needed for efficient proliferation (Fig. 5 A-B). Interestingly, due to previous stimulation and ex vivo proliferation, almost all cells in their respective group demonstrated similar levels of proliferation, visible by showing only one peak in the cell trace violet analysis. PBMC, on the other hand, showed a more diverse proliferation profile, but similar to the TCR-grafted T cells, at least 28.7 µM arginine was needed for proliferation. Throughout all groups, 2.87 µM of arginine was insufficient and resulted in a singular peak in the analysis, indicating no proliferation had occurred. All these observations were equally true for $CD8^+$ and $CD4^+$ T cells. PD1 expression, usually a marker for T cell activation, a sign of T cell exhaustion, or in this case also just an indicator of global protein expression, was also dependent on the arginine concentration. When comparing the mean fluorescence intensity (MFI), PD1 expression was generally higher in transduced cells than in PBMCs. Similar to proliferation and cytokine expression, approximately 28.7 µM was the threshold for efficient upregulation of PD1. Notably, for the TCR-transduced T cells a background expression of PD1 was noticeable in all groups, even in the absence of arginine.

Taken together, this indicates arginine deprivation can inhibit essential T cell functions, i.e. cytokine production, proliferation, and upregulation of regulatory receptors, and the threshold arginine concentration in this *in vitro* setting was 28.7 µM.

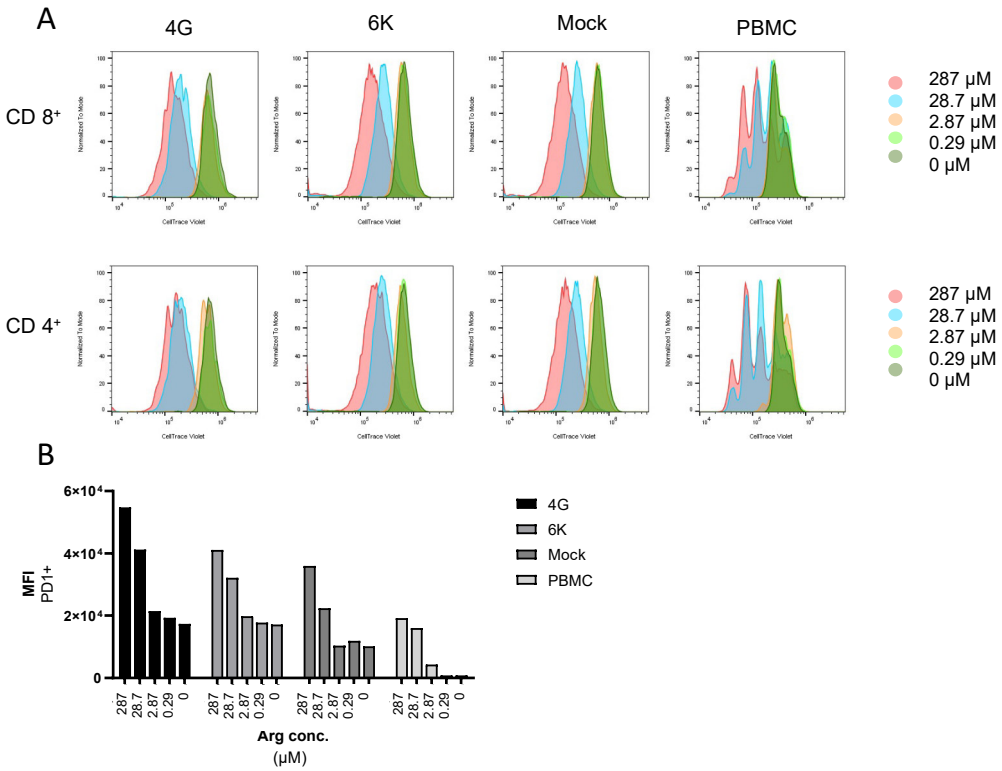

Figure 5 T-cell Activation in Different Arginine Concentrations. T cells were isolated and retrovirally transduced with HBV-specific TCRs (4G+6K) or an unrelated TCR (Mock). Together with T cells directly isolated from peripheral mononuclear blood cells (PBMCs), all cells were then stained using CellTrace violet and activated using αCD3/αCD28-beads in the presence of different concentrations of Arginine. After three days, surface staining was performed, and proliferation (A) and PD1 expression were measured using flow cytometry. Data represents the mean of biological triplicates.

2.1.3. Arginine in HBV infection

To further assess a possible deprivation of arginine from the liver by HBV and investigate the implications of such amino acid depletion on virus replication and viral protein expression, a hepatoma cell-based infection model was used. HepG2-NTCP cells were infected using a high-titer virus stock and cultivated for 10 days in normal medium (HBV), medium deprived of arginine (w/o arg), or Medium that was deprived but then reconstituted with arginine (w/ arg). The supernatant was analyzed every three days, starting on day four, for viral antigen production (Fig 6A), arginine concentration (Fig. 6C-E), and glucose concentration (Fig. 6F+G). Additionally, on day 10, pgRNA was measured from cell lysate.

In all HBV-infected cells, HBeAg expression continuously increased till day 10, while mock-infected cells remained negative (Fig. 6A). This increase was similar in cells cultivated in a standard medium and in a medium where arginine was reconstituted, whereas cells kept in arginine-deprived medium showed a slower and overall lower increase in antigen production. Interestingly, pgRNA, the surrogate marker for viral replication, was higher in cells kept in an arginine-free medium compared to a standard or reconstituted media (Fig.6B).

To check whether HBV infection is depleting arginine from the supernatant, arginine concentration was measured from cells infected with HBV and mock-infected cells (Fig. 6C). On all time points measured, both groups had the same arginine concentration in the supernatant. To assess whether this is also true when the arginine concentration is low at the beginning of cultivation, HBV-infected (Fig. 6D) and mock-infected (Fig. 6E) cells were kept in media containing high (/w arg) and low (w/o arg) amounts of arginine. When compared to the input media, no difference in arginine concentration was observed.

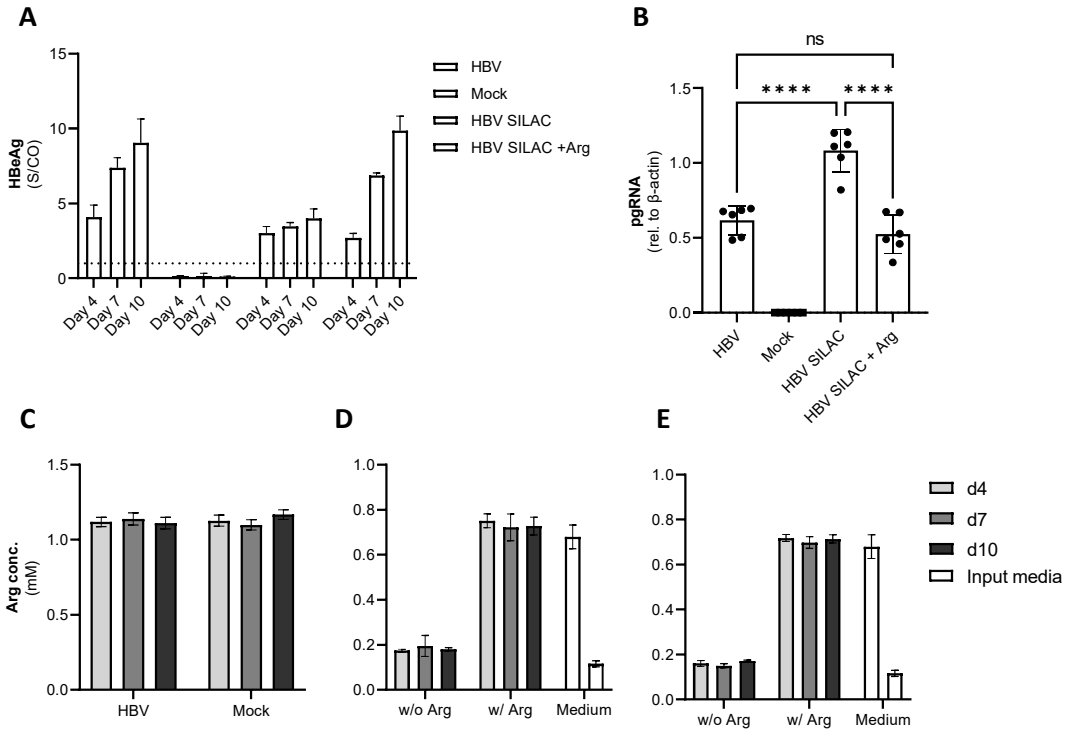

Figure 6 Arginine Concentration in HBV Infection. HepG2-NTCP cells were infected with HBV. For culturing, either normal cell culture Medium (HBV and Mock), Medium deprived of Arginine (Arg) (HBV SILAC), or Medium deprived of Arg and then reconstituted with Arg (HBV SILAC+Arg) was used. (A) HBeAg Elisa was performed from the Supernatant collected at the indicated time points. (B) RT-qPCR for HBV pregenomic RNA (pgRNA) was performed from cell lysate at d10. (C) Arg concentration was measured at different time points from supernatant derived from cells either infected or non-infected with HBV. (D+E) Cells were either infected with HBV (D) or not infected (E) and cultured either in medium containing Arg (w/Arg) or medium deprived of Arg (w/o Arg). Additionally, input Medium was also measured after incubation without cells (Medium). Data is represented as mean ± SD and 6 independent biological replicates per group are shown. Statistical analysis: Student's unpaired t-test with Welch's correction (ns: not significant, ****: p <0.0001)

Taken together, these results show that although arginine concentration in the serum affects viral protein expression and replication, no change in arginine abundance is seen after HBV infection *in vitro*.

2.1.4. Nutrient restriction in HBV infection

One shortcoming of *in vitro* models for metabolic studies is the restrictions of necessary supplements that need to be provided for cell culture. Cell culture Media usually contains a manifold amount of nutrients to ensure the viability of the cells. Nutrient deprivation might not become apparent unless those resources are limited. Therefore, HBV-infected HepG2 cells were cultured in various amounts of cell culture media, ranging from 600 μL to 300 μL, to limit possible ways of compensation. Viral antigens were measured from the supernatant continuously (Fig 7A+B), and at indicated time points, pgRNA was measured

(Fig.7C). From day 10 onwards, all cells were kept in the same standardized amounts of media, i.e. 500 μL, to study the homeostasis of any effects observed.

Normalized expression of HBsAg and HBeAg, as shown in Fig 7A+B, showed a disproportional increase in antigens in the supernatant to what would have been expected due to sheer lower dilution volume. Especially supernatant derived from cells kept in 300 μL, represented by the black bar, had an up to 8-fold increase of HBsAg and up to 6-fold increase of HBeAg compared to supernatant derived from cells kept in 600 μL. Upon cultivation in standardized volume, viral protein concentration remained over 2-fold higher in groups previously kept in lower volumes as compared to those kept in high amounts of media. A trend to higher amounts of pgRNA in cells cultured in 300 μL relative to cells cultured in 600 μL, was observed (Fig 6C).

To summarize, HBV-infected cells cultured in lower amounts of cell culture medium produce a higher amount of viral proteins compared to cells cultured in regular amounts of medium. This is accompanied by a trend of higher amounts of viral pgRNA.

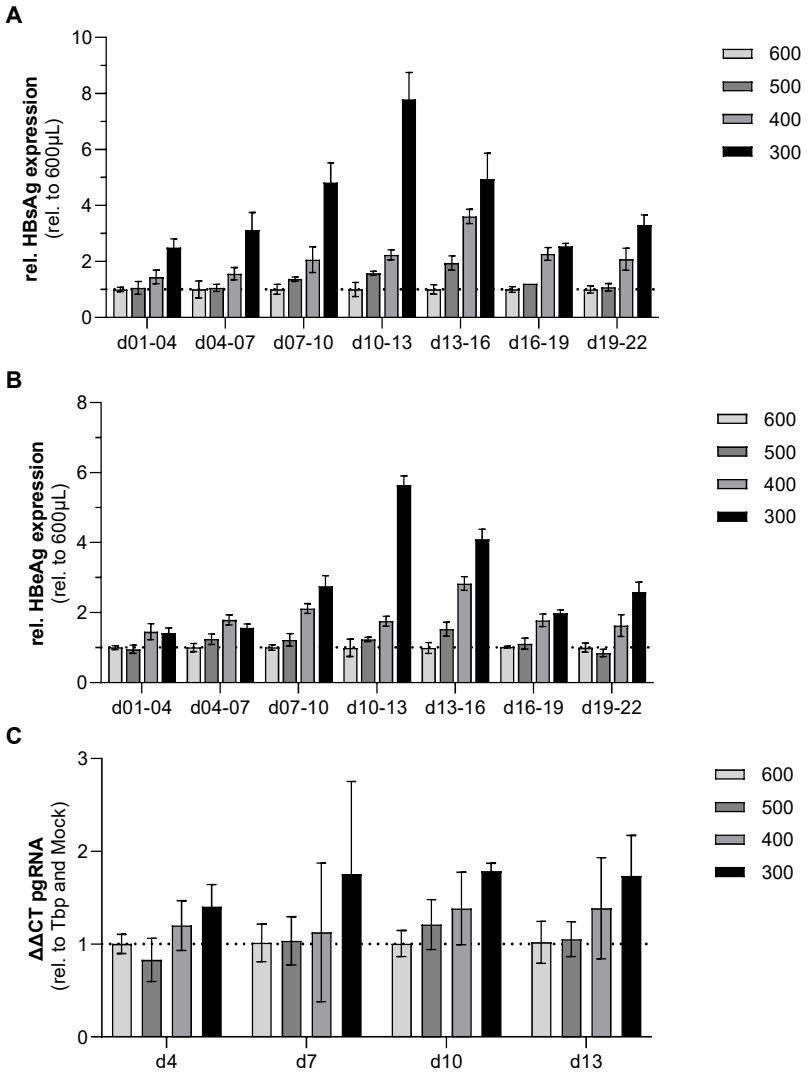

Figure 7 HBV Infection in Different Amounts of Medium. HepG2-NTCP cells were pre-differentiated and infected with HBV. After 24h the cells were washed and cultured in different amounts of cell culture medium, ranging from 300 µL to 600 µL. Supernatant was exchanged every 3 days and HBsAg (A) and HBeAg. (B) were measured. Starting at day 10 post-infection, all cells were kept at 500 µL of medium. (C) At indicated time points HBV pregenomic RNA (pgRNA) was measured using RT-qPCR. Data is represented as mean ± SD and 8 independent biological replicates per group are shown.

2.1.5. Metabolomics of HBV-infected cells

To further investigate the effects of HBV infection on the metabolic signature of cells, mass spectrometry was used to identify the abundance of a range of metabolites in a targeted fashion. A total of 180 metabolites were screened and quantified in non-infected and infected hepatoma cells.

First, changes in the concentration of amino acids, sphingolipids, acylcarnitines, biogenic amines, and glycerophospholipids were compared in hepatoma cells depending on their HBV infection status (Fig. 8). A trend to higher levels of amino acids in non-infected cells could be observed, but this effect was limited to a

specific group but rather applied to all classes of amino acids (Fig. 8A). Interestingly, glycerophospholipids and sphingolipids concentrations were higher in HBV-infected cells. Again, not a specific type of those lipids was accumulated, but rather, a general increase was visible (Fig. 8B+E). For biogenic amines and acylcarnitines, no relevant differences could be observed (Fig.8 C+D).

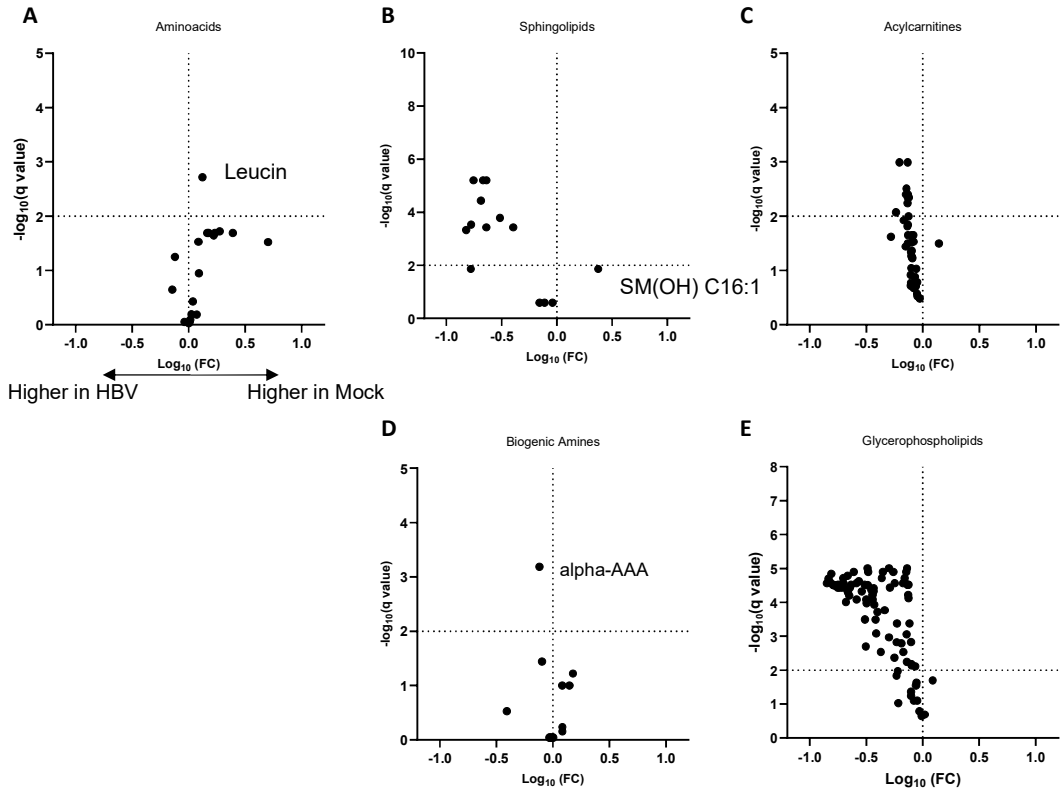

Figure 8 Metabolomics of HepG2-NTCP Cells in HBV Infection. HepG2-NTCP cells were infected or mock-infected and analyzed using targeted metabolomics for (A) amino acids, (B) sphingolipids, (C) acylcarnitines, (D) biogenic amines, and (E) glycerophospholipids. Data shown are 6 independent biological replicates per group.

To further increase sensitivity for HBV-induced metabolic changes, a similar experimental setup as described in 2.1.4. was used; HBV-infected cells were kept under low-medium conditions to limit nutrient availability. Again, slightly higher amino acid levels in non-infect cells (Fig. 9A) and an increase in sphingolipids and glycerophospholipids upon HBV infection could be observed (Fig. 9B+E). Similar to normal culture conditions, the level of biogenic amines and acylcarnitine did not change upon viral infection (Fig. 9C+D).

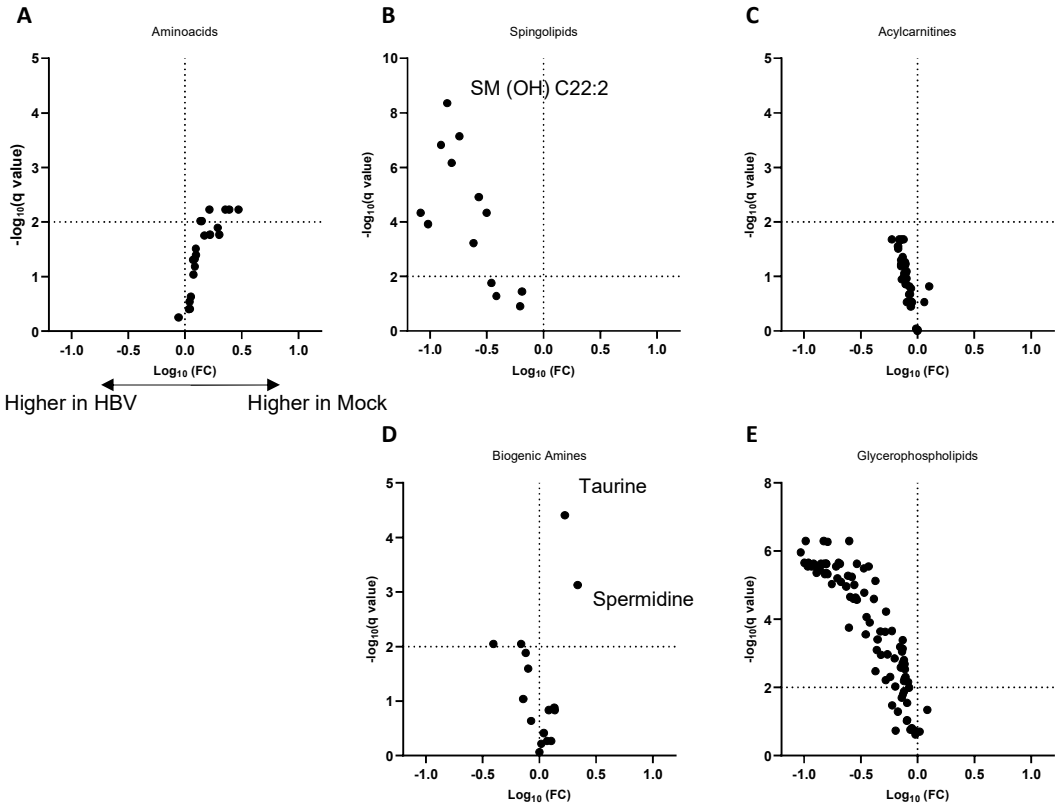

Figure 9 Metabolomics of HepG2-NTCP Cells in HBV Infection under low medium conditions. HepG2-NTCP cells were HBV-infected or mock-infected and kept under low-medium conditions. After 10 days, the cells were analyzed using targeted metabolomics for (A) amino acids, (B) sphingolipids, (C) acylcarnitines, (D) biogenic amines, and (E) glycerophospholipids. Data shown are 6 independent biological replicates per group.

To exclude effects that only confide in different amounts of the medium used, we repeated the measurement in non-infected cells cultured in both medium conditions (Fig. 10). Interestingly, the differences previously observed for sphingolipids and glycerophospholipids were not visible when non-infected cells were compared (Fig. 10 B+E). Differences observed in amino acids were again not limited to a specific group and did not correlate with the previous measurements (Fig. 10A). When looking at acylcarnitines and biogenic amines, carnitine and spermidine showed higher concentrations in cells cultured in higher amounts of medium (Fig. 10 C+D).

Taken together, this data shows that HBV-induced metabolic changes predominantly affect sphingolipids, glycerophospholipids, as well as some amino acids. These changes are even more pronounced under conditions with limited nutrient supply, e.g. reduced amount of cell culture medium.

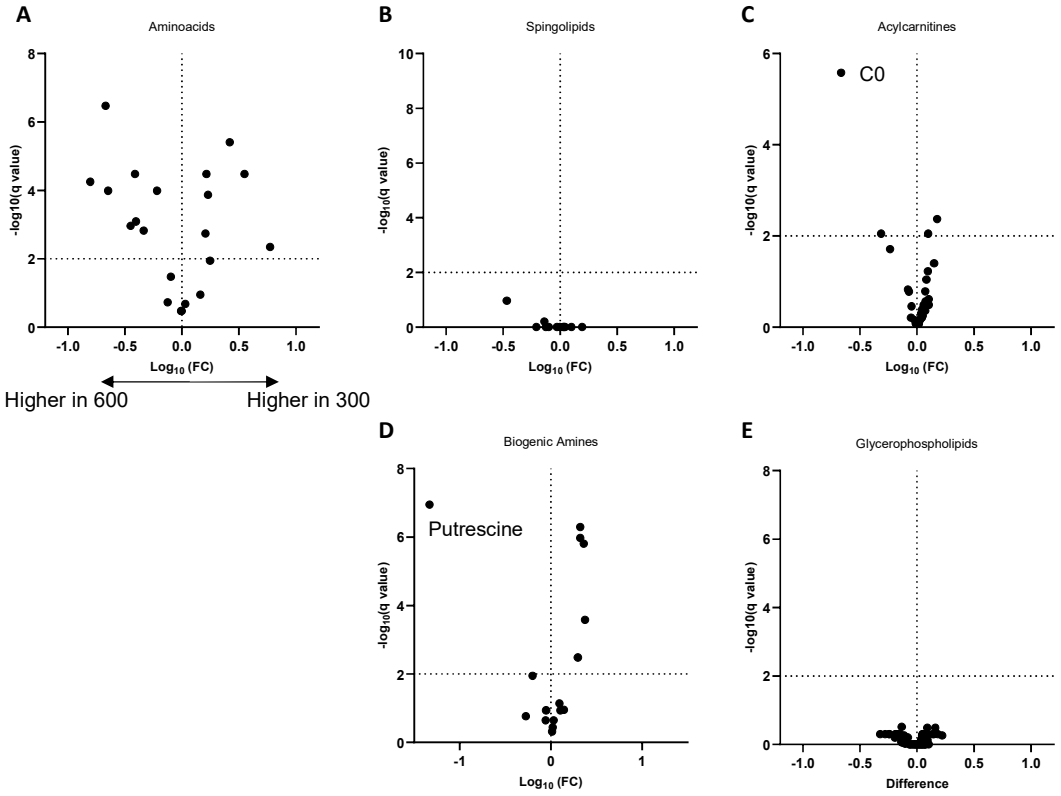

Figure 10 Metabolomics of HepG2-NTCP Cells in low and high medium Conditions. HepG2-NTCP cells were kept under low or high medium conditions. After 10 days, the cells were analyzed using targeted metabolomics for (A) amino acids, (B) sphingolipids, (C) acylcarnitines, (D) biogenic amines, and (E) glycerophospholipids. Data shown are 6 independent biological replicates per group.

2.1.6. RNAseq of HBV-infected cells

To identify the underlying pathways involved in these metabolic changes, gene expression in cells subjected to the same experimental setup was analyzed using RNA sequencing.

Figure 11 shows a volcano plot of differentially expressed genes in cells either infected with HBV or left not infected. Those cells were cultured for ten days under low-medium conditions, RNA was isolated, mRNA was reverse transcribed and bulk sequencing was performed.

Analogous to the metabolomics analysis, different experimental setups were used to only study the effect of different amounts of Medium on non-infected cells (Fig. 12) and low vs high amounts of media used for culturing HBV-infected cells (Fig. 13).

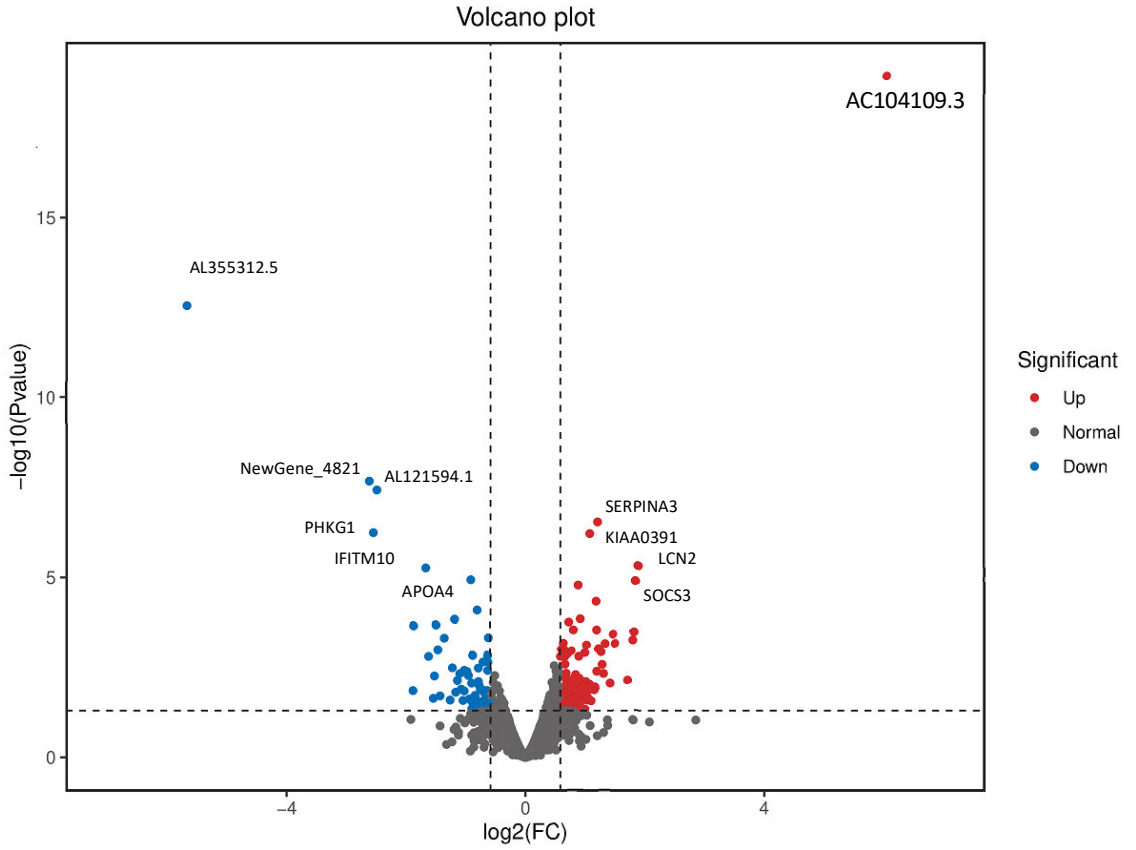

Figure 11 Volcano Plot of Differentially Expressed Genes in HBV-Infected or Non-Infected HepG2-NTCP Cells. HepG2-NTCP cells were either infected with HBV or left non-infected and maintained in low amounts of media for 10 days. RNA sequencing was performed, and differential gene expression analysis was conducted. Blue dots denote down-regulated gene expression, and red dots denote up-regulated gene expression. Data shown are 6 independent biological replicates per group.

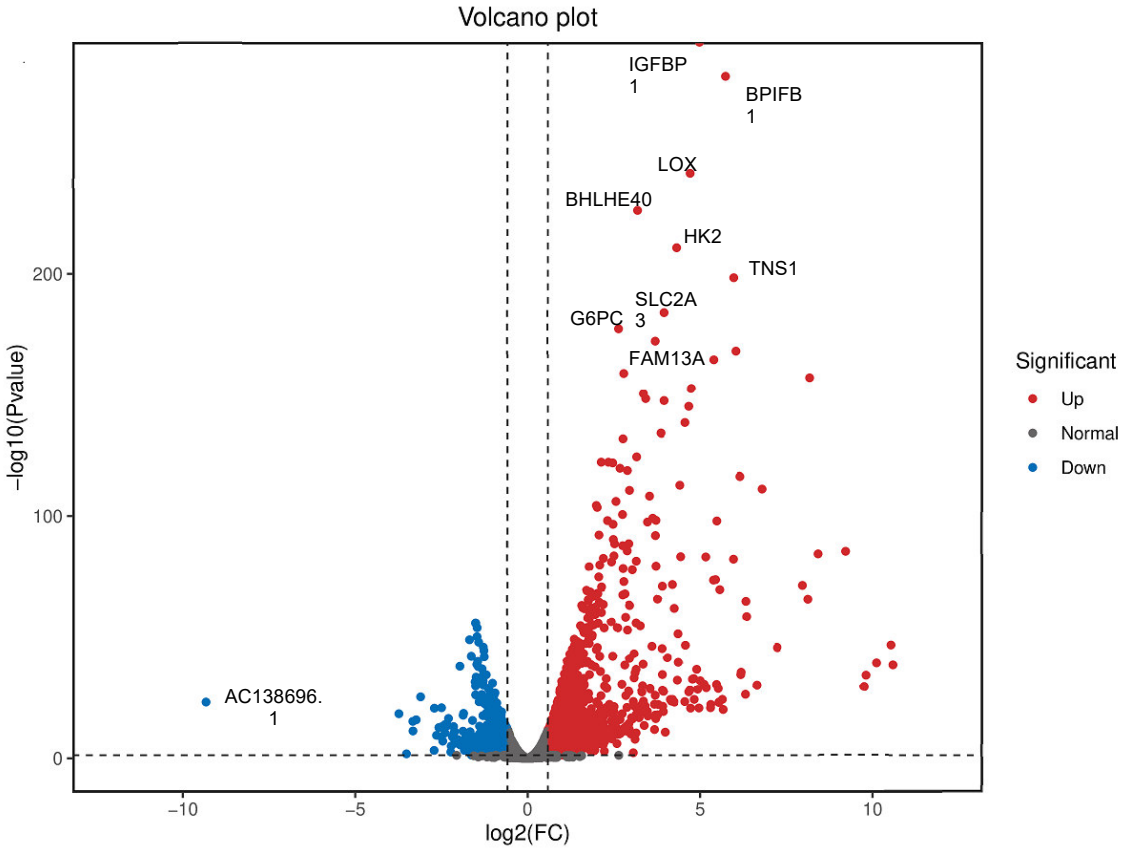

Figure 12 Volcano Plot of Differentially Expressed Genes in HepG2-NTCP Cells Cultured in Low vs High Amounts of Media. HepG2-NTCP cells were seeded and maintained in low (300 µL) or high (600 µL) amounts of media for 10 days. RNA sequencing was performed, and differential gene expression analysis was conducted. Blue dots denote down-regulated gene expression, and red dots denote up-regulated gene expression. Data shown are 6 independent biological replicates per group.

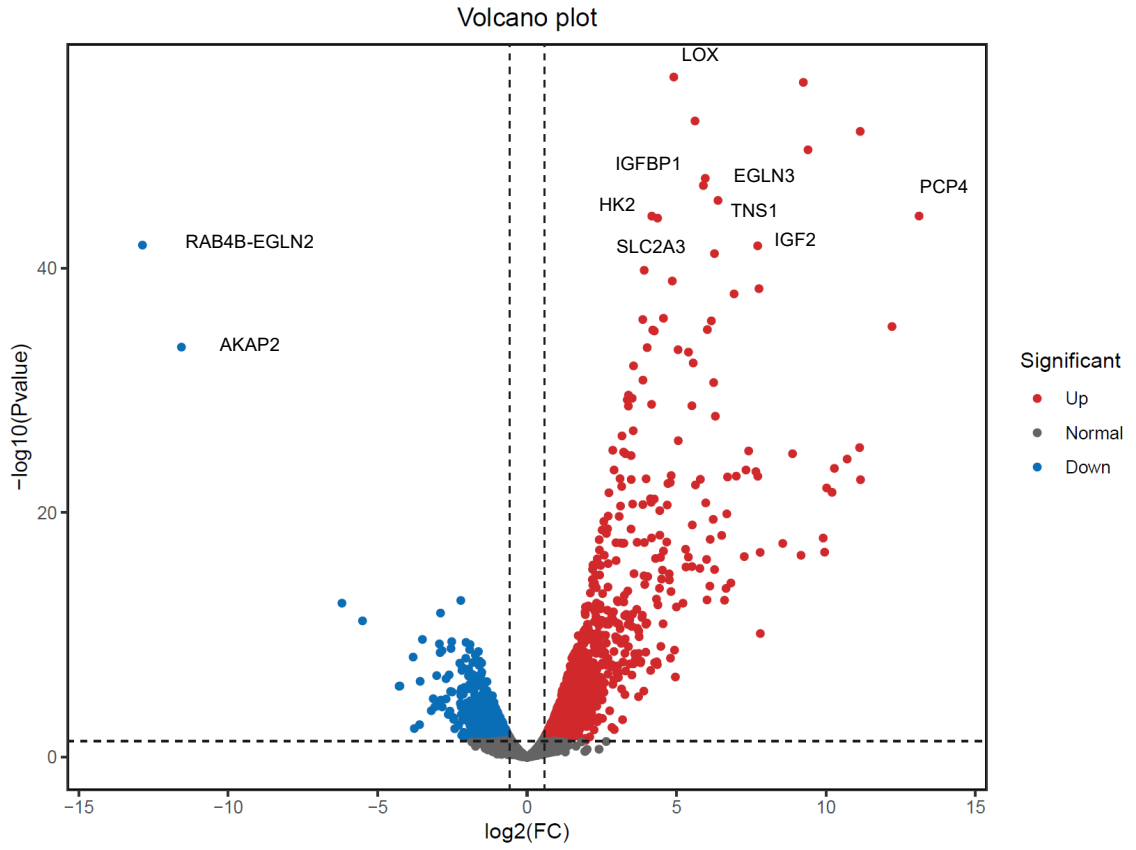

Figure 13 Volcano Plot of Differentially Expressed Genes in HBV-Infected HepG2-NTCP Cells Cultured in Low vs High Amounts of Media. HepG2-NTCP cells were infected with HBV and maintained in low (300 µL) or high (600 µL) amounts of media for 10 days. RNA sequencing was performed, and differential gene expression analysis was conducted. Blue dots denote down-regulated gene expression, and red dots denote up-regulated gene expression. Data shown are 6 independent biological replicates per group.

Interestingly, on a transcriptional level, the amount of medium used seemed to have a higher impact on differentially expressed genes compared to the infection with HBV (Fig. 14). When cells cultivated in low medium are compared with cells cultivated in high medium, 2439 differentially expressed genes are found in uninfected cells (Fig. 14, blue circle) and 3044 for infected cells (Fig. 14, green circle). Cells maintained in the same amount of medium but differing in HBV-infection status, exhibit only 203 differentially expressed genes (Fig 14, red circle).

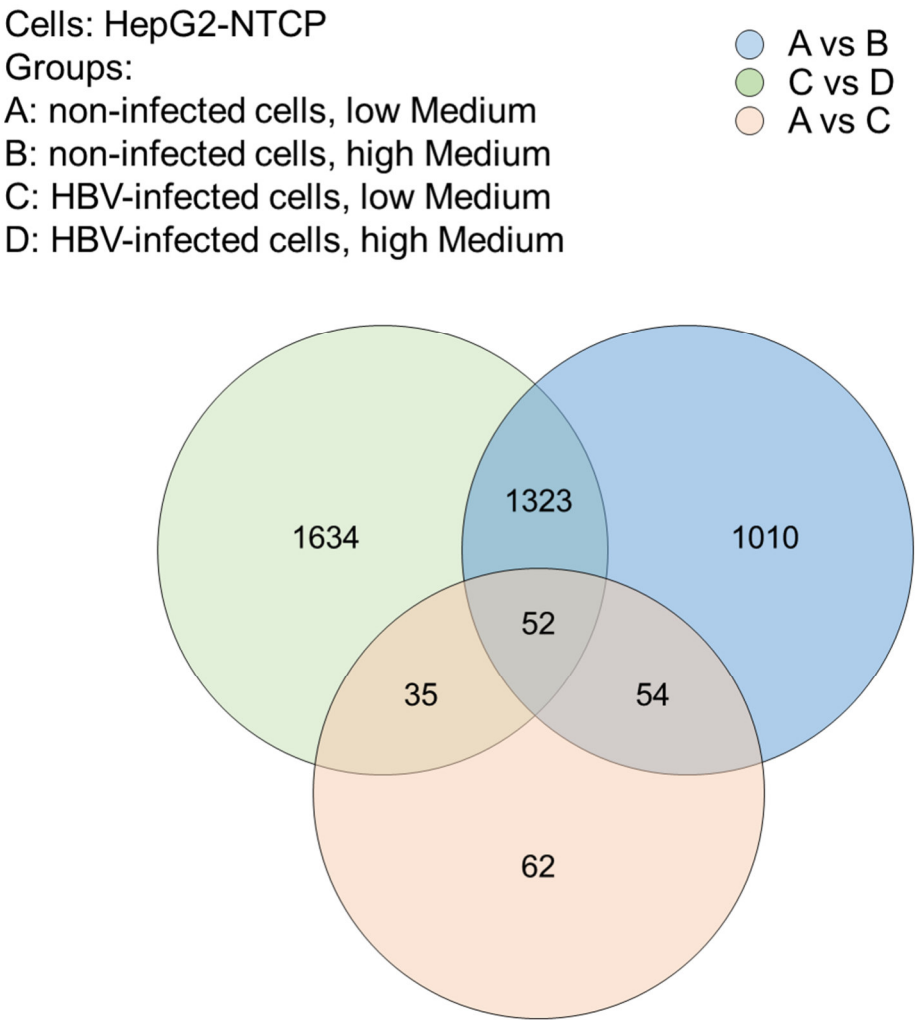

Figure 14 Venn Diagram of Differentially Expressed Genes in HBV or Non-Infected HepG2-NTCP Cells Kept in High or Low Amounts of Media. Differential gene expression analysis was performed on cells kept under certain conditions as stated in Table A. The Venn diagram depicts shared up- or down-regulated genes among the different comparisons.

2.2. Immunometabolism in vivo

According to the aims of this thesis, the second part is focused on investigating immunometabolism in vivo. Mouse models that allow infection with HBV were used to study metabolic changes and their effects on the HBV-specific immune response.

2.2.1. GCN2 in HBV infection

As mentioned previously, GCN2, as a general sensor of amino acid deprivation, serves an important role in the homeostasis of protein synthesis. It has been shown that viruses might exploit the GCN2-eIF2α pathway to escape antiviral responses (Liu, Wang et al. 2020 , Liu, Cheng et al. 2021).

To investigate whether GCN2 is mechanistically involved in the way HBV evades the immune system, GCN2-knockout mice (GCN2k.o.) were infected with AAV carrying the HBV genome (AAV-HBV), which, depending on the dose, either result in a self-resolving infection in low titer mice or persistence of the virus when infected with a high titer.

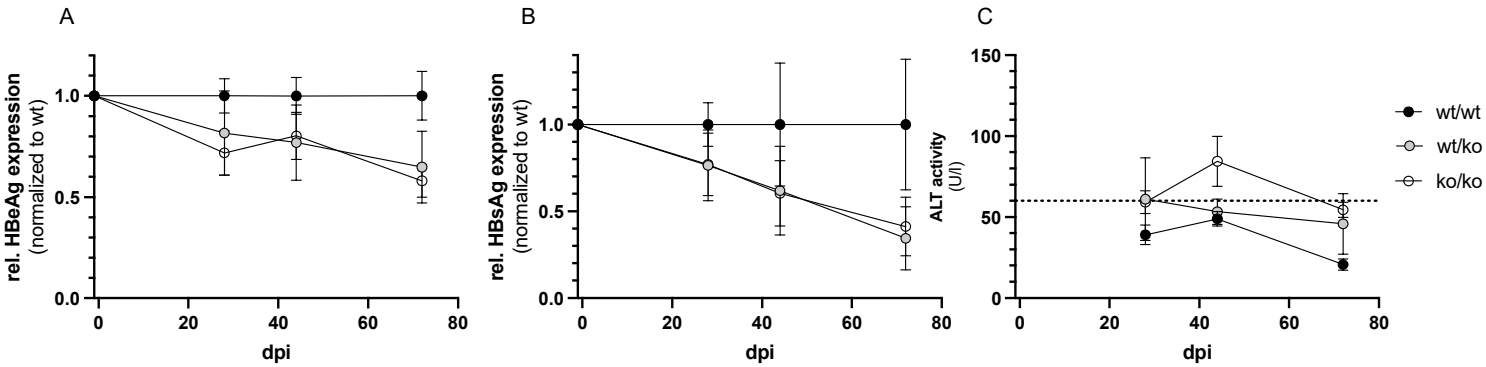

Figure 15 AAV-HBV Infection in GCN2 Knockout Mice. C57BL/6 mice either carrying a wildtype (wt/wt), heterozygous (wt/ko) or homozygous (ko/ko) genotype for General Control Non-derepressible-2 (GCN2) were infected using an AAV-HBV. HBeAg (A), HBsAg (B), and alanine aminotransferase (ALT)(C) was measured from the serum at indicated timepoints. Symbols represent the mean and whiskers the standard error of the mean. Data shown are 4-6 independent biological replicates per group.

Therefore, mice, homozygous (ko/ko) or heterozygous (wt/ko) for a GCN2 knockout, were infected using AAV-HBV and compared to an infection in wt mice. As a marker for viral burden, serum levels for HBeAg and HBsAg can be measured. Relative comparison of HBeAg (Fig.15A) and HBsAg in wt mice (black dots) to either wt/ko (grey dots) or ko/ko (empty dots) mice showed that mice with GCN2-genotype had lower antigenemia compared to wt mice. This effect was

more pronounced for HBsAg than it was for HBeAg. Interestingly, in ko/ko mice, this effect was accompanied by a transient increase in ALT levels above the normal range at week 6 (Fig 15C). Although for wt/ko a slight increase was observed around week 4, all mice returned to normal levels by week 10.

Taken together, this data suggests that mice that carry a knockout allele for GCN2 have lower antigenemia compared to wt mice when infected with AAV-HBV.

2.2.2. Improving HBV-specific immune responses

To achieve a functional cure, an HBV-specific immune response is indispensable due to the cccDNA that persists in hepatocytes even in the absence of viremia. As beforementioned, an elegant way to induce virus-specific immunity is a therapeutic vaccination. While inducing a robust immune response in low-titer infected HBV models, high-titer infection attenuates the effects of the vaccine (Backes, Jager et al.). Complimentary therapies have been applied alongside the vaccination to broaden the applicability. In the context of immunometabolism, although the exact mechanism is yet to be elucidated, a high burden of viral proteins prevents an efficient immune response in the liver. Lowering viral protein expression using siRNA targeting all viral transcripts increases the efficacy of therapeutic vaccination (Michler, Kosinska et al. 2020). Another promising approach is to interfere with the T cell tolerance induced by the immune checkpoints PD-1/PD-L1, as proposed by Patsoukis et al. When PD-L1 is inhibited during therapeutic vaccination, an improved response against HBV is measurable (Liu, Zhang et al. 2014, Bunse, Kosinska et al. 2022).

Together with Anna Kosinska and Edanur Ates Öz (Institute of Virology, Technical University of Munich / Helmholtz Munich) a combinatory approach consisting of siRNA targeting HBV (siHBV), siRNA targeting PD-L1 (siPD-L1) and therapeutic vaccination (TherVacB) was applied to mice infected with AAV-HBV (Fig. 16). First, mice were infected using AAV-HBV. Six weeks later, once viral protein expression reached steady levels, pretreatment with siHBV was performed every 4 weeks, for a total of three times. 14 weeks after infection, TherVacB in combination with siPD-L1 was applied according to the scheme shown in Figure 16 A. The final analysis was performed 36 weeks after the start of vaccination. According to Figure 16 B groups received treatment combinations

corresponding to their name. Control siRNA (Ctrl siRNA) served as a control for siPD-L1. Mice were continuously monitored for HBsAg (Fig. 16C) and HBeAg (Fig. 16D) in the serum.

All mice that received siHBV had a more than 2-$\log_{10}$ reduction in HBsAg and HBeAg. Upon vaccination, a decrease in antigens was detectable in all mice. While HBsAg and HBeAg expression in mice without pretreatment quickly returned to baseline until the end of the experiment, independently whether they were simultaneously treated with siPD-L1, mice that received siHBV further decreased HBeAg levels and became undetectable for HBsAg. Initially reduced to similar levels as the other groups, including siHBV, the combination of siHBV+siPD-L1 without vaccination eventually returned to baseline, too. 16 weeks after initiation of vaccination, mice pretreated with siHBV, but without adjunct checkpoint inhibition, had HBsAg detectable in the serum again, returning to a level that is almost 1-$\log_{10}$ lower compared to control mice. Although the rebound of HBeAg and HBsAg was finally observed in mice receiving triple combination, the levels of the HBV antigens did not return to baseline, but to an overall lower level. The combination of siHBV, siPD-L1, and therapeutic vaccination led to prolonged suppression of HBsAg below the detection limit for up to 32 weeks. Although the rebound in HBeAg expression was observed earlier, around week 12, an overall 67% decrease was detected as compared to the baseline values.

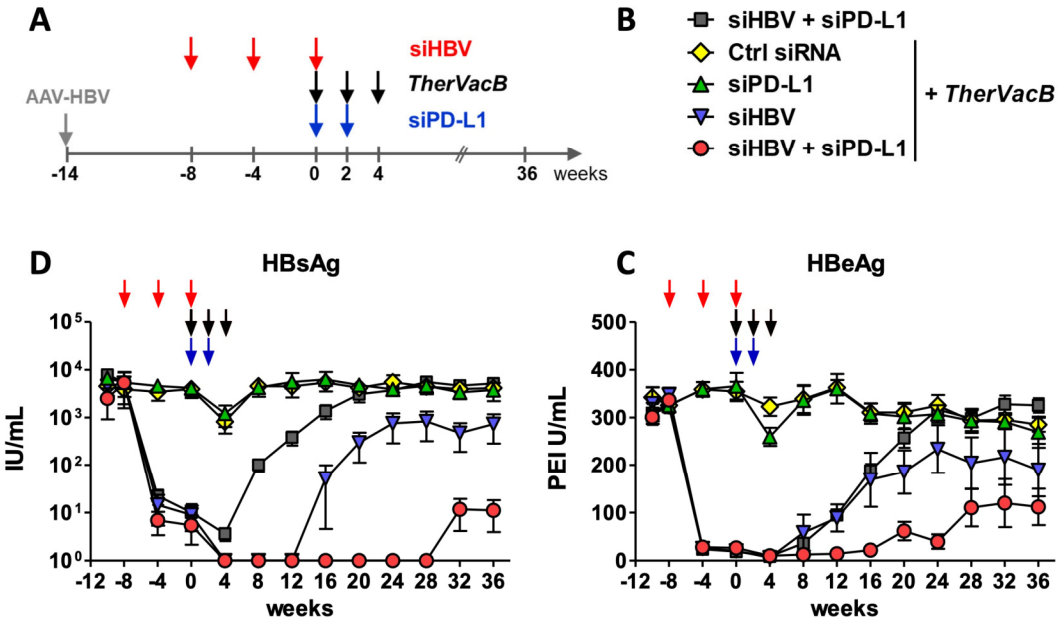

Figure 16 Combinatory Therapy of Viral Protein Knockdown, Checkpoint Inhibition, and Therapeutic Vaccination. Wt C57BL/6 mice were infected using an AAV-HBV. Six weeks later siRNA against HBV transcripts (siHBV) was administered for a total of four times. 14 Weeks after AAV transduction, heterologous prime-boost vaccination (TherVacB) was performed. One day prior to the first two vaccination time points, siRNA against PD-L1 (siPD-L1) was administered. 36 weeks after vaccination start mice were sacrificed for final analysis. (A) In the experimental scheme, arrows indicate respective time points administration. (B) Experimental groups. Viral antigens, i.e., HBsAg (D) and HBsAg (C), were measured from the serum. Symbols represent the mean, and whiskers show SEM. Data shown are 5 independent biological replicates per group.

In conclusion, mice that received a siHBV pretreatment and adjunct siPD-L1 treatment alongside therapeutic vaccination have a greater reduction in viral antigens compared to vaccination alone. For all other groups, only siHBV-pretreated and vaccinated mice had lower antigenemia at the end of the experiments compared to the control groups. siRNA-mediated PD-1/PD-L1 inhibition alone does not increase the efficacy in the high titer setting.

3. Discussion

Despite having an effective prophylactic vaccine, infection with HBV remains a global health burden. Oral treatment with NA can slow down disease progression and reduce infectivity. Nevertheless, life-long treatment is usually necessary, and patients still retain an elevated risk for HCC due to continuous viral protein expression. Especially in low-income countries, healthcare coverage, including regular health checks, availability, costs, and distribution of drugs, are limited. Therefore, novel treatment approaches should be applicable in those settings to eradicate the virus. Here, we investigated the potential mechanism of how HBV is able to evade an effective immune response, and possible implications for future therapies are discussed in the following chapters.

3.1. T-cell cytotoxicity in vitro depends on arginine

Data presented in 2.1. emphasizes Arginine as a critical regulator of cytotoxic T-cell function and shows the important role of arginine in promoting efficient cytotoxicity of T-cells directed against HBV-infected cells. By depriving in vitro cultures of arginine, a delayed onset of cytotoxicity is observed, accompanied by a reduction in IFN-γ production, an antiviral cytokine indispensable for an efficient immune response.

These findings are in line with current literature, highlighting arginine's multifaceted role in T cell activation and effector function. Arginine serves as a substrate for nitric oxide (NO) production (Geiger, Rieckmann et al. 2016), a key mediator of T-cell cytotoxicity against infected cells (Guidotti, Matzke et al. 1995, Majano, García-Monzón et al. 1998). Additionally, arginine metabolism can influence T-cell proliferation, differentiation, and cytokine production (Martí and Reith 2021), further emphasizing its importance in orchestrating effective immune responses against viral pathogens.

The observed delay in cytotoxicity and reduction in IFN-γ release upon arginine deprivation align with previous studies implicating arginine deficiency in immune dysfunction and impaired antiviral responses, by downregulation of CD3

(Feldmeyer, Wabnitz et al. 2012) and reduced IL2-production (Ochoa, Strange et al. 2001). Patients with CHB exhibit reduced serum arginine levels (Das, Hoare et al. 2008), suggesting a potential link between arginine metabolism and disease progression. Thus, targeting arginine metabolism may be a promising therapeutic approach to enhance T cell-mediated clearance of HBV-infected cells. Along those lines, CAR-T cells modified to inhibit arginine-depleting enzymes have been shown to have an increased efficiency in arginine-low microenvironments (Fultang, Booth et al. 2020).

3.2. Arginine-dependency of virus replication

Arginine deprivation in HepG2 cells has been shown to influence HBV replication dynamics and viral protein expression. We showed an attenuation of viral antigen production and replication when arginine was depleted.

Arginine deprivation induces a marked reduction in viral antigen levels, i.e. HBsAg and HBeAg, markers of active viral replication, but an increase in viral pgRNA levels. Suppression of global protein synthesis might not only be limited to host proteins but also might affect viral expression. Interestingly, while the generation of pgRNA seems to be unaffected by this suppression, higher expression of viral RNA might be a way of counteracting negative consequences on viral fitness. Amino acid starvation might rely on a delicate balance between inhibiting the host's antiviral mechanisms and immune response while maintaining an efficient viral replication. For SARS-CoV2 it has been shown that arginine is indispensable for viral replication and arginine depletion was investigated as a potential therapeutic approach (Grimes, Khan et al. 2021). Notably, the antiviral effect of those therapeutic starvation approaches was conveyed by restricting the virus's availability of polyamines rather than the amino acids themselves (Tomé 2021).

Taken together, the link between arginine availability and HBV replication highlights the potential therapeutic implications of targeting arginine metabolism for the treatment of HBV-infected individuals. Strategies aimed at restoring arginine levels or modulating arginine-related pathways should hold the potential to inhibit viral replication and suppress HBV pathogenesis.

3.3. Nutrient Restriction affects Viral Protein Expression

HBV-infected HepG2 cells that were kept in lower amounts of medium expressed more viral proteins. As discussed above, nutrient restriction can also affect viral replication. In this setting, the amount of virus produced unexpectedly increased through an unknown mechanism. Although HBV is termed a stealth virus due to little recognition by the immune system, the virus is able to skew certain pathways, e.g. lipid transport pathways (Esser, Cheng et al. 2023), to favor viral replication over physiological functions. An accumulation of viral proteins might be able to do that in a stronger fashion which would explain why in lower amounts of medium, and therefore also higher concentration of viral protein, a stronger effect was visible. It was described that HBV particles can activate the MyD88-mTOR axis through TLR2 (Li, Wang et al. 2021) an important regulatory pathway for energy metabolism (Zhang, Ma et al. 2019). It is important to understand the mechanism HBV is altering the metabolism to develop a more targeted therapeutic approach. Especially the cellular sensors involved in counteracting might hold valuable potential. Similar to the TLR for the recognition of pathogen- and danger-associated molecular patterns (PAMPs and DAMPs, respectively), homeostasis-altering molecular processes (HAMPs) have been described to sense indirectly molecular perturbations in the cells homeostasis (Liston and Masters 2017). HAMPs involved in detecting HBV-induced metabolic changes might be used to counteract HBV immune evasion and allow for a more efficient immune response against the virus (Diaz, Vidalain et al. 2022).

3.4. Cellular changes upon HBV infection

Metabolic changes in HepG2 cells upon HBV infection predominantly affected in sphingolipids, glycerophospholipids and several amino acids. Although the amount of media was also involved in some changes that were measured, a clear increase in all sphingolipids and glycerophospholipids was observed. These bioactive lipids act on a multitude of cellular pathways. Especially, cell signaling pathways and their connection to the induction of immune response are important in the context of viral infection (Hannun and Obeid 2018).

To further investigate the involved pathways, RNA sequencing was performed. Interestingly, the changes on a transcriptional level are less strong than on a metabolite level. Notably, some of the most upregulated genes, e.g., solute carrier family 2 member 1 (SLC2A) or Insulin-like growth factor binding protein (IGFBP1), are transporter proteins important for metabolic homeostasis. Due to the targeted approach of the metabolomics analysis, we identified the lipidome of infected cells as a promising target for further investigation. Due to the nature of a targeted approach, we could not match RNAseq data with the metabolomics data since the sequencing was performed in an unobserved manner. Nevertheless, targets identified in the sequencing are currently subject to Gene Orthology Analysis to identify pathways involved in metabolic perturbations. Once identified, these pathways might be targeted to clear HBV infection.

3.5. Role of GCN2 in HBV Infection

GCN2, a stress-responsive kinase, is pivotal in integrating cellular stress signals with metabolic adaptations to maintain cellular homeostasis. In the context of viral infections, including HBV, GCN2-mediated signaling regulates the host's antiviral responses and immunometabolic reprogramming (Afroz, Battu et al. 2020) (Liu, Cheng et al. 2021). Here, we evaluated the impact of GCN2 deficiency on HBV infection *in vivo* and explored its implications for viral pathogenesis and immune evasion.

Lower levels of antigenemia compared to wild-type mice upon viral challenge suggest that GCN2 deficiency confers a degree of protection against HBV infection. GCN2-mediated metabolic reprogramming could impact the availability of nutrients crucial for viral replication, attenuating HBV infection in the absence of GCN2 activity (Liu, Wang et al. 2020).

Understanding the role of GCN2 in HBV infection might provide insights into viral pathogenesis and the mechanism of immune evasion through immunometabolism. Targeting GCN2 signaling pathways may be a promising strategy for developing novel antiviral therapies to enhance host immune responses and restrict viral replication (Jaspart, Calmels et al. 2017).

In summary, these results highlight the connection of immunometabolism and viral pathogenesis, in GCN2 deficiency in the context of HBV infection. Further

investigation into the underlying mechanisms is necessary but may lead to novel therapeutic targets for the treatment of CHB.

3.6. Combinatorial Therapies for CHB

As discussed above, a multitude of ways contribute to the persistence of HBV in the liver. Immunotherapy is a promising way to stimulate the patient's immune system to eradicate the virus and develop a sustained response to HBV. Although promising methods exist, none are currently successful as monotherapy. Here we investigated whether a combination of treatments with different modes of action can synergistically clear the virus.

The main effector of this approach is the therapeutic vaccination. Especially in high titer-infected individuals, HBV-specific T cells are scarce and often exhausted (Baudi, Kawashima and Isogawa 2021) (Rossi, Vecchi et al. 2023). The rationale of the vaccine design is the heterologous use of particulate protein to prime T and B cells, followed up by a booster vaccination sing an attenuated modified Vaccinia virus Ankara (MVA) (Backes, Jager et al. 2016).

Continuous exposure to high levels of viral proteins is known to induce tolerance and prevent efficient effector function of T cells. Therefore, siRNA-mediated knockdown of HBV proteins was chosen as an additional therapy. An siRNA that targets the 3' end of all HBV RNAs was coupled to GalNAc for efficient delivery into hepatocytes (Michler, Große et al. 2016, Michler, Kosinska et al. 2020).

Additionally, due to the overexpression of PD1 on circulating HBV-specific T cells in CHB patients (Peng, Li et al. 2008), enhancing therapeutic efficacy through targeting of immune checkpoints, such as programmed cell death ligand 1 (PD-L1), seems to be promising and was already successful in a similar approach (Bunse, Kosinska et al. 2022). Inhibition of PD-L1 using siRNA aims to alleviate T-cell exhaustion and restore antiviral immune responses.

The synergy between siRNA-mediated viral protein knockdown, checkpoint inhibition using siPD-L1, and therapeutic vaccination represents a promising combinatorial approach to treat chronic HBV infection. Targeting multiple aspects of viral pathogenesis is an effective way to modulate the host immune response.

In conclusion, combinatorial therapies for HBV infection represent a promising strategy for improving treatment outcomes and achieving functional cure. By

facilitating the synergistic effects of siRNA-mediated viral protein knockdown, checkpoint inhibition, and therapeutic vaccination, viral eradication is achievable in even more patients than with individual treatments alone.

4. Materials and methods

4.1. Materials

4.1.1. Antibodies

Antibody	Supplier
Granzyme B-PE	Invitrogen
mCD3-PerCP-Cy5.5	eBiosciences
mCD4-PE-Cy7	eBiosciences
mCD4-V500	BD Biosciences
mCD8-PE	BD Biosciences
mCD8-PE-Cy7	Biolegend
mCD8-PerCP-C7	eBioscience
mCD8-V500	BD Biosciences
mCTLA-4-PerCP-Cy5.5	eBioscience
mIFN-γ-APC	BD Biosciences
mIFN-γ-FITC	BD Biosciences
mPD-1-FITC	eBioscience
mPD-1-PacBlue	eBioscience
mTIM-3-APC	Biolegend
mTNF-α-PE-Cy7	BD Biosciences

4.1.2. Buffers

Buffer	Ingredients
ACK lysis buffer	150 nM NH_4Cl 10mM $KHCO_3$ 0.1 mM Na_2EDTA pH 7.2 – 7.4 in H_2O

FACS buffer	0.1 % BSA in PBS
Lysis buffer	2.5ml 1M Tris 2.5ml 5M NaCl 0.3ml 0.5M EDTA 0.075g EGTA 0.5 Triton X100 250µl NP40 5ml Glycerol 0.558g $Na_4P_2O_7$
SDS-Loading dye	3.75 ml 1M Tris/Cl pH 6.8 6 ml glycerol 1.2g SDS 0.93g DTT 6 mg bromphenol blue in 10 ml H_2O
10xTBS	12.1g Tris 40g NaCl Adjust to pH 7.4 In 500 ml H_2O
TBS-T	100 ml 10x TBS 1ml Tween-20 In 1l H_2O
10x SDS Running buffer	30.3g Tris 145g Glycin 100 ml 10% SDS In 1l H_2O
10x Transfer buffer	30.3g Tris 144,1g Glycin In 1l H_2O
Transfer buffer	100ml 10x Transfer buffer 200ml Methanol in 1l H_2O

4.1.3. Cell culture media

Medium	Ingredients
DMEM full medium	DMEM 500 ml FCS 50 ml Pen/Strep, 10,000 U/ml 5.5 ml L-Glutamine, 200 mM 5.5 ml NEAA, 100x 5.5 ml

	Sodium pyruvate, 100 mM 5.5 ml
Freezing medium	FCS 90 % DMSO 10 %
HepG2 Diff medium	DMEM 500 ml FSC 5 ml Pen/Strep, 10,000 U/ml 5.5 ml L-Glutamine, 200 mM 5.5 ml NEAA, 100x 5.5 ml Sodium pyruvate, 100mM 5.5 ml DMSO 10.5 ml
SILAC Medium + varying amounts of Arg	DMEM SILAC 500 ml dialysed FCS 5 ml Pen/Strep, 10,000 U/ml 5.5 ml L-Glutamine, 200 mM 5.5 ml Sodium pyruvate, 100mM 5.5 ml DMSO 10.5 ml + indicated amounts of L-Arginine
Human T cell medium	RPMI 1640 500 ml FSC 50 ml Pen/Strep, 10,000 U/ml 5.5 ml L-Glutamine, 200 mM 5.5 ml NEAA, 100x 5.5 ml Sodium pyruvate, 100 mM 5.5 ml HEPES 5.5 ml Gentamicin 208 □l
LB medium pH 7.0	Tryptone 10 g Yeast extract 5 g NaCl 10 g in 1 liter H2O
RPMI full medium	RPMI 1640 500 ml FCS 50 ml Pen/Strep, 10,000 U/ml 5.5 ml

	L-Glutamine, 200 mM 5.5 ml NEAA, 100x 5.5 ml Sodium pyruvate, 100 mM 5.5 ml
Transfection medium	DMEM 500 ml FCS 50 ml L-Glutamine, 200 mM 5.5 ml NEAA, 100x 5.5 ml Sodium pyruvate, 100 mM 5.5 ml
Wash medium	RPMI 1640 500 ml Pen/Strep, 10,000 U/ml 5.5 ml

4.1.4. Cell lines

Name	Description
HEK293	Human embryonic kidney cells, transformed with fragments of adenovirus type 5 DNA (Graham, Smiley et al. 1977)
HepG2-NTCP	HepG2 cells with a stable expressing of sodium taurocholate co-transporting polypeptide (NTCP) (Ko, Chakraborty et al. 2018)

4.1.5. Chemicals and reagents

Chemical or reagent	Supplier
Agar-agar	Roth, Karlsruhe, Germany
Agarose	Peqlab, Erlangen, Germany
Amersham ECL Prime Western Blotting Detection Reagent	GE Healthcare Life Sciences, Freiburg, Germany
Ampicillin	Roth, Karlsruhe, Germany

Collagen R	Serva Electrophoreses, Heidelberg, Germany
DMSO	Sigma-Aldrich, Steinheim, Germany
Dulbecco´s modified Eagle´s Medium	Gibco/Invitrogen, Carlsbad, USA
Ethanol	Roth, Karlsruhe, Germany
Ethidium bromide	Merck, Darmstadt, Germany
FCS (heat-inactivated)	Gibco/Invitrogen, Carlsbad, USA
Formaldehyde	Roth, Karlsruhe, Germany
Gentamicin	Ratiopharm, Ulm, Germany
Glutamine	Sigma-Adrich, Steinheim, Germany
Glycine	Roth, Karlsuhe, Germany
HBsAg, recombinant	Dynavax
HBcAg, recombinant	Dr. Dišlers,APP Latvijas Biomedicīnas (Riga, Latvia)
IFN-α	Roche, Vienna, Austria
IFN-γ	Boehringer Ingelheim, Vienna, Austria
Isopropanol	Roth, Karlsruhe, Germany
Lipofectamine 2000/3000	Life Technologies, Carlsbad, USA
Lipofectamine RNAiMAX	Life Technologies, Carlsbad, USA
Methanol	Roth, Karlsruhe, Germany
Milk powder	Roth, Karlsruhe, Germany
NaCl	Roth, Karlsruhe, Germany
NaOH	Roth, Karlsruhe, Germany
Non-essential amino acids 100x	Gibco/Invitrogen, Carlsbad, USA

OptiMEM	Gibco/Invitrogen, Carlsbad, USA
Page Ruler Plus Prestained protein ladder	Thermo Scientific, Waltham, USA
PBS	Gibco/Invitrogen, Carlsbad, USA
PEG6000	Merck, Hohenbrunn, Germany
Penicillin/streptomycin	Gibco/Invitrogen, Carlsbad, USA
Pierce RIPA buffer	Thermo Scientific, Rockford, USA
Polyacrylamide	Roth, Karlsruhe, Germany
Protease inhibitor (Comlpete)	Roche, Mannheim, Germany
RotiSafe	Roth, Karlsruhe, Germany
SDS	Roth, Karlsruhe, Germany
SmartLadder DNA (small fragment)	Eurogentec, Liege, Belgium
Sodium citrate	Roth, Karlsruhe, Germany
Sodium pyruvate	Gibco/Invitrogen, Carlsbad, USA
Sucrose	Roth, Karlsruhe, Germany
T5 exonuclease	New England Biolabs, Ipswich, USA
TEMED	Roth, Karlsruhe, Germany
Tris base	Roth, Karlsruhe, Germany
Tris HCL	Roth, Karlsruhe, Germany
Trypan blue	Gibco/Invitrogen, Carlsbad, USA
Trypsin	Gibco/Invitrogen, Carlsbad, USA
Tryptone	Roth, Karlsruhe, Germany
Tween 20	Roth, Karlsruhe, Germany

4.1.6. Kits

Product	Supplier
AllPrep DNA/RNA Kit	Qiagen, Valencia, CA, USA
CellTiter-Blue Cell Viability Assay	Promega BioSciences, CA, USA
Dual-Luciferase Reporter Assay	Promega BioSciences, CA, USA
GeneJet Gel Extraction Kit	Fermentas, St. Leon-Rot, Germany
GeneJet Plasmid Miniprep Kit	Thermo Scientific, Schwerte, Germany
Human IFN- γ ELISA MAX Standard Sets	Biolegend, San Diego, CA, USA
LightCycler 480 SYBR Green I Master mix	Roche, Mannheim, Germany
Liver In Vivo Transfection Kit	Altogen Biosystems, NV, USA
NucleoSpin RNA isolation Kit	Macherey-Nagel, Düren, Germany
NucleoSpin Tissue Kit	Macherey-Nagel, Düren, Germany
SuperScript III First-Strand Synthesis SuperMix for qRT-PCR	Invitrogen, Karlsruhe, Germany
TA Cloning Kit	Invitrogen, Karlsruhe, Germany

4.1.7. Laboratory equipment and consumables

Product	Supplier
BEP (HBeAg measurement)	GE Healthcare Life Sciences, Freiburg, Germany
Cell culture flasks and plates	TPP, Trasadingen, Switzerland
Cell culture incubator HERAcell 150i	Thermo Scientific, Rockford, USA
Centrifuge 5417C / 5417R	Eppendorf, Hamburg, Germany

Cryo vials	Geiner Bio One, Kremsmünster, Austria
ELISA 96well plates Nunc	Thermo Scientific, Rockford, USA
Falcon tubes 15ml, 50ml	Greiner Bio One, Kremsmünster, Austria
Fluorescence microscope CKX41	Olympus, Hamburg, Germany
Freezing container	Thermo Fisher Scientific, Waltham, USA
Fusion Fx7 (chemiluminescence detection; UV light system)	Peqlab, Erlangen, Germany
Gel chambers (agarose gel electrophoresis)	Peglab, Erlangen, Germany
Gel chambers (SDS-PAGE)	Bio-Rad, Hercules, USA
Heating block	Eppendorf, Hamburg, Germany
Hemocytometer	Brand, Wertheim, Germany
Hyperflask	Corning, Amsterdam, The Netherlands
Light Cycler 480 II	Roche, Mannheim, Germany
Light Cycler 96	Roche, Mannheim, Germany
Pipette “Accu-jet pro”	Brand, Wertheim, Germany
Pipette filter tips	Starlab, Ahrensburg, Germany
Pipette tips 2 – 50ml	Greiner Bio One, Kremsmünster, Austria
Pipettes	Eppendorf, Hamburg, Germany
PVDF membrane	Bio-Rad, Hercules, USA
qPCR 96-well plates	4titude, Berlin, Germany

Reaction tubes	Eppendorf, Hamburg, Germany
Reflotron ALT stripes	Roche, Mannheim, Germany
Reflotron Reflovet Plus (ALT reader)	Roche, Mannheim, Germany
Sterile hood	Heraeus, Hanau, Germany
Tecan plate reader Infinite F200	Tecan, Männerdorf, Switzerland
Ultracentrifuge Beckman SW40 rotor	Beckman Coulter, Brea, USA
Western Blotting Chamber	Bio-Rad, Hercules, USA
Whatman paper	Bio-Rad, Hercules, USA

4.1.8. Mouse strains

Mouse line	Description	Source
Wildtype	C57BL/6J wildtype	Janvier
GCN2k.o.	Homozygous knock-out Eif2ak4tm1.2Dron mice (sometimes referred to as GCN2-KO mice) have a deletion of exon XII of the eukaryotic translation initiation factor 2 alpha kinase 4 (Eif2ak4 or GCN2) gene. (Harding, Novoa et al. 2000)	Kindly provided by Prof. Peter Murray, MPI of Biochemistry

4.1.9. siRNA

siRNA Name	Sequence Sense (antisense)
siPD-L1	GGAGAAAUGUGGCGUUGAA (UUCAACGCCACAUUUCUCCAC)
siCtrl	GCAGCACGACUUCUUCAAG

4.1.10. Software

Software name	Supplier
FlowJo, version 10.7	BD Biosciences
LightCycler 480 SW 1.5.1	Roche
Prism 9	GraphPad Software Inc.
ImageJ	NIH
RTCA Software 2.0	ACEA Biosciences
Serial Cloner	SerialBasics

4.2. Methods

4.2.1. Cell culture

Adherent cell lines were cultured under sterile conditions in DMEM full medium and incubated at 37°C, 5% CO_2, and 95% humidity, unless indicated otherwise. Cells were passaged every three to four days, depending on their confluency. Single-cell suspensions were obtained by treatment with trypsin (5-10 min, 37°C). For the cultivation of Hepatoma cells, tissue culture plates and culture flasks were pre-treated with collagen prior to the seeding of the cells.

4.2.2. RNA isolation

Nucleic acids were either isolated immediately after cell lysis or organ harvesting or stored after stabilizing using RNAlater and stored at -80°C. Samples were disrupted using a Tissue Lyser LT according to the manufacturer's instructions. For RNA isolation, the Nucleo Spin RNA Kit was used according to the manufacturer's instructions.

4.2.3. DNA isolation

Cellular DNA was isolated using the NucleoSpin tissue Kit according to the manufacturer's instructions.

4.2.4. Nucleic acids quantification

DNA and RNA concentrations were determined using a NanoDrop One using the respective solvent solution as a blank.

4.2.5. cDNA synthesis

For cDNA synthesis, RNA was reversely transcribed using the SuperScript III Kit according to the manufacturer's instructions. cDNA was additionally diluted for further analysis.

4.2.6. quantitative PCR

Quantitative PCR was performed using a LightCycler 480 system in combination with the SYBR green master mix according to the manufacturer's instructions.

4.2.7. Counting of cells

For automated cell counting, a single-cell suspension was obtained and 20 µL were mixed with 1 µL DAPPI Staining Reagent and counted using the NucleoCounter.

4.2.8. Isolation of human PBMC

Isolation of human PBMC was performed by mixing freshly drawn blood from healthy volunteers with heparin and pre-warmed RPMI wash medium in a 1:1 ratio. Then, 25 mL of the solution was layered onto 12,5 mL Bicoll and centrifuged for 25 min at 1200 g with the breaks turned off. The now visible lymphocyte layer was collected, diluted with RPMI wash medium, and subjected to another centrifugation at 80 g for 20 min. The supernatant is discarded, and the pellet is again diluted in RPMi wash medium and centrifuged for 5 min at 350 g. Cells were then counted, and the cell number was adjusted to $2x10^6$ and frozen at -80°C using the freezing medium.

4.2.9. In vitro HBV infection

HepG2-NTCP cells were differentiated using HepG2 Diff medium 48h prior to HBV infection. Cells were infected using a MOI of 200 in the presence of 5% PEG for 24h. High-titer HBV stocks were kindly provided by Jochen Wettengel.

4.2.10. Mice experiments

Animal experiments were performed following the Society for Laboratory Animal Science (GV-Solas) regulations. All mice were kept in a pathogen-free (SPF) facility.

4.2.11. AAV-HBV transduction

Eight to ten weeks old C57BL/6 male mice were transduced using $4\text{-}6x10^9$ genome equivalents (GE) of AAV-HBV1.2 vector (diluted with PBS in 100 µl)

injected through the tail vein. Persistent viral protein expression was established six weeks after the AAV-HBV transduction. Mice were bled shortly before the first immunization and allocated into groups with comparable HBeAg and HBsAg levels.

4.2.12. Therapeutic vaccination

Protein vaccination was performed by intramuscular (i.m.) injection of 10µg HBsAg, 10µg HBcAg and 10µg ci-di-AMP diluted in an appropriate volume. For MVA-Boost, $1x10^7$ plaque-forming units (pfu) of MVA-HBsAg and $1x10^7$ pfu MVAHBcAg were injected i.m. MVA stocks were kindly provided by Anna Kosinska.

4.2.13. Bleeding and serum analysis

Blood drawing from mice was performed by punctation of the v. facialis. Blood was collected in Microvette 500 LH-Gel tubes and centrifuged at 10,000x g for 5 min at RT.

Serum alanine aminotransferase (ALT) activity was measured using Reflotron Reflovet Plus according to the manufacturer´s protocol.

HBsAg, HBeAg, anti-HBs, and anti-HBe measurements from serum were performed using the ARCHITECT system according to the manufacturer´s protocol.

4.2.14. Flow cytometry

Surface staining was performed in 96-well plates using antibodies diluted in a final volume of 50 µl/well in FACS buffer. Cells were incubated with the antibodies for 30 min on ice in the dark. After washing, cells were resuspended in 200 µl FACS buffer and analyzed using a CytoFLEX S flow cytometer.

Dead cells were stained using fixable viability dye eF780 according to the manufacturer's protocol.

For multimer staining MHC I streptamers that bind to HBV-specific TCRs were used. The streptamers were labeled with Strep-Tactin according to the manufacturers protocol. Labeled multimers were added to the cell surface antibody mix, following the protocol for standard surface staining.

Intracellular cytokine staining was performed after cell permeabilization using the Fixation/Permeabilization Solution Kit BD Bioscience according to the manufactures protocol. Antibodies for intracellular staining were diluted with Perm/Wash buffer and incubated in the dark. After washing, cells were resuspended in 200 µl Perm/Wash buffer and analyzed using a CytoFLEX S flow cytometer.

4.2.15. Metabolomic analysis

Targeted metabolomics analysis was performed at the Helmholtz Zentrum München, Metabolomics and Proteomics Core, in Neuherberg, Germany. Metabolites were quantified using liquid chromatography- and flow injection-electrospray ionization-tandem mass spectrometry (LC- and FIA-ESI-MS/MS) and the AbsoluteIDQTM p180 Kit (biocrates Life Sciences AG, Innsbruck, Austria). The assay allows simultaneous quantification of 188 metabolites out of plasma or other biological samples, including free carnitine, 39 acylcarnitines, 21 amino acids (19 proteinogenic + citrulline + ornithine), 21 biogenic amines, hexoses (sum of hexoses – about 90-95 % glucose), 90 glycerophospholipids (14 lysophosphatidylcholines and 76 phosphatidylcholines), and 15 sphingolipids. The method of AbsoluteIDQTM p180 Kit has been proven to be in conformance with the EMEA-Guideline "Guideline on bioanalytical method validation (July 21st, 2011) which implies proof of reproducibility within a given error range. The assay procedures of the AbsoluteIDQTM Kit p180 as well as the metabolite nomenclature have been described in full detail previously (Zukunft, Sorgenfrei et al. 2013).

Cell homogenate supernatants were used for measurements, which have been prepared as follows: 80 mg of glass beads (diameter 0.5 mm) were added to each sample of harvested adherent cells. Directly afterwards, samples were homogenized using a Precellys24 (PeqLab Biotechnology, Erlangen, Germany) at 0-4 °C for two times over 25 seconds at 5,500 rpm. First, an aliquot of the thoroughly vortexed homogenate was taken from each sample for performing the Hoechst Assay. The results of the Hoechst Assay were used for the normalization of the metabolomics data to an equivalent of the cell number (Muschet, Möller et al. 2016) . Subsequently, samples were centrifuged at 4 °C and 10,000 x g for 5 minutes and 10 µL of the supernatants were placed into the cavities of the 96-

well filter plate of the p180 assay. The filter inserts were dried in a nitrogen stream for 30 min. Amino acids and biogenic amines were derivatized with an excess of 5 % phenylisothiocyanate for 20 min and the filter inserts dried again in a nitrogen stream. Samples were extracted for 30 min at RT with 300 µL methanol containing 5 mM ammonium acetate. The LC run was performed using an Agilent XDB-C18 column (3 x 100 mm, 3.5 µm). Sample handling was performed by a Hamilton Microlab STARTM robot (Hamilton Bonaduz AG, Bonaduz, Switzerland) and a Ultravap nitrogen evaporator (Porvair Sciences, Leatherhead, U.K.), beside standard laboratory equipment. Mass spectrometric analyses were done on an API 4000 triple quadrupole system (SCIEX Deutschland GmbH, Darmstadt, Germany) equipped with a 1260 Series HPLC (Agilent Technologies Deutschland GmbH, Böblingen, Germany) and an HTC-xc PAL auto sampler (CTC Analytics, Zwingen, Switzerland) controlled by the software Analyst 1.6.2. For the LC-part, compounds were identified and quantified based on scheduled multiple reaction monitoring measurements (sMRM), for the FIA-part on MRM. Data evaluation for quantification of metabolite concentrations and quality assessment were performed with the software MultiQuant 3.0.1 (SCIEX) and the MetIDQ™ software package, which is an integral part of the AbsoluteIDQ™ Kit. Metabolite concentrations were calculated using internal standards and reported in µmol/L (µM) for cell homogenate supernatants, reference plasma, and quality control samples.

4.2.16. xCelligence Experiments

The xCELLigence system is an impedance-based method to monitor cell viability in real-time. Microelectrodes on the bottom of a 96-well cell culture plate detect changes in impedance caused by cell growth or cell detachment. Cell viability is illustrated as a cell index normalized to 1 at the beginning of the co-culture experiment.

5. Figures

6. References

Afroz, S., S. Battu, J. Giddaluru and N. Khan (2020). "Dengue Virus Induced COX-2 Signaling Is Regulated Through Nutrient Sensor GCN2." Front Immunol **11**: 1831.

Alonso, D. and W. J. Nungester (1956). "Comparative study of host resistance of guinea pigs and rats. V. The effect of pneumococcal products on glycolysis and oxygen uptake by polymorphonuclear leucocytes." J Infect Dis **99**(2): 174-181.

Backes, S., C. Jager, C. J. Dembek, A. D. Kosinska, T. Bauer, A. S. Stephan, A. Dislers, G. Mutwiri, D. H. Busch, L. A. Babiuk, G. Gasteiger and U. Protzer "Protein-prime/modified vaccinia virus Ankara vector-boost vaccination overcomes tolerance in high-antigenemic HBV-transgenic mice." (1873-2518 (Electronic)).

Backes, S., C. Jager, C. J. Dembek, A. D. Kosinska, T. Bauer, A. S. Stephan, A. Dislers, G. Mutwiri, D. H. Busch, L. A. Babiuk, G. Gasteiger and U. Protzer (2016). "Protein-prime/modified vaccinia virus Ankara vector-boost vaccination overcomes tolerance in high-antigenemic HBV-transgenic mice." Vaccine **34**(7): 923-932.

Baudi, I., K. Kawashima and M. Isogawa (2021). "HBV-Specific CD8+ T-Cell Tolerance in the Liver." Front Immunol **12**: 721975.

Braun, M. Y. (2021). "The Natural History of T Cell Metabolism." Int J Mol Sci **22**(13).

Brunner, J. S., L. Vulliard, M. Hofmann, M. Kieler, A. Lercher, A. Vogel, M. Russier, J. B. Brüggenthies, M. Kerndl, V. Saferding, B. Niederreiter, A. Junza, A. Frauenstein, C. Scholtysek, Y. Mikami, K. Klavins, G. Krönke, A. Bergthaler, J. J. O'Shea, T. Weichhart, F. Meissner, J. S. Smolen, P. Cheng, O. Yanes, J. Menche, P. J. Murray, O. Sharif, S. Blüml and G. Schabbauer (2020). "Environmental arginine controls multinuclear giant cell metabolism and formation." Nat Commun **11**(1): 431.

Budanov, A. V. and M. Karin (2008). "p53 Target Genes Sestrin1 and Sestrin2 Connect Genotoxic Stress and mTOR Signaling." Cell **134**(3): 451-460.

Bunse, T., A. D. Kosinska, T. Michler and U. Protzer (2022). "PD-L1 Silencing in Liver Using siRNAs Enhances Efficacy of Therapeutic Vaccination for Chronic Hepatitis B." Biomolecules **12**(3).

Carpenter, K. L., C. van der Veen, S. E. Taylor, S. J. Hardwick, K. Clare, L. Hegyi and M. J. Mitchinson (1995). "Macrophages, lipid oxidation, ceroid accumulation and alpha-tocopherol depletion in human atherosclerotic lesions." Gerontology **41 Suppl 2**: 53-67.

Carr, E. L., A. Kelman, G. S. Wu, R. Gopaul, E. Senkevitch, A. Aghvanyan, A. M. Turay and K. A. Frauwirth (2010). "Glutamine uptake and metabolism are coordinately regulated by ERK/MAPK during T lymphocyte activation." J Immunol **185**(2): 1037-1044.

Chakraborty, A., C. Ko, C. Henning, A. Lucko, J. M. Harris, F. Chen, X. Zhuang, J. M. Wettengel, S. Roessler, U. Protzer and J. A. McKeating (2020). "Synchronised infection identifies early rate-limiting steps in the hepatitis B virus life cycle." Cell Microbiol **22**(12): e13250.

Chang, C. H., J. D. Curtis, L. B. Maggi, Jr., B. Faubert, A. V. Villarino, D. O'Sullivan, S. C. Huang, G. J. van der Windt, J. Blagih, J. Qiu, J. D. Weber, E. J. Pearce, R. G. Jones and E. L. Pearce (2013). "Posttranscriptional control of T cell effector function by aerobic glycolysis." Cell **153**(6): 1239-1251.

Cobbold, S. P., E. Adams, C. A. Farquhar, K. F. Nolan, D. Howie, K. O. Lui, P. J. Fairchild, A. L. Mellor, D. Ron and H. Waldmann (2009). "Infectious tolerance via the consumption of essential amino acids and mTOR signaling." Proc Natl Acad Sci U S A **106**(29): 12055-12060.

Cornberg, M., U. Protzer, J. Petersen, H. Wedemeyer, T. Berg, W. Jilg, A. Erhardt, S. Wirth, C. Sarrazin, M. M. Dollinger, P. Schirmacher, K. Dathe, I. B. Kopp, S. Zeuzem, W. H. Gerlich, M. P. Manns and Awmf (2011). "[Prophylaxis, diagnosis and therapy of hepatitis B virus infection - the German guideline]." Z Gastroenterol **49**(7): 871-930.

Crawford, J. and H. J. Cohen (1985). "The essential role of L-glutamine in lymphocyte differentiation in vitro." J Cell Physiol **124**(2): 275-282.

Das, A., M. Hoare, N. Davies, A. R. Lopes, C. Dunn, P. T. Kennedy, G. Alexander, H. Finney, A. Lawson, F. J. Plunkett, A. Bertoletti, A. N. Akbar and M. K. Maini (2008). "Functional skewing of the global CD8 T cell population in chronic hepatitis B virus infection." J Exp Med **205**(9): 2111-2124.

Dennis, M. D., N. K. McGhee, L. S. Jefferson and S. R. Kimball (2013). "Regulated in DNA damage and development 1 (REDD1) promotes cell survival during serum deprivation by sustaining repression of signaling through the mechanistic target of rapamycin in complex 1 (mTORC1)." Cellular Signalling **25**(12): 2709-2716.

Diaz, O., P.-O. Vidalain, C. Ramière, V. Lotteau and L. Perrin-Cocon (2022). "What role for cellular metabolism in the control of hepatitis viruses?" Frontiers in Immunology **13**.

Dion, S., M. Bourgine, O. Godon, F. Levillayer and M. L. Michel (2013). "Adeno-associated virus-mediated gene transfer leads to persistent hepatitis B virus replication in mice expressing HLA-A2 and HLA-DR1 molecules." J Virol **87**(10): 5554-5563.

Dong, J., H. Qiu, M. Garcia-Barrio, J. Anderson and A. G. Hinnebusch (2000). "Uncharged tRNA Activates GCN2 by Displacing the Protein Kinase Moiety from a Bipartite tRNA-Binding Domain." Molecular Cell **6**(2): 269-279.

Donnelly, R. P., R. M. Loftus, S. E. Keating, K. T. Liou, C. A. Biron, C. M. Gardiner and D. K. Finlay (2014). "mTORC1-dependent metabolic reprogramming is a prerequisite for NK cell effector function." J Immunol **193**(9): 4477-4484.

Doughty, C. A., B. F. Bleiman, D. J. Wagner, F. J. Dufort, J. M. Mataraza, M. F. Roberts and T. C. Chiles (2006). "Antigen receptor-mediated changes in glucose metabolism in B lymphocytes: role of phosphatidylinositol 3-kinase signaling in the glycolytic control of growth." Blood **107**(11): 4458-4465.

Esser, K., X. Cheng, J. M. Wettengel, J. Lucifora, L. Hansen-Palmus, K. Austen, A. A. Roca Suarez, S. Heintz, B. Testoni, F. Nebioglu, M. T. Pham, S. Yang, A. Zernecke, D. Wohlleber, M. Ringelhan, M. Broxtermann, D. Hartmann, N. Hüser, J. Mergner, A. Pichlmair, W. E. Thasler, M. Heikenwalder, G. Gasteiger, A. Blutke, A. Walch, P. A. Knolle, R. Bartenschlager and U. Protzer (2023). "Hepatitis B Virus Targets Lipid Transport Pathways to Infect Hepatocytes." Cellular and Molecular Gastroenterology and Hepatology **16**(2): 201-221.

European Association for the Study of the Liver. Electronic address, e. e. e. (2017). "EASL 2017 Clinical Practice Guidelines on the management of hepatitis B virus infection." J Hepatol **67**(2): 370-398.

Everts, B., E. Amiel, S. C. Huang, A. M. Smith, C. H. Chang, W. Y. Lam, V. Redmann, T. C. Freitas, J. Blagih, G. J. van der Windt, M. N. Artyomov, R. G. Jones, E. L. Pearce and E. J. Pearce (2014). "TLR-driven early glycolytic reprogramming via the kinases TBK1-IKKε supports the anabolic demands of dendritic cell activation." Nat Immunol **15**(4): 323-332.

Feldmeyer, N., G. Wabnitz, S. Leicht, C. Luckner-Minden, M. Schiller, T. Franz, R. Conradi, P. Kropf, I. Müller, A. D. Ho, Y. Samstag and M. Munder (2012). "Arginine deficiency leads to impaired cofilin dephosphorylation in activated human T lymphocytes." Int Immunol **24**(5): 303-313.

Freigang, S., F. Ampenberger, A. Weiss, T. D. Kanneganti, Y. Iwakura, M. Hersberger and M. Kopf (2013). "Fatty acid-induced mitochondrial uncoupling elicits inflammasome-independent IL-1α and sterile vascular inflammation in atherosclerosis." Nat Immunol **14**(10): 1045-1053.

Fultang, L., S. Booth, O. Yogev, B. Martins da Costa, V. Tubb, S. Panetti, V. Stavrou, U. Scarpa, A. Jankevics, G. Lloyd, A. Southam, S. P. Lee, W. B. Dunn, L. Chesler, F. Mussai and C. De Santo (2020). "Metabolic engineering against the arginine microenvironment enhances CAR-T cell proliferation and therapeutic activity." Blood **136**(10): 1155-1160.

Gan, W., N. Gao, L. Gu, Z. Mo, X. Pang, Z. Lei and Z. Gao (2023). "Reduction in Intrahepatic cccDNA and Integration of HBV in Chronic Hepatitis B Patients with a Functional Cure." Journal of Clinical and Translational Hepatology **11**(2): 314-322.

Gane, E. J. (2017). "Future anti-HBV strategies." Liver Int **37 Suppl 1**: 40-44.

Gao, W. and J. Hu (2007). "Formation of hepatitis B virus covalently closed circular DNA: removal of genome-linked protein." J Virol **81**(12): 6164-6174.

Geiger, R., J. C. Rieckmann, T. Wolf, C. Basso, Y. Feng, T. Fuhrer, M. Kogadeeva, P. Picotti, F. Meissner, M. Mann, N. Zamboni, F. Sallusto and A.

Lanzavecchia (2016). "L-Arginine Modulates T Cell Metabolism and Enhances Survival and Anti-tumor Activity." Cell **167**(3): 829-842.e813.

Gerriets, V. A., R. J. Kishton, A. G. Nichols, A. N. Macintyre, M. Inoue, O. Ilkayeva, P. S. Winter, X. Liu, B. Priyadharshini, M. E. Slawinska, L. Haeberli, C. Huck, L. A. Turka, K. C. Wood, L. P. Hale, P. A. Smith, M. A. Schneider, N. J. MacIver, J. W. Locasale, C. B. Newgard, M. L. Shinohara and J. C. Rathmell (2015). "Metabolic programming and PDHK1 control CD4+ T cell subsets and inflammation." J Clin Invest **125**(1): 194-207.

Graham, F. L., J. Smiley, W. C. Russell and R. Nairn (1977). "Characteristics of a Human Cell Line Transformed by DNA from Human Adenovirus Type 5." Journal of General Virology **36**(1): 59-72.

Grimes, J. M., S. Khan, M. Badeaux, R. M. Rao, S. W. Rowlinson and R. D. Carvajal (2021). "Arginine depletion as a therapeutic approach for patients with COVID-19." Int J Infect Dis **102**: 566-570.

Gubser, P. M., G. R. Bantug, L. Razik, M. Fischer, S. Dimeloe, G. Hoenger, B. Durovic, A. Jauch and C. Hess (2013). "Rapid effector function of memory CD8+ T cells requires an immediate-early glycolytic switch." Nat Immunol **14**(10): 1064-1072.

Guidotti, L. G., B. Matzke, H. Schaller and F. V. Chisari (1995). "High-level hepatitis B virus replication in transgenic mice." J Virol **69**(10): 6158-6169.

Hamilton, J. A., G. Vairo and S. R. Lingelbach (1986). "CSF-1 stimulates glucose uptake in murine bone marrow-derived macrophages." Biochem Biophys Res Commun **138**(1): 445-454.

Hannun, Y. A. and L. M. Obeid (2008). "Principles of bioactive lipid signalling: lessons from sphingolipids." Nat Rev Mol Cell Biol **9**(2): 139-150.

Hannun, Y. A. and L. M. Obeid (2018). "Sphingolipids and their metabolism in physiology and disease." Nature Reviews Molecular Cell Biology **19**(3): 175-191.

Harding, H. P., I. Novoa, Y. Zhang, H. Zeng, R. Wek, M. Schapira and D. Ron (2000). "Regulated translation initiation controls stress-induced gene expression in mammalian cells." Mol Cell **6**(5): 1099-1108.

Harding, H. P., Y. Zhang, H. Zeng, I. Novoa, P. D. Lu, M. Calfon, N. Sadri, C. Yun, B. Popko, R. Paules, D. F. Stojdl, J. C. Bell, T. Hettmann, J. M. Leiden and D. Ron (2003). "An Integrated Stress Response Regulates Amino Acid Metabolism and Resistance to Oxidative Stress." Molecular Cell **11**(3): 619-633.

Haschemi, A., P. Kosma, L. Gille, C. R. Evans, C. F. Burant, P. Starkl, B. Knapp, R. Haas, J. A. Schmid, C. Jandl, S. Amir, G. Lubec, J. Park, H. Esterbauer, M. Bilban, L. Brizuela, J. A. Pospisilik, L. E. Otterbein and O. Wagner (2012). "The sedoheptulose kinase CARKL directs macrophage polarization through control of glucose metabolism." Cell Metab **15**(6): 813-826.

Hu, J. (2016). Hepatitis B Virus Virology and Replication. Hepatitis B Virus in Human Diseases. Y.-F. Liaw and F. Zoulim. Cham, Springer International Publishing**:** 1-34.

Huang, L. R., Y. A. Gäbel, S. Graf, S. Arzberger, C. Kurts, M. Heikenwalder, P. A. Knolle and U. Protzer (2012). "Transfer of HBV genomes using low doses of adenovirus vectors leads to persistent infection in immune competent mice." Gastroenterology **142**(7): 1447-1450.e1443.

Huynh, A., M. DuPage, B. Priyadharshini, P. T. Sage, J. Quiros, C. M. Borges, N. Townamchai, V. A. Gerriets, J. C. Rathmell, A. H. Sharpe, J. A. Bluestone and L. A. Turka (2015). "Control of PI(3) kinase in Treg cells maintains homeostasis and lineage stability." Nat Immunol **16**(2): 188-196.

Indolfi, G., P. Easterbrook, G. Dusheiko, G. Siberry, M.-H. Chang, C. Thorne, M. Bulterys, P.-L. Chan, M. H. El-Sayed, C. Giaquinto, M. M. Jonas, T. Meyers, N. Walsh, S. Wirth and M. Penazzato (2019). "Hepatitis B virus infection in children and adolescents." The Lancet Gastroenterology & Hepatology **4**(6): 466-476.

Infantino, V., P. Convertini, L. Cucci, M. A. Panaro, M. A. Di Noia, R. Calvello, F. Palmieri and V. Iacobazzi (2011). "The mitochondrial citrate carrier: a new player in inflammation." Biochem J **438**(3): 433-436.

Jaspart, A., C. Calmels, O. Cosnefroy, P. Bellecave, P. Pinson, S. Claverol, V. Guyonnet-Dupérat, B. Dartigues, M. S. Benleulmi, E. Mauro, P. A. Gretteau, V. Parissi, M. Métifiot and M. L. Andreola (2017). "GCN2 phosphorylates HIV-1 integrase and decreases HIV-1 replication by limiting viral integration." Sci Rep **7**(1): 2283.

Jha, A. K., S. C. Huang, A. Sergushichev, V. Lampropoulou, Y. Ivanova, E. Loginicheva, K. Chmielewski, K. M. Stewart, J. Ashall, B. Everts, E. J. Pearce, E. M. Driggers and M. N. Artyomov (2015). "Network integration of parallel metabolic and transcriptional data reveals metabolic modules that regulate macrophage polarization." Immunity **42**(3): 419-430.

Kennedy, E. M., A. V. Kornepati and B. R. Cullen (2015). "Targeting hepatitis B virus cccDNA using CRISPR/Cas9." Antiviral Res **123**: 188-192.

Kennedy, P. T. F., E. Sandalova, J. Jo, U. Gill, I. Ushiro-Lumb, A. T. Tan, S. Naik, G. R. Foster and A. Bertoletti (2012). "Preserved T-cell function in children and young adults with immune-tolerant chronic hepatitis B." Gastroenterology **143**(3): 637-645.

Kilberg, M. S., J. Shan and N. Su (2009). "ATF4-dependent transcription mediates signaling of amino acid limitation." Trends in Endocrinology & Metabolism **20**(9): 436-443.

Ko, C., A. Chakraborty, W. M. Chou, J. Hasreiter, J. M. Wettengel, D. Stadler, R. Bester, T. Asen, K. Zhang, K. Wisskirchen, J. A. McKeating, W. S. Ryu and U. Protzer (2018). "Hepatitis B virus genome recycling and de novo secondary infection events maintain stable cccDNA levels." J Hepatol **69**(6): 1231-1241.

Ko, C., J. Su, J. Festag, R. Bester, A. D. Kosinska and U. Protzer (2021). "Intramolecular recombination enables the formation of hepatitis B virus (HBV) cccDNA in mice after HBV genome transfer using recombinant AAV vectors." Antiviral Res **194**: 105140.

Lee, G. K., H. J. Park, M. Macleod, P. Chandler, D. H. Munn and A. L. Mellor (2002). "Tryptophan deprivation sensitizes activated T cells to apoptosis prior to cell division." Immunology **107**(4): 452-460.

Lee, J., M. C. Walsh, K. L. Hoehn, D. E. James, E. J. Wherry and Y. Choi (2014). "Regulator of fatty acid metabolism, acetyl coenzyme a carboxylase 1, controls T cell immunity." J Immunol **192**(7): 3190-3199.

Li, F., Z. Wang, F. Hu and L. Su (2020). "Cell Culture Models and Animal Models for HBV Study." Adv Exp Med Biol **1179**: 109-135.

Li, Q., J. Wang, H. Islam, C. Kirschning, H. Lu, D. Hoffmann, U. Dittmer and M. Lu (2021). "Hepatitis B virus particles activate B cells through the TLR2-MyD88-mTOR axis." Cell Death Dis **12**(1): 34.

Lin, C. L. and J. H. Kao (2023). "Development of hepatocellular carcinoma in treated and untreated patients with chronic hepatitis B virus infection." Clin Mol Hepatol **29**(3): 605-622.

Liston, A. and S. L. Masters (2017). "Homeostasis-altering molecular processes as mechanisms of inflammasome activation." Nat Rev Immunol **17**(3): 208-214.

Liu, J., E. Zhang, Z. Ma, W. Wu, A. Kosinska, X. Zhang, I. Moller, P. Seiz, D. Glebe, B. Wang, D. Yang, M. Lu and M. Roggendorf (2014). "Enhancing virus-specific immunity in vivo by combining therapeutic vaccination and PD-L1 blockade in chronic hepadnaviral infection." PLoS Pathog **10**(1): e1003856.

Liu, Y., A. Cheng, M. Wang, S. Mao, X. Ou, Q. Yang, Y. Wu, Q. Gao, M. Liu, S. Zhang, J. Huang, R. Jia, D. Zhu, S. Chen, X. Zhao, Y. Yu, Y. Liu, L. Zhang, B. Tian and L. Pan (2021). "Duck Hepatitis A Virus Type 1 Induces eIF2α Phosphorylation-Dependent Cellular Translation Shutoff via PERK/GCN2." Frontiers in Microbiology **12**.

Liu, Y., A. Cheng, M. Wang, S. Mao, X. Ou, Q. Yang, Y. Wu, Q. Gao, M. Liu, S. Zhang, J. Huang, R. Jia, D. Zhu, S. Chen, X. Zhao, Y. Yu, Y. Liu, L. Zhang, B. Tian and L. Pan (2021). "Duck Hepatitis A Virus Type 1 Induces eIF2α Phosphorylation-Dependent Cellular Translation Shutoff via PERK/GCN2." Front Microbiol **12**: 624540.

Liu, Y., M. Wang, A. Cheng, Q. Yang, Y. Wu, R. Jia, M. Liu, D. Zhu, S. Chen, S. Zhang, X. X. Zhao, J. Huang, S. Mao, X. Ou, Q. Gao, Y. Wang, Z. Xu, Z. Chen, L. Zhu, Q. Luo, Y. Liu, Y. Yu, L. Zhang, B. Tian, L. Pan, M. U. Rehman and X. Chen (2020). "The role of host eIF2α in viral infection." Virol J **17**(1): 112.

Lok, A. S., B. J. McMahon, R. S. Brown, Jr., J. B. Wong, A. T. Ahmed, W. Farah, J. Almasri, F. Alahdab, K. Benkhadra, M. A. Mouchli, S. Singh, E. A. Mohamed, A. M. Abu Dabrh, L. J. Prokop, Z. Wang, M. H. Murad and K. Mohammed (2016).

"Antiviral therapy for chronic hepatitis B viral infection in adults: A systematic review and meta-analysis." Hepatology **63**(1): 284-306.

Lucifora, J., Y. Xia, F. Reisinger, K. Zhang, D. Stadler, X. Cheng, M. F. Sprinzl, H. Koppensteiner, Z. Makowska, T. Volz, C. Remouchamps, W. M. Chou, W. E. Thasler, N. Hüser, D. Durantel, T. J. Liang, C. Münk, M. H. Heim, J. L. Browning, E. Dejardin, M. Dandri, M. Schindler, M. Heikenwalder and U. Protzer (2014). "Specific and nonhepatotoxic degradation of nuclear hepatitis B virus cccDNA." Science **343**(6176): 1221-1228.

Luo, W., H. Hu, R. Chang, J. Zhong, M. Knabel, R. O'Meally, R. N. Cole, A. Pandey and G. L. Semenza (2011). "Pyruvate kinase M2 is a PHD3-stimulated coactivator for hypoxia-inducible factor 1." Cell **145**(5): 732-744.

MacMicking, J., Q. W. Xie and C. Nathan (1997). "Nitric oxide and macrophage function." Annu Rev Immunol **15**: 323-350.

MacMicking, J. D., C. Nathan, G. Hom, N. Chartrain, D. S. Fletcher, M. Trumbauer, K. Stevens, Q. W. Xie, K. Sokol, N. Hutchinson and et al. (1995). "Altered responses to bacterial infection and endotoxic shock in mice lacking inducible nitric oxide synthase." Cell **81**(4): 641-650.

Majano, P. L., C. García-Monzón, M. López-Cabrera, E. Lara-Pezzi, E. Fernández-Ruiz, C. García-Iglesias, M. J. Borque and R. Moreno-Otero (1998). "Inducible nitric oxide synthase expression in chronic viral hepatitis. Evidence for a virus-induced gene upregulation." J Clin Invest **101**(7): 1343-1352.

Malandrino, M. I., R. Fucho, M. Weber, M. Calderon-Dominguez, J. F. Mir, L. Valcarcel, X. Escoté, M. Gómez-Serrano, B. Peral, L. Salvadó, S. Fernández-Veledo, N. Casals, M. Vázquez-Carrera, F. Villarroya, J. J. Vendrell, D. Serra and L. Herrero (2015). "Enhanced fatty acid oxidation in adipocytes and macrophages reduces lipid-induced triglyceride accumulation and inflammation." Am J Physiol Endocrinol Metab **308**(9): E756-769.

Martí, I. L. A. A. and W. Reith (2021). "Arginine-dependent immune responses." Cell Mol Life Sci **78**(13): 5303-5324.

Mason, W. S. (2015). "Animal models and the molecular biology of hepadnavirus infection." Cold Spring Harb Perspect Med **5**(4).

McMahon, B. J. (2009). "The natural history of chronic hepatitis B virus infection." Hepatology **49**(5 Suppl): S45-55.

Michalek, R. D., V. A. Gerriets, S. R. Jacobs, A. N. Macintyre, N. J. MacIver, E. F. Mason, S. A. Sullivan, A. G. Nichols and J. C. Rathmell (2011). "Cutting edge: distinct glycolytic and lipid oxidative metabolic programs are essential for effector and regulatory CD4+ T cell subsets." J Immunol **186**(6): 3299-3303.

Michl, J., D. J. Ohlbaum and S. C. Silverstein (1976). "2-Deoxyglucose selectively inhibits Fc and complement receptor-mediated phagocytosis in mouse peritoneal macrophages. I. Description of the inhibitory effect." J Exp Med **144**(6): 1465-1483.

Michler, T., S. Große, S. Mockenhaupt, N. Röder, F. Stückler, B. Knapp, C. Ko, M. Heikenwalder, U. Protzer and D. Grimm (2016). "Blocking sense-strand activity improves potency, safety and specificity of anti-hepatitis B virus short hairpin RNA." EMBO Mol Med **8**(9): 1082-1098.

Michler, T., A. D. Kosinska, J. Festag, T. Bunse, J. Su, M. Ringelhan, H. Imhof, D. Grimm, K. Steiger, C. Mogler, M. Heikenwalder, M. L. Michel, C. A. Guzman, S. Milstein, L. Sepp-Lorenzino, P. Knolle and U. Protzer (2020). "Knockdown of Virus Antigen Expression Increases Therapeutic Vaccine Efficacy in High-titer HBV Carrier Mice." Gastroenterology.

Miller, R. H., S. Kaneko, C. T. Chung, R. Girones and R. H. Purcell (1989). "Compact organization of the hepatitis B virus genome." Hepatology **9**(2): 322-327.

Mukhopadhyay, R., J. Jia, A. Arif, P. S. Ray and P. L. Fox (2009). "The GAIT system: a gatekeeper of inflammatory gene expression." Trends Biochem Sci **34**(7): 324-331.

Munn, D. H., E. Shafizadeh, J. T. Attwood, I. Bondarev, A. Pashine and A. L. Mellor (1999). "Inhibition of T cell proliferation by macrophage tryptophan catabolism." J Exp Med **189**(9): 1363-1372.

Murphy, C. and P. Newsholme (1998). "Importance of glutamine metabolism in murine macrophages and human monocytes to L-arginine biosynthesis and rates of nitrite or urea production." Clin Sci (Lond) **95**(4): 397-407.

Muschet, C., G. Möller, C. Prehn, M. H. de Angelis, J. Adamski and J. Tokarz (2016). "Removing the bottlenecks of cell culture metabolomics: fast normalization procedure, correlation of metabolites to cell number, and impact of the cell harvesting method." Metabolomics **12**(10): 151.

Nakaya, M., Y. Xiao, X. Zhou, J. H. Chang, M. Chang, X. Cheng, M. Blonska, X. Lin and S. C. Sun (2014). "Inflammatory T cell responses rely on amino acid transporter ASCT2 facilitation of glutamine uptake and mTORC1 kinase activation." Immunity **40**(5): 692-705.

Newsholme, P., R. Curi, S. Gordon and E. A. Newsholme (1986). "Metabolism of glucose, glutamine, long-chain fatty acids and ketone bodies by murine macrophages." Biochem J **239**(1): 121-125.

O'Sullivan, D., G. J. van der Windt, S. C. Huang, J. D. Curtis, C. H. Chang, M. D. Buck, J. Qiu, A. M. Smith, W. Y. Lam, L. M. DiPlato, F. F. Hsu, M. J. Birnbaum, E. J. Pearce and E. L. Pearce (2014). "Memory CD8(+) T cells use cell-intrinsic lipolysis to support the metabolic programming necessary for development." Immunity **41**(1): 75-88.

Ochoa, J. B., J. Strange, P. Kearney, G. Gellin, E. Endean and E. Fitzpatrick (2001). "Effects of L-arginine on the proliferation of T lymphocyte subpopulations." JPEN J Parenter Enteral Nutr **25**(1): 23-29.

Okamoto, A., T. Nikaido, K. Ochiai, S. Takakura, M. Saito, Y. Aoki, N. Ishii, N. Yanaihara, K. Yamada, O. Takikawa, R. Kawaguchi, S. Isonishi, T. Tanaka and M. Urashima (2005). "Indoleamine 2,3-dioxygenase serves as a marker of poor prognosis in gene expression profiles of serous ovarian cancer cells." Clin Cancer Res **11**(16): 6030-6039.

Pallett, L. J., U. S. Gill, A. Quaglia, L. V. Sinclair, M. Jover-Cobos, A. Schurich, K. P. Singh, N. Thomas, A. Das, A. Chen, G. Fusai, A. Bertoletti, D. A. Cantrell, P. T. Kennedy, N. A. Davies, M. Haniffa and M. K. Maini (2015). "Metabolic regulation of hepatitis B immunopathology by myeloid-derived suppressor cells." Nat Med **21**(6): 591-600.

Palsson-McDermott, E. M., A. M. Curtis, G. Goel, M. A. Lauterbach, F. J. Sheedy, L. E. Gleeson, M. W. van den Bosch, S. R. Quinn, R. Domingo-Fernandez, D. G. Johnston, J. K. Jiang, W. J. Israelsen, J. Keane, C. Thomas, C. Clish, M. Vander Heiden, R. J. Xavier and L. A. O'Neill (2015). "Pyruvate kinase M2 regulates Hif-1α activity and IL-1β induction and is a critical determinant of the warburg effect in LPS-activated macrophages." Cell Metab **21**(1): 65-80.

Patsoukis, N., K. Bardhan, P. Chatterjee, D. Sari, B. Liu, L. N. Bell, E. D. Karoly, G. J. Freeman, V. Petkova, P. Seth, L. Li and V. A. Boussiotis (2015). "PD-1 alters T-cell metabolic reprogramming by inhibiting glycolysis and promoting lipolysis and fatty acid oxidation." Nat Commun **6**: 6692.

Peng, G., S. Li, W. Wu, X. Tan, Y. Chen and Z. Chen (2008). "PD-1 upregulation is associated with HBV-specific T cell dysfunction in chronic hepatitis B patients." Mol Immunol **45**(4): 963-970.

Pesce, J. T., T. R. Ramalingam, M. M. Mentink-Kane, M. S. Wilson, K. C. El Kasmi, A. M. Smith, R. W. Thompson, A. W. Cheever, P. J. Murray and T. A. Wynn (2009). "Arginase-1-expressing macrophages suppress Th2 cytokine-driven inflammation and fibrosis." PLoS Pathog **5**(4): e1000371.

Pfefferkorn, E. R. (1984). "Interferon gamma blocks the growth of Toxoplasma gondii in human fibroblasts by inducing the host cells to degrade tryptophan." Proc Natl Acad Sci U S A **81**(3): 908-912.

Protzer, U. (2017). "Viral hepatitis: The bumpy road to animal models for HBV infection." Nat Rev Gastroenterol Hepatol **14**(6): 327-328.

Rath, M., I. Müller, P. Kropf, E. I. Closs and M. Munder (2014). "Metabolism via Arginase or Nitric Oxide Synthase: Two Competing Arginine Pathways in Macrophages." Front Immunol **5**: 532.

Rodríguez-Prados, J. C., P. G. Través, J. Cuenca, D. Rico, J. Aragonés, P. Martín-Sanz, M. Cascante and L. Boscá (2010). "Substrate fate in activated macrophages: a comparison between innate, classic, and alternative activation." J Immunol **185**(1): 605-614.

Rodriguez, P. C., D. G. Quiceno and A. C. Ochoa (2007). "L-arginine availability regulates T-lymphocyte cell-cycle progression." Blood **109**(4): 1568-1573.

Rodriguez, P. C., A. H. Zea, K. S. Culotta, J. Zabaleta, J. B. Ochoa and A. C. Ochoa (2002). "Regulation of T cell receptor CD3zeta chain expression by L-arginine." J Biol Chem **277**(24): 21123-21129.

Rossi, M., A. Vecchi, C. Tiezzi, V. Barili, P. Fisicaro, A. Penna, I. Montali, S. Daffis, S. P. Fletcher, A. Gaggar, J. Medley, M. Graupe, L. Lad, A. Loglio, R. Soffredini, M. Borghi, T. Pollicino, C. Musolino, A. Alfieri, F. Brillo, D. Laccabue, M. Massari, C. Boarini, G. Abbati, G. Pedrazzi, G. Missale, P. Lampertico, C. Ferrari and C. Boni (2023). "Phenotypic CD8 T cell profiling in chronic hepatitis B to predict HBV-specific CD8 T cell susceptibility to functional restoration in vitro." Gut **72**(11): 2123-2137.

Schaefer, S. (2007). "Hepatitis B virus taxonomy and hepatitis B virus genotypes." World J Gastroenterol **13**(1): 14-21.

Schroten, H., B. Spors, C. Hucke, M. Stins, K. S. Kim, R. Adam and W. Däubener (2001). "Potential role of human brain microvascular endothelial cells in the pathogenesis of brain abscess: inhibition of Staphylococcus aureus by activation of indoleamine 2,3-dioxygenase." Neuropediatrics **32**(4): 206-210.

Seeger, C. and W. S. Mason (2015). "Molecular biology of hepatitis B virus infection." Virology **479-480**: 672-686.

Shi, L. Z., R. Wang, G. Huang, P. Vogel, G. Neale, D. R. Green and H. Chi (2011). "HIF1alpha-dependent glycolytic pathway orchestrates a metabolic checkpoint for the differentiation of TH17 and Treg cells." J Exp Med **208**(7): 1367-1376.

Shoelson, S. E., J. Lee and A. B. Goldfine (2006). "Inflammation and insulin resistance." The Journal of Clinical Investigation **116**(7): 1793-1801.

Spiegel, S. and S. Milstien (2011). "The outs and the ins of sphingosine-1-phosphate in immunity." Nat Rev Immunol **11**(6): 403-415.

Tannahill, G. M., A. M. Curtis, J. Adamik, E. M. Palsson-McDermott, A. F. McGettrick, G. Goel, C. Frezza, N. J. Bernard, B. Kelly, N. H. Foley, L. Zheng, A. Gardet, Z. Tong, S. S. Jany, S. C. Corr, M. Haneklaus, B. E. Caffrey, K. Pierce, S. Walmsley, F. C. Beasley, E. Cummins, V. Nizet, M. Whyte, C. T. Taylor, H. Lin, S. L. Masters, E. Gottlieb, V. P. Kelly, C. Clish, P. E. Auron, R. J. Xavier and L. A. O'Neill (2013). "Succinate is an inflammatory signal that induces IL-1β through HIF-1α." Nature **496**(7444): 238-242.

Tennant, B. C. and J. L. Gerin (2001). "The woodchuck model of hepatitis B virus infection." Ilar j **42**(2): 89-102.

Terrault, N. A., A. S. F. Lok, B. J. McMahon, K. M. Chang, J. P. Hwang, M. M. Jonas, R. S. Brown, Jr., N. H. Bzowej and J. B. Wong (2018). "Update on prevention, diagnosis, and treatment of chronic hepatitis B: AASLD 2018 hepatitis B guidance." Hepatology **67**(4): 1560-1599.

Tomé, D. (2021). "Amino acid metabolism and signalling pathways: potential targets in the control of infection and immunity." Nutr Diabetes **11**(1): 20.

Urban, S., R. Bartenschlager, R. Kubitz and F. Zoulim (2014). "Strategies to inhibit entry of HBV and HDV into hepatocytes." Gastroenterology **147**(1): 48-64.

Uyttenhove, C., L. Pilotte, I. Théate, V. Stroobant, D. Colau, N. Parmentier, T. Boon and B. J. Van den Eynde (2003). "Evidence for a tumoral immune resistance mechanism based on tryptophan degradation by indoleamine 2,3-dioxygenase." Nat Med **9**(10): 1269-1274.

Van de Velde, L. A., C. Subramanian, A. M. Smith, L. Barron, J. E. Qualls, G. Neale, A. Alfonso-Pecchio, S. Jackowski, C. O. Rock, T. A. Wynn and P. J. Murray (2017). "T Cells Encountering Myeloid Cells Programmed for Amino Acid-dependent Immunosuppression Use Rictor/mTORC2 Protein for Proliferative Checkpoint Decisions." J Biol Chem **292**(1): 15-30.

van der Windt, G. J., B. Everts, C. H. Chang, J. D. Curtis, T. C. Freitas, E. Amiel, E. J. Pearce and E. L. Pearce (2012). "Mitochondrial respiratory capacity is a critical regulator of CD8+ T cell memory development." Immunity **36**(1): 68-78.

Velkov, S., J. J. Ott, U. Protzer and T. Michler (2018). "The Global Hepatitis B Virus Genotype Distribution Approximated from Available Genotyping Data." Genes **9**(10): 495.

Wallace, C. and D. Keast (1992). "Glutamine and macrophage function." Metabolism **41**(9): 1016-1020.

Wei, L. and A. Ploss (2021). "Mechanism of Hepatitis B Virus cccDNA Formation." Viruses **13**(8).

Weichhart, T., M. Hengstschläger and M. Linke (2015). "Regulation of innate immune cell function by mTOR." Nat Rev Immunol **15**(10): 599-614.

Wisskirchen, K., J. Kah, A. Malo, T. Asen, T. Volz, L. Allweiss, J. M. Wettengel, M. Lütgehetmann, S. Urban, T. Bauer, M. Dandri and U. Protzer (2019). "T cell receptor grafting allows virological control of Hepatitis B virus infection." J Clin Invest **129**(7): 2932-2945.

Xu, D., W. Dai, L. Kutzler, H. A. Lacko, L. S. Jefferson, M. D. Dennis and S. R. Kimball (2020). "ATF4-Mediated Upregulation of REDD1 and Sestrin2 Suppresses mTORC1 Activity during Prolonged Leucine Deprivation." The Journal of Nutrition **150**(5): 1022-1030.

Yan, H., B. Peng, Y. Liu, G. Xu, W. He, B. Ren, Z. Jing, J. Sui and W. Li (2014). "Viral entry of hepatitis B and D viruses and bile salts transportation share common molecular determinants on sodium taurocholate cotransporting polypeptide." J Virol **88**(6): 3273-3284.

Yan, Z., J. Zeng, Y. Yu, K. Xiang, H. Hu, X. Zhou, L. Gu, L. Wang, J. Zhao, J. A. T. Young and L. Gao (2017). "HBVcircle: A novel tool to investigate hepatitis B virus covalently closed circular DNA." Journal of Hepatology **66**(6): 1149-1157.

Yao, F., Y. Chen, J. Shi, K. Ming, J. Liu, W. Xiong, M. Song, H. Du, Y. Wang, S. Zhang, Y. Wu, D. Wang and Y. Hu (2016). "Replication cycle of duck hepatitis A virus type 1 in duck embryonic hepatocytes." Virology **491**: 73-78.

Yoshida, R. and O. Hayaishi (1978). "Induction of pulmonary indoleamine 2,3-dioxygenase by intraperitoneal injection of bacterial lipopolysaccharide." Proc Natl Acad Sci U S A **75**(8): 3998-4000.

Yuen, M. F., E. J. Gane, D. J. Kim, F. Weilert, H. L. Yuen Chan, J. Lalezari, S. G. Hwang, T. Nguyen, O. Flores, G. Hartman, S. Liaw, O. Lenz, T. N. Kakuda, W. Talloen, C. Schwabe, K. Klumpp and N. Brown (2019). "Antiviral Activity, Safety, and Pharmacokinetics of Capsid Assembly Modulator NVR 3-778 in Patients with Chronic HBV Infection." Gastroenterology **156**(5): 1392-1403.e1397.

Zhang, B. Y., D. P. Chai, Y. H. Wu, L. P. Qiu, Y. Y. Zhang, Z. H. Ye and X. P. Yu (2019). "Potential Drug Targets Against Hepatitis B Virus Based on Both Virus and Host Factors." Curr Drug Targets **20**(16): 1636-1651.

Zhang, E., Z. Ma, Q. Li, H. Yan, J. Liu, W. Wu, J. Guo, X. Zhang, C. J. Kirschning, H. Xu, P. A. Lang, D. Yang, U. Dittmer, H. Yan and M. Lu (2019). "TLR2 Stimulation Increases Cellular Metabolism in CD8(+) T Cells and Thereby Enhances CD8(+) T Cell Activation, Function, and Antiviral Activity." J Immunol **203**(11): 2872-2886.

Zukunft, S., M. Sorgenfrei, C. Prehn, G. Möller and J. Adamski (2013). "Targeted Metabolomics of Dried Blood Spot Extracts." Chromatographia **76**(19): 1295-1305.

7. Acknowledgment

First, I would like to express my gratitude to my supervisor, Prof. Dr. Ulrike Protzer, for providing me with the opportunity to work on my second thesis at the Institute of Virology. The past few years have been an interesting and challenging period in virology, and I am thankful for the role I have been able to play in addressing these challenges. I am particularly appreciative of her unwavering support throughout the project and her scientific guidance.

I extend special thanks to Prof. Dr. Peter Murray and Prof. Dr. Stefanie Eyerich for serving as supervisors for my project and for their contributions during thesis committee meetings.

I am very thankful to my colleagues at the Institute of Virology for their support in the laboratory and for providing such a welcoming working environment. I would like to extend my gratitude to Theresa Asen, Anna Kosinska, Merve Gülcan, Philipp Hagen, Susanne Miko, and Edanur Öz for their fruitful discussions and assistance with experiments. Additionally, I wish to thank the entire Diagnostics department for their warm welcome, with special mention to Samuel Jeske, Natalia Graf, Dr. Jochen Wettengel, Dr. Dieter Hoffmann, Catharina Crista, and Mehmet Tekinsoy.

I also want to express my heartfelt appreciation to my friends for their unwavering support.

I am grateful to Dr. Anindita Chakraborty and Dr. Anna Kosinska for their assistance in proofreading the thesis and providing corrections.

Ganz besonders möchte ich auch meiner Familie für die bedingungslose Unterstützung danken.

Publications and meetings

Articles in peer-reviewed journals

Wettengel JM*, **Bunse T***, Jeske SD, Wölfel R, Zange S, Taeubner J, Goelnitz U, Protzer U. Implementation and clinical evaluation of an Mpox virus laboratory-developed test on a fully automated random-access platform. J Med Virol. 2023 Aug;95(8):e29022. doi: 10.1002/jmv.29022. PMID: 37565757.

Bunse T, Koerber N, Wintersteller H, Schneider J, Graf A, Radonic A, Thuermer A, von Kleist M, Blum H, Spinner CD, Bauer T, Knolle PA, Protzer U, Schulte EC. T-Cell-Dominated Immune Response Resolves Protracted SARS-CoV-2 Infection in the Absence of Neutralizing Antibodies in an Immunocompromised Individual. Microorganisms. 2023 Jun 12;11(6):1562. doi: 10.3390/microorganisms11061562. PMID: 37375064; PMCID: PMC10304262.

Bunse T, Kosinska AD, Michler T, Protzer U. PD-L1 Silencing in Liver Using siRNAs Enhances Efficacy of Therapeutic Vaccination for Chronic Hepatitis B. Biomolecules. 2022 Mar 18;12(3):470. doi: 10.3390/biom12030470. PMID: 35327662; PMCID: PMC8946278.

Malin JJ, **Bunse T**, Spinner CD, Protzer U. Antivirale Medikamente: Potente Wirkstoffe, Hoffnungsträger bei COVID-19 und therapeutische Grenzen [Antiviral drugs : Potent agents, promising therapies for COVID-19 and therapeutic limitations]. Internist (Berl). 2022 Jan;63(1):118-128. German. doi: 10.1007/s00108-021-01233-4. Epub 2022 Jan 5. PMID: 34988607; PMCID: PMC8730307.

Michler T, Kosinska AD, Festag J, **Bunse T**, Su J, Ringelhan M, Imhof H, Grimm D, Steiger K, Mogler C, Heikenwalder M, Michel ML, Guzman CA, Milstein S, Sepp-Lorenzino L, Knolle P, Protzer U. Knockdown of Virus Antigen Expression Increases Therapeutic Vaccine Efficacy in High-Titer Hepatitis B Virus Carrier Mice. Gastroenterology. 2020 May;158(6):1762-1775.e9. doi: 10.1053/j.gastro.2020.01.032. Epub 2020 Jan 28. PMID: 32001321.

International conferences

2022 International HBV Meeting-The Molecular Biology of Hepatitis B Viruses
September 18-22, 2022, Paris, France

Poster: PD-L1 silencing in liver using siRNAs enhances efficacy of therapeutic vaccination for chronic hepatitis B

8. Appendix

8.1. RNAseq Results Tables

Genes were identified using differential gene expression analysis and sorted by their p-value. Tables contain the top 100 genes.

8.1.1. Table corresponding to Fig. 11

#ID	Symbol	P-Value	Log_2-FC
ENSG00000145920	CPLX2	0.000140054206318497	0.918015807048732
ENSG00000167244	IGF2	0.000148163379994263	-117.926.178.574.262
ENSG00000090339	ICAM1	0.000174170594032383	0.72499011373201
ENSG00000101323	HAO1	0.000211203385015674	-149.666.137.498.652
ENSG00000163993	S100P	0.000286876474394777	0.80144832570023
ENSG00000177144	NUDT4B	0.000288826940044758	119.242.826.421.185
NewGene_18258	NewGene_18258	0.000326284153777415	181.941.829.314.912
ENSG00000254536	AL360181.3	0.000380152787373057	147.054.632.377.499
NewGene_9341	NewGene_9341	0.000488599812278491	-135.933.815.065.186
ENSG00000130821	SLC6A8	0.000491189985974744	-0.613256666371041
ENSG00000168003	SLC3A2	0.000674559629770851	0.63371551024271
ENSG00000196917	HCAR1	0.000694046044119451	133.424.996.026.859
ENSG00000164749	HNF4G	0.00069651899483483	15.037.558.267.788
ENSG00000285162	AC004593.3	0.000762881855802685	10.226.077.088.285
ENSG00000256206	AC018523.2	0.000956714628050848	1.227.053.589.799
ENSG00000115902	SLC1A4	0.000979190770007608	0.607529968092801
NewGene_13835	NewGene_13835	0.00102890170496359	-146.668.250.847.067
ENSG00000224389	C4B	0.00105831696937011	0.648663718767798
ENSG00000103888	CEMIP	0.00106584853821091	0.657961128430256
ENSG00000128165	ADM2	0.0011014320140836	0.772738877794545
ENSG00000197859	ADAMTSL2	0.00118624168981975	127.426.796.528.782
NewGene_1232	NewGene_1232	0.00125013792072751	10.033.158.875.341
ENSG00000077238	IL4R	0.00131838827725265	0.714203304419411
ENSG00000283782	AC116366.3	0.00146902837169228	-0.883396750717592

ENSG00000124253	PCK1	0.00147972298684545	-0.634086730309562
ENSG00000285953	AC000120.3	0.00156402461909905	-162.220.603.320.872
ENSG00000109321	AREG	0.00159704842748876	0.901383654345699
ENSG00000118785	SPP1	0.0016062102114406	0.594428105270724
ENSG00000139514	SLC7A1	0.00162817255217958	0.664664692268883
ENSG00000148795	CYP17A1	0.00222809778139004	-0.628683852739597
ENSG00000087266	SH3BP2	0.00264766342522567	0.670364167752369
ENSG00000167680	SEMA6B	0.00267727030041404	129.250.896.137.948
ENSG00000170509	HSD17B13	0.00330372184268716	-0.788578088645969
ENSG00000258674	AC011448.1	0.00381382024450159	-102.456.022.107.127
ENSG00000243955	GSTA1	0.00383520489944064	-0.63346899922361
NewGene_11957	NewGene_11957	0.00410883675668158	-0.97951149155941
ENSG00000173212	MAB21L3	0.00416019590529355	120.213.347.408.555
ENSG00000104880	ARHGEF18	0.0047333406181037	0.690023741882028
ENSG00000203896	LIME1	0.00478949372344931	131.508.622.957.502
ENSG00000137309	HMGA1	0.0051690595926689	0.848047695673117
ENSG00000196616	ADH1B	0.00533192810743368	-0.95413280296045
NewGene_20569	NewGene_20569	0.00547927337046768	-152.312.984.961.557
NewGene_14681	NewGene_14681	0.00611704213773918	0.857228016255082
ENSG00000163814	CDCP1	0.00648010664989684	0.864358737322791
NewGene_15534	NewGene_15534	0.00648378008924749	0.906183363611139
ENSG00000103257	SLC7A5	0.0066037506225039	0.696036708260075
ENSG00000185022	MAFF	0.00665223367286755	0.852877919369769
ENSG00000196924	FLNA	0.00666709443306443	0.686362033538247
ENSG00000171791	BCL2	0.00704002573065965	0.793964022524359
ENSG00000168477	TNXB	0.00704150062603942	0.913765549098277
ENSG00000167861	HID1	0.00708941228815871	0.695038896968764
ENSG00000277957	SENP3-EIF4A1	0.007149654626916	171.084.310.349.357
ENSG00000019186	CYP24A1	0.00729143365594214	0.924175512884015
ENSG00000258653	AC005520.1	0.00731518829466067	-113.892.907.806.285
ENSG00000231852	CYP21A2	0.00776463859891081	0.743785303537818

ENSG00000187867	PALM3	0.00780483632667628	-0.787030668393374
NewGene_2458	NewGene_2458	0.00806413847297719	101.974.210.806.493
ENSG00000266086	AC015813.2	0.00862924081180162	-0.900804208498367
ENSG00000273259	AL049839.2	0.00883790946298391	142.507.547.228.811
ENSG00000274588	DGKK	0.0092862886284359	0.707733661036445
ENSG00000106006	HOXA6	0.00955439124058572	108.161.426.371.199
ENSG00000155760	FZD7	0.00986229168293552	0.949615188206668
ENSG00000134470	IL15RA	0.00989032929519209	0.913780562227174
ENSG00000120833	SOCS2	0.00991908665000559	0.812403462652194
ENSG00000137331	IER3	0.00994304992744921	0.685024310806063
ENSG00000167600	CYP2S1	0.0101379726749029	0.852017622695889
ENSG00000187134	AKR1C1	0.0101634838188978	-0.773004419573138
ENSG00000174721	FGFBP3	0.0109420608906913	0.960162456295076
ENSG00000070019	GUCY2C	0.0109765211081781	0.947908412208164
ENSG00000213928	IRF9	0.0113171409861942	117.199.915.968.072
ENSG00000156535	CD109	0.0115796602060558	0.715645431672836
ENSG00000187860	CCDC157	0.0126916052005923	-107.490.075.883.938
ENSG00000072201	LNX1	0.0129260046702808	100.393.318.237.804
ENSG00000148965	SAA4	0.0130506111734083	-0.752536007051433
ENSG00000183153	GJD3	0.0132063294673745	115.338.238.923.407
NewGene_14837	NewGene_14837	0.0132186318920058	-0.726905355209143
ENSG00000132470	ITGB4	0.0133591534073216	0.75689291411513
ENSG00000159842	ABR	0.0136996677531392	0.609185319916733
ENSG00000244474	UGT1A4	0.0138454436182287	-0.716066424859887
ENSG00000253710	ALG11	0.0139102753938321	-0.640456135319352
ENSG00000188223	AD000671.1	0.0139812415761053	-188.273.180.798.384
ENSG00000124313	IQSEC2	0.0142880941019588	-10.257.529.116.417
ENSG00000142627	EPHA2	0.014901321510704	0.680581362221538
ENSG00000197951	ZNF71	0.0150585596149948	0.918509207117285
ENSG00000237649	KIFC1	0.0154999205284621	-116.803.063.682.988
ENSG00000196660	SLC30A10	0.0158536773105582	-0.690377097500201

ENSG00000148400	NOTCH1	0.0161319992080622	0.894474740314891

8.1.2. Table corresponding to Fig. 12

#ID	Symbol	P-Value	Log_2-FC
ENSG00000146678	IGFBP1	1,62E-301	498.199.089.790.128
ENSG00000125999	BPIFB1	2,86E-268	573.696.984.248.757
ENSG00000113083	LOX	3,29E-228	471.159.287.328.356
ENSG00000134107	BHLHE40	6,21E-213	318.614.183.359.968
ENSG00000159399	HK2	1,65E-197	431.983.265.328.975
ENSG00000079308	TNS1	4,01E-185	597.590.917.824.527
ENSG00000059804	SLC2A3	1,03E-170	395.516.544.687.838
ENSG00000131482	G6PC	4,84E-164	263.524.476.416.685
ENSG00000138640	FAM13A	6,18E-159	369.815.777.630.402
NewGene_6341	NewGene_6341	8,17E-155	603.953.741.923.546
ENSG00000170509	HSD17B13	2,31E-146	280.019.251.068.251
ENSG00000129521	EGLN3	2,68E-139	474.737.048.344.157
ENSG00000182022	CHST15	4,08E-137	337.138.959.284.358
ENSG00000114268	PFKFB4	4,53E-136	343.624.623.850.058
ENSG00000106366	SERPINE1	2,93E-134	396.926.529.028.838
ENSG00000186910	SERPINA11	6,86E-132	468.527.059.887.139
ENSG00000167244	IGF2	3,44E-125	457.389.651.737.078
ENSG00000172765	TMCC1	1,30E-118	276.406.425.273.808
ENSG00000109107	ALDOC	3,56E-111	316.001.784.490.229
ENSG00000118523	CTGF	5,51E-109	213.307.212.060.944
ENSG00000152952	PLOD2	5,75E-109	234.171.813.508.867
ENSG00000182534	MXRA7	1,11E-108	246.690.374.188.696
ENSG00000162267	ITIH3	1,77E-106	267.705.260.148.536
ENSG00000137642	SORL1	1,54E-105	289.136.106.319.015
ENSG00000107159	CA9	5,11E-103	61.536.500.764.465
NewGene_8715	NewGene_8715	1,85E-100	441.166.043.375.989
ENSG00000257017	HP	2,41E-97	295.155.478.627.305

ENSG00000152256	PDK1	5,92E-96	353.371.761.443.553
ENSG00000124253	PCK1	9,06E-93	25.600.569.256.209
ENSG00000136881	BAAT	4,31E-91	199.151.836.366.102
ENSG00000164406	LEAP2	2,53E-90	201.695.285.574.814
ENSG00000185100	ADSSL1	2,22E-87	275.033.392.601.107
ENSG00000213213	CCDC183	7,92E-86	362.697.995.211.556
ENSG00000140107	SLC25A47	5,68E-85	372.043.835.316.817
ENSG00000122884	P4HA1	7,51E-85	231.531.414.499.731
ENSG00000078898	BPIFB2	1,06E-84	548.548.486.925.317
ENSG00000100593	ISM2	2,87E-84	347.441.312.765.706
ENSG00000104419	NDRG1	2,45E-83	247.610.282.885.193
ENSG00000114480	GBE1	6,65E-79	206.813.910.189.186
ENSG00000136859	ANGPTL2	1,14E-78	370.471.771.070.871
ENSG00000155093	PTPRN2	4,57E-77	248.419.051.396.257
ENSG00000170525	PFKFB3	1,67E-75	27.563.268.699.911
ENSG00000111674	ENO2	2,64E-75	29.327.010.574.255
ENSG00000116260	QSOX1	2,75E-75	251.955.140.423.442
ENSG00000130173	ANGPTL8	2,29E-72	288.593.735.898.913
ENSG00000183036	PCP4	3,37E-72	921.870.994.906.164
NewGene_21559	NewGene_21559	3,98E-71	842.127.298.993.631
ENSG00000130821	SLC6A8	2,76E-70	25.021.043.484.362
NewGene_16243	NewGene_16243	5,94E-70	443.658.466.429.912
ENSG00000118729	CASQ2	7,56E-70	516.410.116.235.792
ENSG00000102144	PGK1	2,89E-69	219.435.475.194.397
ENSG00000145287	PLAC8	6,25E-69	596.801.563.643.499
ENSG00000105707	HPN	4,16E-68	314.837.239.803.047
ENSG00000171766	GATM	8,73E-68	243.098.298.509.343
ENSG00000158874	APOA2	1,63E-66	209.058.519.078.322
ENSG00000134333	LDHA	8,70E-66	178.342.398.486.115
ENSG00000148926	ADM	4,31E-65	276.776.990.179.692
ENSG00000119938	PPP1R3C	1,92E-61	207.538.849.006.113

ENSG00000111452	ADGRD1	1,69E-60	544.732.181.537.313
ENSG00000047457	CP	2,71E-60	538.827.666.419.263
NewGene_2226	NewGene_2226	1,77E-58	419.746.408.998.925
ENSG00000135636	DYSF	8,70E-58	3.905.721.791.175
ENSG00000113739	STC2	2,69E-57	215.690.509.495.487
ENSG00000142583	SLC2A5	2,41E-56	557.153.401.411.105
ENSG00000214491	SEC14L6	5,62E-56	27.722.795.827.661
ENSG00000104765	BNIP3L	6,76E-56	171.948.936.964.674
ENSG00000067225	PKM	3,34E-55	183.024.981.319.237
ENSG00000197930	ERO1A	1,18E-54	203.500.063.590.646
ENSG00000170345	FOS	2,06E-54	28.360.988.568.703
ENSG00000269190	FBXO17	4,16E-54	195.301.871.162.581
ENSG00000073060	SCARB1	8,28E-54	198.263.548.125.662
ENSG00000100060	MFNG	1,73E-53	187.878.798.924.985
NewGene_21191	NewGene_21191	2,12E-52	812.473.564.768.551
ENSG00000061656	SPAG4	2,84E-52	377.743.604.716.294
ENSG00000110436	SLC1A2	2,94E-52	17.568.598.703.216
ENSG00000180758	GPR157	1,11E-51	176.075.487.138.764
ENSG00000133401	PDZD2	1,61E-51	632.866.907.442.068
ENSG00000197496	SLC2A10	3,86E-51	20.759.890.476.328
ENSG00000081051	AFP	7,82E-50	156.722.405.475.655
ENSG00000196557	CACNA1H	8,20E-50	295.448.808.737.504
ENSG00000112715	VEGFA	3,47E-49	196.637.403.460.279
ENSG00000116285	ERRFI1	6,92E-49	159.635.860.184.636
ENSG00000145192	AHSG	1,07E-48	184.891.739.211.095
ENSG00000105220	GPI	1,77E-48	164.636.775.736.712
ENSG00000130822	PNCK	2,01E-48	426.344.657.067.213
ENSG00000149573	MPZL2	4,41E-47	195.916.824.233.559
ENSG00000244187	TMEM141	6,33E-47	213.831.552.149.112
ENSG00000074800	ENO1	1,45E-46	179.970.096.250.445
NewGene_8789	NewGene_8789	3,28E-45	635.062.929.997.562

NewGene_16563	NewGene_16563	6,12E-45	284.068.404.302.933
ENSG00000157557	ETS2	1,15E-44	174.331.752.740.634
ENSG00000115414	FN1	3,40E-44	179.913.881.447.578
ENSG00000156222	SLC28A1	6,17E-43	243.586.917.109.429
ENSG00000285043	AC093512.2	1,36E-42	314.422.473.957.089
ENSG00000272196	HIST2H2AA4	1,51E-42	-151.281.375.768.514
ENSG00000203812	HIST2H2AA3	1,54E-42	-150.420.894.751.657
ENSG00000110245	APOC3	2,50E-42	205.803.582.065.583
ENSG00000130208	APOC1	1,30E-41	192.862.111.855.749
ENSG00000134716	CYP2J2	1,92E-41	326.551.198.848.318
ENSG00000283932	AL121722.1	2,76E-41	154.541.764.258.722

8.1.3. Table corresponding to Fig. 13

#ID	Symbol	P-Value	Log_2-FC
ENSG00000113083	LOX	2,36E-42	490.903.586.288.228
NewGene_21559	NewGene_21559	6,61E-40	111.450.407.183.105
NewGene_6341	NewGene_6341	9,32E-39	561.882.651.710.707
ENSG00000146678	IGFBP1	4,56E-34	596.221.444.787.126
ENSG00000129521	EGLN3	1,76E-33	589.731.421.966.473
ENSG00000079308	TNS1	2,93E-32	638.747.348.057.046
ENSG00000183036	PCP4	5,49E-31	131.146.530.313.845
ENSG00000159399	HK2	5,60E-31	417.200.048.717.157
ENSG00000059804	SLC2A3	8,15E-31	436.672.094.536.622
ENSG00000171570	RAB4B-EGLN2	1,32E-28	-128.667.598.267.624
ENSG00000167244	IGF2	6,53E-28	626.903.459.703.235
ENSG00000186910	SERPINA11	1,14E-25	485.811.850.051.613
ENSG00000145287	PLAC8	4,81E-25	775.916.773.361.966
ENSG00000078898	BPIFB2	1,29E-24	692.571.604.486.139
ENSG00000135636	DYSF	1,27E-22	456.271.623.420.174
NewGene_2226	NewGene_2226	1,40E-22	425.559.099.979.442
ENSG00000106366	SERPINE1	1,62E-22	387.128.962.099.919
ENSG00000118729	CASQ2	2,07E-22	616.636.646.478.723

NewGene_21191	NewGene_21191	6,03E-22	122.092.822.081.266
ENSG00000047457	CP	1,08E-21	603.251.802.256.315
ENSG00000138640	FAM13A	1,16E-21	420.500.350.150.465
ENSG00000172264	MACROD2	7,49E-21	540.081.585.588.762
ENSG00000241978	AKAP2	2,92E-20	-115.627.222.993.523
ENSG00000114268	PFKFB4	3,21E-20	401.854.354.797.477
NewGene_8715	NewGene_8715	4,76E-20	505.133.156.252.081
ENSG00000152256	PDK1	9,94E-19	356.111.660.729.531
ENSG00000109107	ALDOC	1,46E-17	387.665.053.607.565
ENSG00000142583	SLC2A5	2,33E-17	624.316.649.161.022
ENSG00000172765	TMCC1	2,46E-17	339.328.546.033.063
NewGene_16243	NewGene_16243	1,82E-16	551.496.416.479.053
ENSG00000182022	CHST15	4,48E-16	351.729.510.459.512
ENSG00000130821	SLC6A8	5,92E-16	335.237.211.239.633
ENSG00000136859	ANGPTL2	1,39E-15	416.541.703.261.722
ENSG00000185100	ADSSL1	1,94E-15	338.941.680.566.232
ENSG00000149043	SYT8	1,30E-14	629.904.758.408.451
ENSG00000182534	MXRA7	7,90E-14	286.685.038.995.506
ENSG00000124253	PCK1	5,32E-13	317.523.313.196.658
ENSG00000061656	SPAG4	1,31E-12	505.726.238.025.427
ENSG00000100593	ISM2	2,18E-12	348.128.245.814.411
ENSG00000283247	AC096582.3	9,09E-12	741.328.407.133.564
ENSG00000111674	ENO2	1,12E-11	322.961.262.954.151
ENSG00000107159	CA9	1,53E-11	888.113.359.679.382
NewGene_22906	NewGene_22906	1,05E-10	699.896.262.652.476
ENSG00000104419	NDRG1	3,27E-10	291.070.354.888.011
ENSG00000140107	SLC25A47	3,48E-10	478.924.343.301.983
ENSG00000111452	ADGRD1	9,31E-10	482.110.730.615.678
ENSG00000133401	PDZD2	1,22E-09	670.702.675.400.536
ENSG00000156222	SLC28A1	1,67E-09	310.976.545.927.944
ENSG00000134716	CYP2J2	1,72E-09	398.377.370.310.278

NewGene_19620	NewGene_19620	1,89E-09	579.765.907.039.859
ENSG00000170509	HSD17B13	1,95E-09	348.464.806.365.362
ENSG00000089356	FXYD3	2,03E-09	11.156.299.546.378
ENSG00000134107	BHLHE40	7,26E-09	316.645.575.975.647
ENSG00000183873	SCN5A	2,20E-08	10.204.854.004.383
ENSG00000102144	PGK1	2,38E-08	27.384.009.001.891
NewGene_4014	NewGene_4014	1,61E-07	597.715.360.140.378
ENSG00000148926	ADM	2,00E-07	35.316.374.866.823
ENSG00000213213	CCDC183	2,20E-07	38.743.394.596.658
NewGene_13835	NewGene_13835	2,40E-07	468.895.390.665.848
ENSG00000171766	GATM	2,92E-07	312.558.804.945.412
ENSG00000162267	ITIH3	5,31E-07	256.739.642.367.108
ENSG00000164442	CITED2	6,91E-07	443.964.838.991.654
NewGene_8789	NewGene_8789	1,27E-06	668.277.101.840.083
ENSG00000122884	P4HA1	1,93E-06	271.352.545.924.145
ENSG00000170345	FOS	2,04E-06	308.098.616.543.091
NewGene_18254	NewGene_18254	3,57E-06	622.789.612.021.135
NewGene_13015	NewGene_13015	1,02E-05	552.732.677.543.564
ENSG00000170525	PFKFB3	2,10E-05	269.335.758.364.767
ENSG00000074211	PPP2R2C	2,21E-05	347.777.727.842.177
ENSG00000114480	GBE1	2,65E-05	251.096.727.939.811
ENSG00000167601	AXL	2,71E-05	36.816.085.252.969
ENSG00000119227	PIGZ	3,25E-05	320.030.280.159.098
ENSG00000155093	PTPRN2	5,13E-05	265.437.630.142.709
ENSG00000130173	ANGPTL8	6,99E-05	444.211.480.710.563
ENSG00000186352	ANKRD37	1,18E-04	416.670.052.411.267
ENSG00000153902	LGI4	1,21E-04	990.627.023.161.435
ENSG00000119938	PPP1R3C	1,65E-04	241.306.164.800.094
ENSG00000244242	IFITM10	2,54E-04	467.306.411.930.927
ENSG00000134363	FST	2,82E-04	392.381.522.643.205
ENSG00000180448	ARHGAP45	2,88E-04	297.307.478.445.667

ENSG00000214491	SEC14L6	3,03E-04	25.843.017.336.079
ENSG00000011347	SYT7	3,05E-04	312.884.439.864.508
ENSG00000169403	PTAFR	3,17E-04	323.980.720.252.153
ENSG00000160182	TFF1	3,31E-04	855.326.804.428.656
ENSG00000189334	S100A14	9,96E-04	530.425.636.395.527
NewGene_4895	NewGene_4895	1,79E-03	779.860.835.905.002
ENSG00000160180	TFF3	4,36E-03	539.647.727.481.674
NewGene_11297	NewGene_11297	4,61E-03	446.581.613.541.014
ENSG00000143595	AQP10	5,68E-03	429.813.435.999.912
ENSG00000272398	CD24	6,00E-03	234.915.189.804.425
ENSG00000116260	QSOX1	8,36E-03	297.910.199.204.992
ENSG00000152952	PLOD2	1,47E-02	271.234.233.945.939
ENSG00000149573	MPZL2	1,93E-02	220.664.071.763.507
ENSG00000257017	HP	2,10E-02	246.270.021.139.034
ENSG00000118523	CTGF	2,18E-02	225.719.563.084.303
ENSG00000127241	MASP1	2,60E-02	551.640.100.698.009
ENSG00000181378	CFAP65	2,81E-02	531.517.509.264.177
NewGene_22437	NewGene_22437	3,65E-02	578.151.546.896.799
ENSG00000197496	SLC2A10	3,73E-02	211.762.479.358.756
ENSG00000197930	ERO1A	4,39E-02	219.091.846.156.901

8.2. Metabolom Analysis Results

Targeted metabolomics analysis was performed and absolute quantification of each metabolite is given in the following tables (μM).

8.2.1. Aminoacids

	Ala	Arg	Asn	Asp	Cit	Gln	Glu	Gly	His	Ile	Leu	Lys	Met	Orn	Phe	Pro	Ser	Thr	Trp	Tyr	Val
01H_300	22,5	3,61	6,52	29,3	0,136	56,5	174	78,5	11,6	2,41	1,96	9,41	1,54	0,304	3,99	14,4	169	43,2	0,88	12,9	5,65
02H_300	22,5	4,11	7,9	26,3	0,591	44,6	191	94,5	9,87	1,46	1,29	8,94	0,992	0,258	2,85	12,6	198	53,7	0,79	14,1	4,3
03H_300	21,6	4,51	9,15	33	0,128	48,8	187	102	8,71	0,99	1,42	11,9	0,858	0,308	2,28	13,8	182	44,4	0,871	13,4	3,36
04H_300	18,6	4,74	7,39	31,8	0,105	40,1	175	101	7,25	0,883	0,756	11,2	0,764	0,279	1,81	14,3	218	45,2	0,844	13,5	3,19
05H_300	19,9	3,14	7,18	42	0,127	34,8	192	76,3	5,74	0,718	0,709	8,11	0,642	0,237	1,53	13,7	163	43,6	0,771	9,99	2,38
06H_300	19,8	4,09	7,19	42,2	0,142	41,7	171	98,1	6,06	0,823	1,14	11,4	0,778	0,236	1,52	14,7	197	43,9	0,907	11,4	2,42
07H_600	84,3	2,16	5,65	14,6	0,17	34,9	208	41,7	13,1	12,3	8,86	7,08	2,87	0,35	10,7	81,4	60,1	62,9	1,72	14	13,8
08H_600	68,9	4,14	5,62	30,1	0,492	27,7	209	45,2	11,6	9,72	7,04	6,35	2,66	0,305	8,08	67	68,4	52,7	1,76	14	10,7
09H_600	61,4	2,52	4,22	12,6	0,212	1,91	218	32,7	5,14	9,65	6,65	7,42	2,21	0,297	8,21	97,9	34,9	52,5	1,49	14	11,2
10H_600	52,5	2,51	4,67	23,4	0,203	7,03	174	36	4,72	5,78	4,44	6,44	1,76	0,415	5,33	66,9	54,1	43,9	1,31	10,9	7,77
11H_600	51,9	2,73	4,57	16,7	0,168	2,18	189	36,3	3,08	6,81	4,53	7,35	1,81	0,494	6,38	82,6	53,5	49,5	1,51	12,8	7,93
12H_600	42,7	2,68	4,64	37,7	0,318	9,95	211	37,7	4,15	4,58	3,52	5,84	1,67	0,386	3,9	43,8	91,1	45,9	1,45	11,5	6,82
01M_300	40,1	4,62	10,2	44,1	0,159	79,4	223	95,1	14,7	4,13	2,24	12,7	2,13	0,408	5,96	24	225	66,8	1,17	17,3	8,16
02M_300	43,2	4,96	13,1	54	0,138	77,7	264	111	15,9	4,05	3,02	14,3	2,24	0,313	6,2	24,2	258	62,7	1,21	18,1	8,54
03M_300	45,1	6,14	15,2	43,3	0,172	91,9	376	144	17	4,79	2,74	18,8	2,1	0,35	7,47	28,4	319	73,9	1,39	20,6	10,5
04M_300	40,4	6,98	12,8	42,6	0,207	76,7	291	161	17,7	3,49	2,65	18,7	1,87	0,383	6,63	22,4	336	72,4	1,33	21,7	9,94
05M_300	56,1	6,26	16,1	56,1	0,363	100	337	138	20,9	4,98	3,93	17,7	2,99	0,519	8,7	30,5	314	77,5	1,64	21,1	12,2
06M_300	46,5	7,01	14,9	48,3	0,163	89,8	329	151	18,3	4,51	3,8	17,8	2,47	0,401	7,62	25,6	303	74,7	1,37	21,8	11,8
07M_600	101	3,12	5,41	15,4	0,181	51,1	218	55,3	16,8	15,4	11,7	10,2	3,45	0,284	14,2	104	78,7	62,1	2,04	18,1	17,4
08M_600	112	3,83	6,46	38,3	0,195	72,4	255	61	21,8	18	14,3	11,6	4,72	0,332	14,2	86,2	115	71	2,11	20,5	18,5
09M_600	127	3,77	5,14	13,8	0,338	28,7	262	50,7	19,1	20,2	15,9	12,3	4,05	0,475	18,7	150	42,9	74,5	2,37	25,2	20,9
10M_600	137	3,89	8,13	30	0,238	63	351	71,7	19,9	17,3	14,2	12,2	4,13	0,372	14,9	92,2	103	83,1	2,25	21,1	18,6
11M_600	118	3,97	6,86	21,5	0,194	50	289	69,3	19,2	18,6	15	13	4,21	0,413	16,7	112	93,4	70	2,44	22	22,1
12M_600	126	4,16	8,33	57,9	0,29	85,6	338	77	23,8	17,5	14,1	13,2	4,74	0,424	13,2	65,2	168	77,4	2,41	20,5	18,2

8.2.2. Biogenic amines

	Ac-Orn	ADMA	alpha-AAA	c4-OH-Pro	Carnosine	Creatinine	DOPA	Dopamine	Histamine	Kynurenine	Met-SO	Nitro-Tyr	PEA	Putrescine	SDMA	Serotonin	Spermidine	Spermine	t4-OH-Pro	Taurine	total DMA
01H_300	0,089	0,138	0,377	0	0,014	5,09	0	0	0	0,222	0,361	0	0,001	0,116	0	0	0,168	0,07	0,008	66,4	0,099
02H_300	0,078	0,044	0,664	0	0,018	4,97	0	0	0,001	0,228	0,455	0	0,001	0,119	0,082	0	0,238	0,084	0	73,5	0,148
03H_300	0,109	0,117	0,695	0	0,017	4,86	0	0	0	0,265	0,377	0	0,001	0,145	0	0	0,201	0,089	0	64,9	0,132
04H_300	0,11	0,161	0,611	0	0,01	5,25	0	0	0,001	0,256	0,398	0	0,001	0,174	0	0	0,263	0,072	0	63,3	0,15
05H_300	0,066	0,096	0,456	0	0,009	4,99	0	0	0	0,225	0,308	0	0,001	0,116	0	0	0,16	0,073	0	62,9	0,092
06H_300	0,09	0,084	0,512	0	0,013	5,16	0	0	0	0,259	0,34	0	0,001	0,147	0,116	0	0,206	0,081	0	66,5	0,138
07H_600	0,088	0,071	0,27	0	0,022	5,65	0	0	0,001	0,249	0,199	0	0,002	0,12	0	0	0,159	0,23	0,309	93	0,063
08H_600	0,085	0,133	0,142	0	0,025	5,47	0	0	0,011	0,192	0,318	0	0,002	0,103	0	0	0,15	0,178	0,233	81,1	0,073
09H_600	0,121	0,061	0,147	0	0,03	5,6	0	0	0	0,217	0,208	0	0,002	0,093	0	0	0,163	0,378	0,337	97,8	0,067
10H_600	0,083	0,161	0,174	0	0,017	5,64	0	0	0,001	0,205	0,198	0	0,001	0,083	0	0	0,134	0,195	0,217	90,2	0,055
11H_600	0,077	0,107	0,266	0	0,02	5,61	0	0	0	0,242	0,199	0	0,001	0,055	0	0	0,096	0,198	0,26	85,5	0,051
12H_600	0,047	0,053	0,322	0	0,023	5,37	0	0	0,001	0,228	0,179	0	0,001	0,069	0	0	0,124	0,167	0,145	88,5	0,052
01M_300	0,087	0,202	0,47	0	0,023	5,24	0	0	0	0,242	0,392	0	0,001	0,237	0	0	0,706	0,601	0	91,7	0,171
02M_300	0,086	0,096	0,615	0	0,024	5,33	0	0	0	0,222	0,487	0	0,001	0,299	0,048	0	0,645	0,138	0,021	88,7	0,16
03M_300	0,142	0,163	0,844	0	0,028	5,37	0	0	0,001	0,217	0,548	0	0,001	0,307	0,056	0	0,598	0,114	0,016	97	0,218
04M_300	0,152	0,174	0,626	0	0,022	5,37	0	0	0,001	0,199	0,544	0	0,001	0,34	0,079	0	0,662	0,093	0,017	92,3	0,225
05M_300	0,137	0,166	0,52	0	0,026	5,23	0	0	0,001	0,218	0,583	0	0,001	0,341	0,052	0	0,473	0,07	0,017	107	0,221
06M_300	0,118	0,134	0,605	0	0,018	5,21	0	0	0,001	0,22	0,519	0	0,001	0,275	0	0	0,447	0,079	0,016	96,7	0,202
07M_600	0,092	0,073	0,24	0	0,033	5,54	0	0	0,001	0,238	0,249	0	0,002	0,128	0	0	0,185	0,228	0,45	113	0,085
08M_600	0,111	0,125	0,484	0	0,024	5,28	0	0	0	0,234	0,26	0	0,002	0,153	0,047	0	0,205	0,18	0,352	120	0,088
09M_600	0,087	0,118	0,24	0	0,036	6,15	0	0	0,001	0,227	0,285	0	0,002	0,144	0	0	0,351	1,05	0,594	120	0,1
10M_600	0,112	0,177	0,325	0	0,027	5,89	0	0	0,001	0,224	0,263	0	0,002	0,169	0,039	0	0,316	0,28	0,401	131	0,108
11M_600	0,117	0,158	0,299	0	0,039	5,85	0	0	0,001	0,262	0,26	0	0,002	0,187	0	0	0,314	0,264	0,442	117	0,098
12M_600	0,127	0,114	0,605	0	0,024	5,59	0	0	0,001	0,256	0,324	0	0,001	0,187	0,058	0	0,332	0,14	0,233	129	0,109

Metabolom Analysis Results
8.2.3. Acylcarnitines(1/2)

	C0	C2	C3	-DC (C4-O	C3-OH	C3:1	C4	C4:1	C5	C5-DC (C6-OH)	C5-M-DC	C5-OH (C3-DC-M)	C5:1	C5:1-DC	C6 (C4:1-DC)	C6:1	C7-DC	C8	C9	C10
01H_300	1,76	0,124	0,036	0,035	0,019	0,012	0,027	0,026	0,027	0,021	0,028	0,026	0,015	0,016	0,043	0,022	0,033	0,077	0,01	0,051
02H_300	2,01	0,082	0,035	0,035	0,018	0,012	0,033	0,018	0,026	0,019	0,023	0,027	0,016	0,018	0,03	0,02	0,027	0,071	0,008	0,041
03H_300	1,92	0,096	0,043	0,033	0,024	0,011	0,027	0,027	0,025	0,021	0,029	0,037	0,02	0,021	0,037	0,02	0,031	0,077	0,008	0,047
04H_300	1,94	0,117	0,036	0,039	0,019	0,009	0,025	0,022	0,019	0,02	0,019	0,029	0,013	0,016	0,038	0,022	0,026	0,073	0,009	0,042
05H_300	1,76	0,158	0,039	0,03	0,015	0	0,018	0,018	0,024	0,02	0,032	0,024	0,018	0,017	0,038	0,014	0,024	0,071	0,007	0,043
06H_300	2,03	0,148	0,052	0,037	0,026	0,011	0,031	0,021	0,031	0,024	0,029	0,028	0,017	0,024	0,033	0,017	0,031	0,085	0,012	0,043
07H_600	1,34	1,06	0,041	0,04	0,021	0,015	0,034	0,023	0,026	0,02	0,028	0,029	0,014	0,022	0,045	0,015	0,027	0,077	0,011	0,047
08H_600	1,28	1,12	0,037	0,048	0,024	0,017	0,03	0,026	0,034	0,024	0,023	0,038	0,017	0,022	0,035	0,021	0,021	0,069	0,013	0,048
09H_600	0,848	1,35	0,041	0,042	0,018	0,01	0,026	0,019	0,029	0,019	0,025	0,028	0,018	0,021	0,041	0,019	0,021	0,072	0,008	0,04
10H_600	0,9	1,19	0,035	0,042	0,02	0,01	0,026	0,015	0,031	0,019	0,03	0,029	0,018	0,016	0,03	0,018	0,019	0,073	0,005	0,039
11H_600	0,916	1,33	0,045	0,049	0,022	0,017	0,028	0,018	0,031	0,02	0,028	0,036	0,017	0,023	0,036	0,023	0,028	0,075	0,008	0,044
12H_600	0,866	1,29	0,043	0,046	0,023	0,01	0,026	0,021	0,026	0,022	0,029	0,038	0,02	0,019	0,039	0,018	0,021	0,071	0,007	0,045
01M_300	2,33	0,168	0,035	0,036	0,021	0,012	0,037	0,022	0,026	0,027	0,027	0,033	0,017	0,021	0,039	0,019	0,027	0,075	0,008	0,041
02M_300	2,35	0,164	0,035	0,036	0,021	0,013	0,041	0,021	0,028	0,022	0,023	0,035	0,015	0,017	0,039	0,022	0,021	0,066	0	0,042
03M_300	2,57	0,205	0,044	0,034	0,019	0,017	0,04	0,022	0,031	0,024	0,026	0,03	0,018	0,022	0,036	0,021	0,033	0,079	0,009	0,046
04M_300	2,75	0,184	0,043	0,037	0,023	0,023	0,049	0,02	0,035	0,02	0,027	0,035	0,02	0,022	0,044	0,023	0,026	0,08	0,009	0,045
05M_300	2,52	0,252	0,049	0,037	0,021	0,01	0,039	0,023	0,028	0,022	0,035	0,032	0	0,025	0,041	0,022	0,03	0,067	0,009	0,05
06M_300	2,62	0,217	0,043	0,04	0,019	0,013	0,034	0,016	0,029	0,024	0,028	0,03	0,013	0,019	0,044	0,024	0,027	0,066	0,009	0,048
07M_600	1,58	1,02	0,049	0,044	0,016	0,016	0,032	0,023	0,032	0,026	0,031	0,038	0,02	0,024	0,04	0,021	0,03	0,078	0,009	0,043
08M_600	2,02	0,923	0,058	0,042	0,024	0,018	0,04	0,027	0,033	0,028	0,027	0,026	0,021	0,027	0,046	0,021	0,031	0,086	0,011	0,047
09M_600	1,81	1,22	0,049	0,046	0,023	0,014	0,038	0,023	0,036	0,019	0,028	0,039	0,015	0,024	0,048	0,022	0,027	0,072	0,008	0,046
10M_600	1,75	1,02	0,044	0,041	0,017	0,012	0,039	0,025	0,029	0,022	0,023	0,028	0,018	0,018	0,046	0,019	0,025	0,075	0,008	0,041
11M_600	1,93	1,19	0,046	0,045	0,023	0,015	0,032	0,021	0,035	0,018	0,025	0,03	0,021	0,023	0,03	0,021	0,032	0,074	0,009	0,044
12M_600	2,35	0,823	0,041	0,04	0,016	0,012	0,034	0,022	0,032	0,021	0,031	0,036	0,017	0,019	0,036	0,018	0,02	0,062	0,008	0,039

Metabolom Analysis Results
8.2.4. Acylcarnitines(2/2)

	C10:1	C10:2	C12	C12-DC	C12:1	C14	C14:1	C14:1-OH	C14:2	C14:2-OH	C16	C16-OH	C16:1	C16:1-OH	C16:2	C16:2-OH	C18	C18:1	C18:1-OH	C18:2
01H_300	0,072	0,023	0,018	0,146	0,069	0,01	0,004	0,004	0,003	0,01	0,006	0,006	0,026	0,007	0,007	0,009	0,006	0,011	0,022	0,006
02H_300	0,057	0,024	0,015	0,127	0,046	0,01	0,004	0,006	0,006	0,006	0,011	0,006	0,021	0,008	0,006	0,006	0,007	0,008	0,021	0,005
03H_300	0,069	0,027	0,017	0,136	0,053	0,01	0,004	0,006	0,005	0,006	0,007	0,008	0,023	0,009	0,008	0,008	0,006	0,009	0,021	0,006
04H_300	0,059	0,025	0,017	0,137	0,051	0,01	0	0,005	0,004	0,006	0,007	0,006	0,024	0,005	0,008	0,009	0,005	0,01	0,02	0,006
05H_300	0,061	0,02	0,017	0,135	0,047	0,01	0,004	0,004	0,004	0,008	0,007	0,005	0,027	0,007	0,007	0,009	0,005	0,011	0,017	0,005
06H_300	0,077	0,023	0,017	0,144	0,065	0,012	0,006	0,006	0,003	0,007	0,008	0,007	0,023	0,008	0,009	0,009	0,006	0,012	0,022	0,006
07H_600	0,061	0,021	0,015	0,142	0,059	0,011	0,005	0,005	0	0,005	0,018	0,006	0,029	0,007	0,005	0,008	0,006	0,019	0,017	0,007
08H_600	0,052	0,026	0,019	0,128	0,045	0,013	0,003	0,006	0,004	0,007	0,023	0,006	0,029	0,009	0,007	0,012	0,016	0,02	0,019	0,007
09H_600	0,052	0,021	0,018	0,121	0,041	0,014	0,004	0,006	0	0,007	0,026	0,005	0,028	0,006	0,006	0,009	0,007	0,022	0,017	0,006
10H_600	0,046	0,021	0,018	0,13	0,041	0,014	0,003	0,005	0,004	0,006	0,021	0,006	0,031	0,005	0,007	0,01	0,007	0,015	0,017	0,007
11H_600	0,048	0,021	0,018	0,135	0,046	0,014	0,007	0,005	0,003	0,006	0,027	0,006	0,032	0,009	0,011	0,01	0,009	0,021	0,023	0,007
12H_600	0,049	0,021	0,015	0,14	0,052	0,012	0,005	0,005	0,004	0,005	0,02	0,005	0,028	0,007	0,008	0,008	0,004	0,017	0,02	0,006
01M_300	0,059	0,023	0,016	0,123	0,045	0,009	0,004	0,005	0,005	0,007	0,005	0,007	0,021	0,005	0,006	0,009	0,004	0,01	0,018	0,006
02M_300	0,046	0,023	0,017	0,124	0,045	0,01	0,004	0,004	0,004	0,007	0,006	0,005	0,021	0,005	0,006	0,007	0,007	0,008	0,018	0,008
03M_300	0,072	0,028	0,022	0,146	0,062	0,011	0,004	0	0,005	0,009	0,008	0,006	0,023	0,006	0,008	0,008	0,005	0,011	0,021	0,005
04M_300	0,063	0,021	0,015	0,128	0,057	0,013	0,004	0,005	0,003	0,01	0,009	0,005	0,02	0,006	0,007	0,009	0	0,009	0,02	0,009
05M_300	0,051	0,026	0,014	0,128	0,042	0,009	0,004	0,006	0,004	0,007	0,009	0	0,023	0,006	0,007	0,009	0,007	0,013	0,021	0,007
06M_300	0,061	0,029	0,017	0,135	0,042	0,01	0,005	0,004	0,005	0,009	0,009	0,007	0,022	0,006	0,008	0,009	0,006	0,012	0,022	0,011
07M_600	0,068	0,027	0,014	0,138	0,061	0,013	0,005	0,005	0,005	0,007	0,02	0,006	0,029	0,008	0,007	0,008	0,007	0,023	0,017	0,006
08M_600	0,072	0,025	0,015	0,145	0,048	0,015	0,004	0,009	0,006	0,007	0,017	0,007	0,03	0,008	0,007	0,01	0,006	0,018	0,019	0,006
09M_600	0,057	0,022	0,018	0,131	0,051	0,015	0,006	0,004	0,004	0,005	0,023	0,007	0,031	0,007	0,007	0,01	0,004	0,026	0,017	0,008
10M_600	0,047	0,028	0,015	0,113	0,036	0,013	0,004	0,005	0,004	0,006	0,014	0,006	0,029	0,007	0	0,009	0,005	0,017	0,019	0,005
11M_600	0,064	0,028	0,023	0,137	0,071	0,011	0,006	0,007	0,004	0,006	0,023	0,006	0,03	0,008	0,006	0,012	0,005	0,021	0,018	0,007
12M_600	0,048	0,028	0,019	0,131	0,038	0,011	0,003	0,008	0,005	0,008	0,011	0,006	0,027	0,007	0,007	0,008	0,005	0,017	0,018	0,008

8.2.5. Glycerophospholipids(1/5)

	lysoPCa C14:0	lysoPCa C16:0	lysoPCa C16:1	lysoPCa C17:0	lysoPCa C18:0	lysoPCa C18:1	lysoPCa C18:2	lysoPCa C20:3	lysoPCa C20:4	lysoPCa C24:0	lysoPCa C26:0	lysoPCa C26:1	lysoPCa C28:0	lysoPCa C28:1	PCaa C24:0	PCaa C26:0	PCaa C28:1	PCaa C30:0	PCaa C30:2	PCaa C32:0
01H_300	0,23	0,263	0,193	0,015	0,177	0,254	0,042	0,071	0,022	0,232	0	0,023	0,039	0,055	0,014	0,331	0,198	0,631	0,028	0,311
02H_300	0,211	0,255	0,177	0	0,165	0,275	0,043	0,058	0,024	0,279	0	0,02	0,068	0,044	0,015	0,328	0,204	0,644	0,043	0,27
03H_300	0,249	0,278	0,183	0	0,161	0,28	0,047	0,085	0	0,253	0,028	0	0,068	0,042	0,02	0,339	0,198	0,637	0,047	0,212
04H_300	0,224	0,267	0,198	0	0,164	0,256	0,039	0,072	0,019	0,258	0,032	0,023	0,046	0,053	0,017	0,349	0,236	0,716	0,043	0,361
05H_300	0,212	0,211	0,171	0,02	0,163	0,191	0,042	0,066	0	0,248	0,048	0,021	0,046	0,042	0,021	0,347	0,171	0,595	0,039	0,28
06H_300	0,222	0,283	0,235	0	0,164	0,29	0,047	0,087	0,02	0,239	0	0,021	0,066	0,058	0,019	0,361	0,198	0,659	0,034	0,3
07H_600	0,207	0,403	0,197	0,021	0,202	0,258	0,039	0,07	0,015	0,258	0	0,04	0,051	0,054	0,018	0,346	0,141	0,872	0,045	0,406
08H_600	0,216	0,36	0,212	0,018	0,184	0,308	0	0,059	0	0,289	0,02	0,024	0,05	0,026	0,016	0,322	0,131	0,864	0,045	0,402
09H_600	0,236	0,414	0,195	0,018	0,214	0,305	0,026	0,065	0,021	0,248	0,038	0,028	0,05	0,049	0,022	0,335	0,145	0,982	0,052	0,375
10H_600	0,231	0,36	0,192	0,017	0,204	0,26	0,032	0,063	0	0,271	0,022	0,024	0,05	0,05	0,016	0,352	0,142	1,01	0,057	0,482
11H_600	0,227	0,349	0,209	0,025	0,182	0,271	0,035	0,087	0,026	0,228	0,023	0,03	0,065	0,047	0,022	0,329	0,154	0,987	0,053	0,424
12H_600	0,216	0,348	0,199	0,018	0,171	0,256	0,036	0,066	0,019	0,251	0	0,023	0,05	0,035	0,021	0,365	0,134	0,891	0,046	0,421
01M_300	0,225	0,234	0,222	0	0,157	0,25	0,037	0,061	0	0,227	0,029	0,044	0,047	0,031	0,013	0,322	0,086	0,232	0,018	0,096
02M_300	0,232	0,308	0,224	0	0,17	0,336	0,028	0,07	0,031	0,294	0,032	0,021	0,062	0,031	0,017	0,322	0,081	0,201	0,016	0,058
03M_300	0,209	0,315	0,318	0	0,177	0,407	0,05	0,08	0,034	0,26	0,039	0,023	0,072	0,048	0,019	0,33	0,083	0,18	0,022	0,062
04M_300	0,247	0,311	0,353	0	0,153	0,392	0,063	0,085	0,024	0,285	0,032	0,024	0,055	0,024	0,019	0,333	0,072	0,153	0,025	0,054
05M_300	0,222	0,27	0,37	0	0,136	0,373	0,078	0,067	0,032	0,28	0,033	0,026	0,061	0,045	0,019	0,352	0,06	0,123	0,015	0,044
06M_300	0,253	0,284	0,405	0,014	0,21	0,365	0,066	0,078	0,023	0,295	0,046	0,033	0,051	0,035	0,021	0,337	0,081	0,159	0,018	0,039
07M_600	0,24	0,489	0,228	0	0,198	0,308	0,025	0,075	0	0,282	0,039	0,024	0,076	0,041	0,022	0,328	0,131	0,617	0,039	0,225
08M_600	0,236	0,448	0,234	0	0,204	0,309	0,039	0,082	0	0,29	0,045	0	0,058	0,068	0,013	0,346	0,081	0,379	0,027	0,138
09M_600	0,2	0,503	0,238	0,028	0,215	0,349	0,053	0,076	0	0,263	0,044	0	0,047	0	0,019	0,355	0,068	0,341	0,02	0,14
10M_600	0,216	0,369	0,195	0	0,161	0,298	0,037	0,07	0,026	0,254	0,036	0,026	0,066	0,023	0,017	0,345	0,056	0,207	0,016	0,073
11M_600	0,225	0,49	0,262	0	0,22	0,373	0,053	0,081	0	0,295	0,043	0,028	0,079	0,028	0,017	0,343	0,062	0,25	0,023	0,089
12M_600	0,234	0,352	0,285	0	0,142	0,29	0,05	0,057	0	0,264	0,035	0,051	0,06	0,026	0,026	0,314	0,046	0,152	0,014	0,069

8.2.6. Glycerophospholipids(2/5)

	PC aa C32:1	PC aa C32:2	PC aa C32:3	PC aa C34:1	PC aa C34:2	PC aa C34:3	PC aa C34:4	PC aa C36:0	PC aa C36:1	PC aa C36:2	PC aa C36:3	PC aa C36:4	PC aa C36:5	PC aa C36:6	PC aa C38:0	PC aa C38:1	PC aa C38:3	PC aa C38:4	PC aa C38:5	PC aa C38:6
01H_300	11,1	3,59	0,101	6,51	9,12	0,663	0,083	0,025	0,784	5,27	1,93	1,06	0,569	0,12	0,014	0,003	0,308	0,833	0,97	0,828
02H_300	12,3	3,96	0,117	6,8	10,1	0,758	0,096	0,03	0,806	5,74	2,35	1,17	0,595	0,133	0,012	0	0,352	0,936	0,981	0,845
03H_300	12,1	4,06	0,136	6,1	9,17	0,722	0,087	0,017	0,727	4,82	1,86	0,995	0,543	0,145	0,014	0	0,288	0,74	0,86	0,773
04H_300	12,5	4,25	0,133	6,87	10,3	0,726	0,081	0,029	0,862	5,92	2,18	1,07	0,619	0,137	0,014	0	0,369	0,942	0,939	0,847
05H_300	10,8	3,59	0,11	6,15	8,89	0,691	0,071	0,023	0,784	4,78	1,77	0,962	0,546	0,114	0,014	0	0,272	0,744	0,861	0,739
06H_300	11,7	4,07	0,122	6,22	9,21	0,718	0,089	0,04	0,734	4,85	1,9	0,994	0,569	0,146	0,012	0	0,283	0,779	0,861	0,774
07H_600	12,4	3,57	0,079	6,1	7,59	0,481	0,058	0,03	0,604	3,87	1,34	0,746	0,419	0,098	0,012	0,003	0,218	0,507	0,646	0,584
08H_600	12,5	3,56	0,082	6,34	7,65	0,51	0,063	0,035	0,579	3,95	1,41	0,874	0,438	0,103	0,013	0,006	0,215	0,526	0,705	0,644
09H_600	12,7	3,54	0,07	6,07	7,39	0,442	0,055	0,028	0,611	3,75	1,22	0,693	0,382	0,095	0,017	0,005	0,187	0,463	0,593	0,514
10H_600	14,9	3,99	0,091	7,8	9,12	0,578	0,064	0,022	0,747	4,77	1,61	1,02	0,497	0,111	0,021	0	0,264	0,63	0,772	0,728
11H_600	13,9	3,82	0,094	7,41	8,57	0,514	0,058	0,019	0,756	4,55	1,5	0,778	0,423	0,096	0,016	0	0,251	0,564	0,684	0,618
12H_600	13,4	3,79	0,093	7,3	8,38	0,56	0,068	0,028	0,716	4,31	1,54	0,95	0,516	0,11	0,014	0,001	0,242	0,599	0,776	0,742
01M_300	3,33	1,52	0,051	1,49	2,56	0,238	0,034	0,025	0,143	1,09	0,47	0,305	0,178	0,063	0,007	0,002	0,058	0,182	0,229	0,239
02M_300	3,11	1,63	0,049	1,29	2,48	0,218	0,038	0,021	0,117	1,02	0,434	0,261	0,188	0,066	0,006	0,003	0,048	0,184	0,215	0,204
03M_300	2,42	1,3	0,049	1,01	1,92	0,172	0,027	0,027	0,123	0,78	0,318	0,19	0,127	0,05	0	0,001	0,045	0,134	0,154	0,168
04M_300	1,85	0,96	0,034	0,754	1,41	0,121	0,02	0,028	0,088	0,601	0,258	0,144	0,095	0,047	0,009	0,003	0,03	0,1	0,113	0,128
05M_300	1,09	0,571	0,023	0,524	0,794	0,081	0,016	0,025	0,078	0,365	0,148	0,088	0,06	0,028	0,007	0,004	0,024	0,054	0,071	0,073
06M_300	1,77	0,926	0,032	0,805	1,4	0,115	0,028	0,026	0,101	0,566	0,239	0,157	0,094	0,045	0,008	0,008	0,034	0,105	0,122	0,127
07M_600	8,54	3,1	0,075	3,57	5,17	0,368	0,045	0,018	0,336	2,14	0,803	0,49	0,305	0,095	0,014	0	0,113	0,316	0,416	0,414
08M_600	4,85	1,89	0,049	1,88	2,87	0,22	0,031	0,023	0,144	1,18	0,489	0,319	0,205	0,061	0	0	0,062	0,181	0,253	0,259
09M_600	3,26	1,26	0,027	1,41	1,86	0,142	0,024	0,024	0,145	0,771	0,287	0,168	0,109	0,042	0,008	0,003	0,038	0,098	0,142	0,136
10M_600	2,21	0,887	0,026	0,882	1,29	0,097	0,022	0,026	0,095	0,514	0,203	0,139	0,086	0,028	0,007	0,005	0,029	0,079	0,1	0,108
11M_600	2,61	1,11	0,034	1,13	1,58	0,136	0,023	0,03	0,127	0,666	0,241	0,154	0,098	0,036	0,005	0,003	0,042	0,099	0,122	0,127
12M_600	1,57	0,671	0,025	0,737	0,916	0,078	0,015	0,025	0,086	0,399	0,16	0,12	0,076	0,029	0,009	0,001	0,026	0,063	0,086	0,099

Metabolom Analysis Results
8.2.7. Glycerophospholipids(3/5)

	PC aa C40:1	PC aa C40:2	PC aa C40:3	PC aa C40:4	PC aa C40:5	PC aa C40:6	PC aa C42:0	PC aa C42:1	PC aa C42:2	PC aa C42:4	PC aa C42:5	PC aa C42:6	PC ae C30:0	PC ae C30:1	PC ae C30:2	PC ae C32:1	PC ae C32:2	PC ae C34:0	PC ae C34:1	PC ae C34:2
01H_300	0,161	0,007	0,008	0,028	0,072	0,212	0,025	0,006	0,033	0,008	0,002	0,053	0,036	0,017	0,101	0,114	0,024	0,04	0,489	0,222
02H_300	0,156	0,012	0,009	0,025	0,067	0,217	0,042	0,01	0,035	0,004	0,006	0,044	0,037	0,024	0,099	0,118	0,035	0,034	0,518	0,238
03H_300	0,165	0	0,008	0,027	0,062	0,18	0,042	0,007	0,039	0,005	0,006	0,041	0,036	0,021	0,097	0,119	0,032	0,038	0,438	0,23
04H_300	0,158	0,008	0,007	0,026	0,073	0,206	0,031	0,005	0,039	0,007	0,006	0,043	0,045	0,022	0,107	0,133	0,066	0,037	0,53	0,267
05H_300	0,173	0,007	0	0,026	0,056	0,195	0,042	0,005	0,038	0,004	0	0,038	0,03	0,014	0,097	0,133	0,027	0,033	0,458	0,232
06H_300	0,162	0,007	0,011	0,024	0,057	0,203	0,029	0	0,036	0,005	0,008	0,045	0,036	0,018	0,109	0,123	0,033	0,035	0,468	0,251
07H_600	0,163	0,009	0,01	0,019	0,067	0,181	0,04	0,007	0,035	0	0,01	0,058	0,052	0,022	0,102	0,261	0,039	0,053	0,691	0,298
08H_600	0,154	0,012	0,009	0,02	0,063	0,199	0,029	0	0,034	0,008	0,005	0,044	0,043	0,022	0,099	0,233	0,042	0,048	0,695	0,311
09H_600	0,177	0,008	0,007	0,022	0,063	0,17	0,038	0,003	0,038	0,008	0,005	0,055	0,051	0,016	0,099	0,29	0,048	0,059	0,714	0,319
10H_600	0,162	0,012	0,008	0,033	0,092	0,229	0,03	0,007	0,038	0,004	0,008	0,054	0,039	0,023	0,094	0,277	0,051	0,056	0,858	0,37
11H_600	0,178	0,011	0,009	0,023	0,081	0,184	0,033	0,005	0,041	0,006	0,006	0,044	0,046	0,016	0,103	0,289	0,045	0,062	0,813	0,33
12H_600	0,154	0,009	0,014	0,029	0,079	0,218	0,03	0,005	0,038	0,004	0,005	0,046	0,05	0,022	0,098	0,221	0,041	0,058	0,73	0,313
01M_300	0,163	0,005	0,003	0,01	0,017	0,058	0,036	0,006	0,04	0,005	0,003	0,039	0,029	0,009	0,091	0,042	0,031	0,012	0,128	0,092
02M_300	0,17	0,004	0,009	0,006	0,016	0,052	0,038	0,004	0,037	0,006	0,002	0,035	0,031	0,009	0,103	0,046	0,028	0,018	0,103	0,081
03M_300	0,168	0,008	0,004	0,014	0,01	0,047	0,027	0,008	0,035	0	0,003	0,044	0,031	0,01	0,097	0,036	0,029	0,017	0,085	0,065
04M_300	0,156	0,006	0,005	0,009	0,015	0,036	0,031	0	0,042	0,006	0	0,036	0,026	0,013	0,102	0,027	0,018	0,009	0,068	0,042
05M_300	0,163	0,006	0	0,013	0,013	0,024	0,036	0,011	0,03	0	0,003	0,029	0,026	0,018	0,104	0,019	0,029	0,009	0,044	0,029
06M_300	0,151	0,003	0,005	0	0,012	0,042	0,035	0,008	0,039	0	0,003	0,035	0,028	0,014	0,097	0,025	0,022	0,013	0,062	0,048
07M_600	0,161	0,004	0,005	0,015	0,044	0,115	0,031	0,004	0,037	0	0,006	0,04	0,038	0,014	0,103	0,191	0,034	0,047	0,437	0,243
08M_600	0,158	0,007	0,005	0,017	0,02	0,078	0,038	0,005	0,034	0,004	0,005	0,036	0,038	0,013	0,093	0,096	0,035	0,023	0,229	0,14
09M_600	0,156	0,009	0	0,011	0,021	0,051	0,037	0,006	0,034	0,006	0	0,042	0,026	0,018	0,103	0,099	0,028	0,028	0,186	0,11
10M_600	0,16	0,003	0,005	0,009	0,014	0,038	0,031	0,005	0,037	0,004	0,004	0,033	0,026	0,018	0,095	0,047	0,03	0,017	0,114	0,062
11M_600	0,169	0	0,004	0,012	0,018	0,039	0,032	0,006	0,028	0	0,004	0,037	0,038	0,014	0,108	0,066	0,026	0,015	0,131	0,076
12M_600	0,167	0	0,004	0,007	0,021	0,031	0,037	0,007	0,033	0	0	0,035	0,031	0,02	0,1	0,028	0,028	0,014	0,073	0,048

8.2.8. Glycerophospholipids(4/5)

	PC ae C34:3	PC ae C36:0	PC ae C36:1	PC ae C36:2	PC ae C36:3	PC ae C36:4	PC ae C36:5	PC ae C38:0	PC ae C38:1	PC ae C38:2	PC ae C38:3	PC ae C38:4	PC ae C38:5	PC ae C38:6	PC ae C40:1	PC ae C40:2	PC ae C40:3	PC ae C40:4	PC ae C40:5	PC ae C40:6
01H_300	0,019	0,015	0,122	0,361	0,077	0,024	0,022	0,134	0,012	0,057	0,055	0,071	0,033	0,013	0,019	0,019	0,012	0,029	0,026	0,028
02H_300	0,022	0,013	0,124	0,414	0,081	0,022	0,017	0,128	0,021	0,067	0,049	0,064	0,036	0,013	0,017	0,023	0,012	0,036	0,022	0,028
03H_300	0,022	0,023	0,116	0,34	0,08	0,025	0,023	0,116	0,023	0,059	0,051	0,067	0,029	0,018	0,01	0,019	0,011	0,028	0,014	0,031
04H_300	0,02	0,014	0,137	0,41	0,09	0,023	0,027	0,121	0,027	0,057	0,061	0,064	0,031	0,016	0,022	0,021	0,015	0,031	0,019	0,024
05H_300	0,019	0,016	0,122	0,347	0,069	0,021	0,018	0,122	0,013	0,064	0,049	0,056	0,031	0,012	0,02	0,018	0,011	0,03	0,016	0,024
06H_300	0,018	0,017	0,136	0,341	0,075	0,026	0,019	0,122	0,017	0,054	0,045	0,064	0,039	0,01	0,023	0,021	0,008	0,029	0,018	0,025
07H_600	0,02	0,013	0,151	0,374	0,065	0,021	0,026	0,105	0,02	0,062	0,044	0,043	0,037	0,013	0,01	0,017	0,012	0,032	0,015	0,025
08H_600	0,026	0,019	0,141	0,402	0,07	0,025	0,022	0,115	0,021	0,062	0,046	0,044	0,032	0,014	0,018	0,014	0,017	0,029	0,011	0,025
09H_600	0,026	0,018	0,159	0,38	0,058	0,02	0,022	0,107	0,017	0,069	0,046	0,038	0,032	0,017	0,013	0,022	0,011	0,026	0,018	0,027
10H_600	0,023	0,02	0,176	0,476	0,078	0,02	0,024	0,12	0,02	0,081	0,048	0,051	0,034	0,018	0,015	0,014	0,016	0,034	0,017	0,024
11H_600	0,027	0,013	0,168	0,451	0,071	0,022	0,022	0,103	0,015	0,069	0,046	0,046	0,034	0,021	0,014	0,019	0,019	0,031	0,015	0,022
12H_600	0,018	0,017	0,131	0,402	0,067	0,023	0,022	0,118	0,019	0,066	0,045	0,046	0,038	0,017	0,013	0,018	0,015	0,032	0,017	0,022
01M_300	0,01	0,009	0,048	0,1	0,025	0,009	0	0,074	0,006	0,014	0,017	0,019	0,013	0,004	0,01	0,011	0,006	0,024	0,005	0,019
02M_300	0,011	0,013	0,039	0,093	0,02	0,011	0,007	0,064	0,01	0,015	0,017	0,019	0,016	0,009	0	0	0,006	0,018	0,007	0,014
03M_300	0	0,015	0,042	0,066	0,019	0	0	0,058	0,007	0,012	0,012	0,02	0,016	0,01	0,009	0	0,003	0,021	0,005	0,015
04M_300	0	0,009	0,053	0,054	0,012	0,006	0,009	0,046	0,006	0,014	0,013	0,008	0,018	0,004	0,012	0,005	0,007	0,025	0,003	0,015
05M_300	0,005	0,009	0,035	0,043	0,011	0,009	0	0,043	0,011	0,008	0,01	0,01	0,01	0,007	0,012	0,005	0,007	0,021	0,005	0,015
06M_300	0,01	0,012	0,034	0,069	0,014	0	0	0,052	0,004	0,009	0,017	0,011	0,016	0,006	0,009	0,006	0,006	0,018	0,005	0,01
07M_600	0,02	0,019	0,093	0,25	0,051	0,024	0,013	0,093	0,016	0,044	0,031	0,027	0,021	0,014	0,017	0,012	0,016	0,022	0,012	0,017
08M_600	0,011	0,012	0,051	0,134	0,026	0,01	0,01	0,07	0,008	0,025	0,019	0,023	0,019	0,008	0,01	0,011	0,006	0,021	0,012	0,016
09M_600	0	0,011	0,049	0,099	0,019	0,007	0,011	0,057	0,018	0,015	0,011	0,016	0,012	0,007	0,012	0,007	0	0,027	0,008	0,015
10M_600	0,008	0,013	0,044	0,071	0,017	0,006	0,008	0,062	0,006	0,014	0,014	0,013	0,016	0	0,011	0	0,003	0,027	0	0,012
11M_600	0,011	0,006	0,048	0,08	0,016	0,011	0,009	0,059	0,008	0,012	0,019	0,015	0,013	0,006	0,008	0	0,005	0,021	0,007	0,017
12M_600	0,009	0,01	0,035	0,044	0,012	0,005	0	0,056	0,007	0,012	0,01	0,01	0,013	0,007	0,009	0,006	0	0,023	0	0,011

Metabolom Analysis Results
8.2.9. Glycerophospholipids (5/5)

	PC ae C42:0	PC ae C42:1	PC ae C42:2	PC ae C42:3	PC ae C42:4	PC ae C42:5	PC ae C44:3	PC ae C44:4	PC ae C44:5	PC ae C44:6
01H_300	0,175	0,035	0,015	0,006	0	0,437	0,015	0,033	0,011	0,093
02H_300	0,17	0,036	0	0,005	0	0,464	0,015	0,031	0,021	0,084
03H_300	0,166	0,032	0,011	0	0	0,428	0,015	0,029	0,016	0,085
04H_300	0,18	0,029	0,011	0,008	0	0,462	0,016	0,029	0,017	0,102
05H_300	0,189	0,034	0,012	0,008	0	0,461	0,012	0,03	0,018	0,095
06H_300	0,191	0,034	0,011	0	0	0,475	0,018	0,031	0,011	0,095
07H_600	0,191	0,031	0,012	0,006	0	0,451	0,017	0,031	0,016	0,089
08H_600	0,182	0,037	0,013	0,007	0	0,446	0,021	0,031	0,01	0,091
09H_600	0,178	0,032	0,01	0,005	0	0,455	0,013	0,031	0,014	0,092
10H_600	0,175	0,042	0,009	0,005	0	0,461	0,015	0,031	0,011	0,093
11H_600	0,19	0,031	0	0	0	0,451	0,014	0,031	0,017	0,094
12H_600	0,18	0,037	0,011	0,009	0	0,461	0,013	0,029	0,012	0,092
01M_300	0,17	0,039	0,011	0,002	0	0,435	0,014	0,033	0,015	0,095
02M_300	0,177	0,038	0	0,004	0	0,449	0,012	0,035	0,012	0,095
03M_300	0,159	0,048	0,008	0,007	0	0,419	0,014	0,031	0,013	0,094
04M_300	0,163	0,037	0,007	0	0	0,444	0,016	0,03	0,009	0,09
05M_300	0,16	0,046	0	0,009	0	0,432	0,014	0,027	0,017	0,082
06M_300	0,159	0,042	0,006	0,007	0	0,435	0,015	0,027	0,012	0,083
07M_600	0,166	0,035	0,013	0,004	0	0,438	0,015	0,024	0,016	0,093
08M_600	0,162	0,039	0,013	0,004	0	0,427	0,011	0,033	0,011	0,088
09M_600	0,182	0,048	0	0	0	0,436	0,013	0,033	0,013	0,085
10M_600	0,164	0,033	0,006	0,002	0	0,45	0,012	0,032	0,018	0,097
11M_600	0,172	0,032	0,009	0,005	0	0,442	0,016	0,033	0,02	0,095
12M_600	0,179	0,041	0,006	0	0	0,441	0,014	0,031	0,009	0,092

8.2.10. Sphingolipids

e	SM (OH) C14:1	SM (OH) C16:1	SM (OH) C22:1	SM (OH) C22:2	SM (OH) C24:1	SM C16:0	SM C16:1	SM C18:0	SM C18:1	SM C20:2	SM C22:3	SM C24:0	SM C24:1	SM C26:0	SM C26:1
01H_300	0,217	0,052	0,068	0,138	0	3,47	0,075	0	0,026	0	0	0,148	0,648	0,004	0,006
03H_300	0,235	0,043	0,048	0,143	0,006	3,68	0,086	0	0,034	0,008	0	0,19	0,627	0,003	0,007
05H_300	0,26	0,037	0,058	0,13	0,016	3,82	0,085	0	0,019	0	0	0,127	0,571	0,008	0
07H_600	0,292	0,05	0,051	0,17	0,006	4,58	0,091	0	0,035	0,009	0	0,167	0,676	0	0,01
09H_600	0,225	0,041	0,055	0,132	0,007	3,38	0,081	0	0,024	0,005	0	0,142	0,596	0	0,009
11H_600	0,257	0,047	0,065	0,139	0,006	3,9	0,09	0	0,037	0,001	0	0,155	0,651	0	0,003
01M_300	0,209	0,05	0,046	0,093	0,006	2,77	0,096	0	0,03	0	0	0,172	0,368	0,002	0,002
03M_300	0,181	0,04	0,04	0,086	0,006	2,73	0,078	0	0,035	0	0	0,148	0,429	0	0
05M_300	0,22	0,035	0,05	0,086	0,007	2,78	0,1	0	0,055	0,001	0	0,178	0,368	0,005	0,01
07M_600	0,217	0,04	0,045	0,117	0,007	3,2	0,084	0	0,035	0	0,038	0,199	0,551	0,003	0,005
09M_600	0,23	0,043	0,065	0,109	0,011	3,15	0,093	0	0,027	0,005	0,014	0,222	0,498	0,001	0
11M_600	0,189	0,054	0,054	0,111	0,007	3,04	0,075	0	0,032	0	0	0,186	0,568	0	0,002
02H_300	0,073	0,007	0,016	0,035	0	1,14	0,04	0	0,01	0,002	0,007	0,038	0,124	0,002	0
04H_300	0,05	0,01	0,012	0,019	0,009	0,864	0,033	0	0,019	0,004	0	0,036	0,101	0,003	0
06H_300	0,055	0,004	0,032	0,028	0,009	0,923	0,034	0	0,005	0,001	0,015	0,045	0,127	0	0
08H_600	0,029	0,009	0,033	0,021	0,005	0,686	0	0	0,019	0,003	0,001	0,036	0,12	0	0,002
10H_600	0,005	0	0,029	0,02	0,005	0,476	0,019	0	0,003	0	0,004	0,032	0,127	0,001	0,008
12H_600	0,031	0,001	0,03	0,02	0,006	0,711	0,023	0	0,01	0	0,006	0,034	0,104	0,003	0,011
02M_300	0,137	0,025	0,035	0,046	0	1,87	0,066	0	0,029	0	0,004	0,102	0,233	0,011	0,008
04M_300	0,059	0,012	0,014	0,024	0,011	1,08	0,051	0	0,012	0	0	0,054	0,12	0,006	0,001
06M_300	0,05	0,005	0,028	0,028	0,005	0,834	0,043	0	0,019	0,002	0,008	0,055	0,126	0	0
08M_600	0,017	0,004	0,022	0,013	0,009	0,56	0,024	0	0,008	0	0	0,044	0,097	0,007	0,003
10M_600	0,032	0	0,043	0,022	0,013	0,691	0,033	0	0,006	0	0	0,064	0,14	0,006	0,009
12M_600	0	0	0,029	0,02	0	0,461	0,019	0	0,005	0,002	0,004	0,04	0,113	0,007	0

Metabolom Analysis Results

8.2.11. Hoechst Assay

Normalization was performed by measuring DNA contents using the Hoechst Assay:

All Plates Results - sorted for groups

ample N	mple Nar	Plate	Mean	SD	SNR*
2	04H_300	1	2384,125	275,821	954,799
5	02H_300	1	2013,605	167,417	792,161
5	01H_300	2	1933,133	85,903	545,066
3	03H_300	3	2403,313	118,596	625,999
5	06H_300	3	2269,490	122,757	587,691
6	05H_300	3	2294,945	154,099	594,978
3	10H_600	1	2492,573	339,695	1002,402
7	07H_600	1	2278,205	92,661	908,306
9	08H_600	1	2241,353	109,220	892,130
3	12H_600	2	2303,638	125,164	662,721
7	11H_600	2	2467,308	50,435	714,694
9	09H_600	2	2784,605	57,862	815,453
4	06M_300	1	2547,855	237,128	1026,668
6	03M_300	1	3067,603	168,013	1254,810
1	02M_300	2	3127,263	147,718	924,264
6	04M_300	2	3541,590	158,901	1055,834
8	05M_300	2	3078,058	213,005	908,639
7	01M_300	3	2264,105	58,338	586,150
1	11M_600	1	3221,275	80,700	1322,264
8	07M_600	1	3049,855	64,445	1247,019
2	12M_600	2	3357,358	110,028	997,331
4	13M_600	2	2558,133	60,563	743,536
1	10M_600	3	3275,405	120,705	875,639
2	14M_600	3	2537,663	53,765	664,457
4	08M_600	3	3386,283	110,886	907,378
8	09M_600	3	3373,313	185,407	903,666